



University of Tennessee, Knoxville  
**TRACE: Tennessee Research and Creative  
Exchange**

---

Masters Theses

Graduate School

---

12-2019

## Saltiness Enhancing Odorants Derived from Mushrooms

Jordan Lopez

University of Tennessee, [jlopez22@vols.utk.edu](mailto:jlopez22@vols.utk.edu)

Follow this and additional works at: [https://trace.tennessee.edu/utk\\_gradthes](https://trace.tennessee.edu/utk_gradthes)

---

### Recommended Citation

Lopez, Jordan, "Saltiness Enhancing Odorants Derived from Mushrooms. " Master's Thesis, University of Tennessee, 2019.

[https://trace.tennessee.edu/utk\\_gradthes/5644](https://trace.tennessee.edu/utk_gradthes/5644)

This Thesis is brought to you for free and open access by the Graduate School at TRACE: Tennessee Research and Creative Exchange. It has been accepted for inclusion in Masters Theses by an authorized administrator of TRACE: Tennessee Research and Creative Exchange. For more information, please contact [trace@utk.edu](mailto:trace@utk.edu).

To the Graduate Council:

I am submitting herewith a thesis written by Jordan Lopez entitled "Saltiness Enhancing Odorants Derived from Mushrooms." I have examined the final electronic copy of this thesis for form and content and recommend that it be accepted in partial fulfillment of the requirements for the degree of Master of Science, with a major in Food Science.

John Munafo Jr., Major Professor

We have read this thesis and recommend its acceptance:

John Munafo Jr, Curtis Lockett, Tao Wu

Accepted for the Council:

Dixie L. Thompson

Vice Provost and Dean of the Graduate School

(Original signatures are on file with official student records.)

# **Saltiness Enhancing Odorants Derived from Mushrooms**

A Thesis Presented for the

Master of Science

Degree

The University of Tennessee, Knoxville

Jordan Lopez

May 2020

## ACKNOWLEDGEMENTS

I would like to sincerely thank my advisor, Dr. John P. Munafo Jr., for giving me this opportunity to study food science under his tutelage. His knowledge and dedication to food science has helped me learn and grow as a scientist and I am indebted to him for taking the chance on teaching me. I would also like to express my gratitude to Dr. Curtis Luckett and Dr. Tao Wu for serving on my advisory committee and supporting my studies.

I would also like to thank my lab mates, Melissa Dein, Purni Wickramasinghe, Trent Kerley, Andrew Moore, and Dr. Anne Murray for their help in my projects. I wouldn't be here without their support both in and outside the lab. I'd also like to thank Lindsay Jenkinson and the rest of the sensory lab for their help in this project and all the sensory tests they performed for me.

Thanks to my family for their support and encouragement in my return to school. I'm especially thankful to my wife, Alexa Hamilton, for her relentless encouragement and willingness to put up with my frequent trips to Knoxville.

Thank you to the USDA National Institute of Food and Agriculture Grant #12445956 for funding this project.

## ABSTRACT

New approaches to developing healthy foods with great flavor is crucial in encouraging consumer adoption of nutritious diets and in improving the nutritional quality of the global food supply. Accordingly, interest has significantly increased in the development of flavors that increase consumer appeal and preference for low sodium foods. Gas chromatography-olfactometry (GC-O), coupled with stable isotope dilution assays (SIDA), led to the identification of the odorants responsible for an enhancement in perceived saltiness perception of a low-sodium chicken broth prepared with enzymatically hydrolyzed mushroom protein (eHMP) and cysteine, and reacted under kitchen-like cooking conditions. Comparative aroma extract dilution analysis (cAEDA) of thermally treated eHMP, with and without the addition of cysteine, revealed 36 odorants with flavor dilution (FD) factors within a range of 1–256. In this study, 16 odorants were quantitated and odor activity values (OAVs) were calculated. The key odorants generated during thermal treatment with cysteine were identified as 2-furfurylthiol (coffee, OAV 610.4), 1-(2-furyl)ethanethiol (meaty, OAV 78.2), 3-sulfanylpentan-2-one (catty, OAV 41.9), sotolon (maple, OAV 20.2), indole (animal, OAV 7.6), 2-methyl-3-(methyldithio)furan (meaty, OAV 3.4), and *p*-cresol (barnyard, OAV 1.3). An odor simulation model was generated based on the quantitative data that successfully mimicked the aroma of thermally reacted eHMP and cysteine. A large consumer sensory study ( $n = 96$ ) confirmed that the addition of the aroma simulation model to a low-sodium chicken broth increased the perceived saltiness of the broth ( $p = 0.020$ ). This study illustrates the crossmodal effects of aroma on saltiness perception and provides a foundation for future experiments that explore aroma-taste interaction.

# TABLE OF CONTENTS

1. INTRODUCTION .....	1
2. LITERATURE REVIEW .....	4
2.1. History of Mushrooms in Food .....	4
2.2. Previous Mushroom Aroma Studies.....	5
2.3. Taste-Enhancing Compounds.....	6
2.4. Taste-Aroma Interaction .....	8
2.5. Hydrolysis .....	9
3. MATERIALS AND METHODS .....	12
3.1. Button Mushrooms ( <i>A. bisporus</i> ) .....	12
3.2. Chemicals, Reference Odorants, & Labeled Odorants .....	12
3.2.1. Reference Odorants .....	12
3.2.2. Synthesis of 1-(2-furyl)ethanethiol (8) .....	12
3.2.3. Isotopically Labeled Odorants.....	13
3.2.4. Synthesis of 1-(2-furyl)ethanethiol-d3 (d-8).....	13
3.2.5. Miscellaneous Chemicals and Reagents .....	15
3.3. Preparation of Samples .....	17
3.3.1. Enzymatic Hydrolysis of Mushroom Protein (eHMP).....	17
3.3.2. Thermal Treatment of Sample 1: eHMP (control).....	17
3.3.3. Thermal Treatment of Sample 2: eHMP + cystine (eHMP + cys) .....	17
3.3.4. Thermal Treatment of Sample 3: Thermal treatment of cysteine (alone) .....	18
3.4. Sensory Analysis of eHMP Samples .....	18
3.4.1. Olfactory-Profile Analysis .....	18
3.4.2. Consumer Taste Study .....	20
3.5. Identification & Quantitation of Odorants.....	21
3.5.1. Solvent Assisted Flavor Evaporation (SAFE) .....	21
3.5.2. Gas Chromatography-Olfactometry (GC-O) .....	21
3.5.3. Comparative Aroma Extract Dilution Analysis (cAEDA).....	24
3.6. Quantitation of Odorants.....	24
3.6.1. Quantitation by Stable Isotope Dilution Assay (SIDA).....	24
3.6.2. Gas Chromatography-Mass Spectrometry (GC-MS).....	25
3.6.3. Calculation of Odor Activity Values .....	26

3.7.	Quantitation of Sugar Content.....	27
3.8.	Model Reaction of Mannose and Cysteine .....	28
3.9.	Sensory Analysis of Aroma Simulation Model .....	28
3.9.1.	Aroma Simulation Model.....	28
3.9.2.	Olfactory-Profile Analysis .....	29
3.9.3.	Consumer Taste Evaluation.....	29
4.	RESULTS AND DISCUSSION .....	32
4.1.	First Consumer Sensory Panel .....	32
4.2.	Olfactory-Profile Analysis of eHMP & eHMP + cys .....	34
4.3.	Identification of Odorants by GC-O & GC-MS .....	34
4.3.1.	FD Chromatograms of eHMP .....	36
4.3.2.	FD Chromatograms of eHMP + cys .....	37
4.3.3.	Comparison of Odorants in eHMP & eHMP + cys by cAEDA.....	51
4.4.	Quantitation of Odorants .....	52
4.4.1.	Aroma Profile of eHMP .....	70
4.4.2.	Aroma Profile of eHMP + cys.....	70
4.4.3.	Aroma Simulation Model of eHMP + cys .....	75
4.5.	Second & Third Consumer Taste Panels .....	75
4.6.	Proposed Mechanisms of Formation .....	78
4.6.1.	Sugar Analysis .....	78
4.6.2.	Reaction of Mannose and Cysteine .....	79
4.6.3.	Proposed Mechanisms of Formation .....	79
5.	CONCLUSION.....	86
	REFERENCES .....	88
	APPENDIX .....	95
	VITA .....	98

## LIST OF TABLES

Table 1: Odorants and RFs used in quantitation .....	26
Table 2: Odorants identified in eHMP and eHMP + cys.....	35
Table 3: List of odorants detected at FD 256 in eHMP .....	39
Table 4: List of odorants detected at FD 64 in eHMP .....	41
Table 5: List of odorants detected at FD 16 in eHMP .....	42
Table 6: List of odorants detected at FD 4 in eHMP.....	43
Table 7: List of odorants detected at FD 1 in eHMP .....	44
Table 8: List of odorants detected at FD 256 in eHMP + cys .....	46
Table 9: List of odorants detected at FD 64 in eHMP + cys.....	47
Table 10: List of odorants detected at FD 16 in eHMP + cys .....	48
Table 11: List of odorants detected at FD 4 in eHMP + cys.....	49
Table 12: List of odorants detected at FD 1 in eHMP + cys.....	50
Table 13: Concentrations, odor thresholds, and odor activity values (OAV) of key odorants in eHMP ...	72
Table 14: Concentrations, odor thresholds, and odor activity values (OAV) of key odorants in eHMP + cys.....	73
Table 15: Concentrations of 16 odorants in eHMP and eHMP + cys.....	74
Table 16: Odorants and concentrations used in simulation flavor formula .....	76
Table 17: Sugar content of eHMP as determined by IC-PAD (n = 3) .....	78



## LIST OF FIGURES

Figure 1: Hydrolysis of protein .....	10
Figure 2: Synthetic pathway of 1-(2-furyl)ethanethiol .....	14
Figure 3: Mass Spectrum of 1-(2-furyl)ethanethiol (8) .....	14
Figure 4: Synthetic pathway of 1-(2-furyl)ethanethiol-d3.....	15
Figure 5: Mass spectra of synthesized 1-(2-furyl)ethanethiol (8, top) and 1-(2-furyl)ethanethiol-d3 (d-8, bottom) .....	16
Figure 6: eHMP Before and after thermal treatment .....	18
Figure 7: Reference odorants used for quantitative olfactory-profile analysis .....	19
Figure 8: Solvent Assisted Flavor Evaporation (SAFE) apparatus in use .....	22
Figure 9: Stepwise dilution of sample for cAEDA.....	24
Figure 10: Consumer sensory data comparing eHMP and eHMP + cys saltiness ratings in chicken broth	33
Figure 11: Olfactory-profile analysis of eHMP, cys, and eHMP + cys .....	33
Figure 12: Structures of odorants detected at FD 256 in eHMP.....	39
Figure 13: FD chromatogram of eHMP .....	40
Figure 14: Structures of odorants detected at FD 64 in eHMP .....	41
Figure 15: Structures of odorants detected at FD 16 in eHMP.....	42
Figure 16: Structures of odorants detected at FD 4 in eHMP.....	43
Figure 17: Structures of odorants detected at FD 1 in eHMP.....	44
Figure 18: FD chromatogram of eHMP + cys.....	45
Figure 19: Structures of odorants detected at FD 256 in eHMP + cys .....	46
Figure 20: Structures of odorants detected at FD 64 in eHMP + cys .....	47
Figure 21: Structures of odorants detected at FD 16 in eHMP + cys .....	48
Figure 22: Structures of odorants detected at FD 4 in eHMP + cys .....	49
Figure 23: Structures of odorants detected at FD 1 in eHMP + cys .....	50

Figure 24: Odorants detected at a higher FD in eHMP + cys compared to eHMP .....	51
Figure 25: Total ion chromatogram of eHMP .....	53
Figure 26: Total ion chromatogram of eHMP + cys .....	54
Figure 27: Mass spectra for 1-octen-3-one and 1-octen-3-one-d3.....	55
Figure 28: Mass spectra for 1-(2-furyl)ethanethiol and 1-(2-furyl)ethanethiol-d3 .....	56
Figure 29: Mass spectra for 2-furfurylthiol and 2-furfurylthiol-d2 .....	57
Figure 30: Mass spectra for 3-(methylsulfanyl)propanal and 3-(methylsulfanyl)propanal-d3 .....	58
Figure 31: Mass spectra of 2-ethyl-3,5-dimethylpyrazine and 2-ethyl-d5-3,5-dimethylpyrazine.....	59
Figure 32: Mass spectra of butanoic acid and butanoic acid-d7 .....	60
Figure 33: Mass spectra of 2-acetylthiazole and 2-acetylthiazole- <sup>13</sup> C <sub>2</sub> .....	61
Figure 34: Mass spectra of phenylacetaldehyde and phenylacetaldehyde-d5.....	62
Figure 35: Mass spectra of 3-methylbutanoic acid and 3-methylbutanoic acid-d9.....	63
Figure 36: Mass spectra of HDMF and HDMF- <sup>13</sup> C <sub>2</sub> .....	64
Figure 37: Mass spectra of <i>p</i> -cresol and <i>p</i> -cresol-d7.....	65
Figure 38: Mass spectra of sotolon and sotolon- <sup>13</sup> C <sub>2</sub> .....	66
Figure 39: Mass spectra of indole and indole-d7 .....	67
Figure 40: Mass spectra of phenylacetic acid and phenylacetic acid-d5 .....	68
Figure 41: Mass spectrum for 3-sulfanylpentan-2-one.....	69
Figure 42: Mass spectrum for 2-methyl-3-(methyldithio)furan.....	69
Figure 43: Olfactory-profile analysis of eHMP + aroma model versus eHMP + cys .....	76
Figure 44: Consumer sensory data comparing eHMP vs. eHMP + aroma model saltiness ratings in low sodium chicken broth.....	77
Figure 45: Theoretical pathway of formation of 1-(2-furyl)ethanethiol via the reaction of mannose with cysteine.....	81
Figure 46: Theoretical pathway of formation for 2-furfurylthiol via the reaction of xylose and cysteine.	82

Figure 47: Theoretical pathway of formation for 3-sulfanylpentan-2-one via the reaction of mannose and cysteine. .... 84

Figure 48: Theoretical pathway of formation of 2-methyl-3-(methyldithio)furan via the reaction of xylose and cysteine. .... 85

# 1. INTRODUCTION

Button mushrooms, *Agaricus bisporus* (L.), are a popular ingredient in the cuisines of many cultures because of their pleasantly unique flavor. Many studies have been conducted on mushrooms, including the characterization of odorants, sugars, and amino acids. Mushrooms are a common ingredient in pre-prepared meals and home recipes, imparting a savory and umami-like taste character. Other studies have explored process flavors, such as reacting sugars with cysteine or hydrolyzing proteins to promote a similar umami-like taste. The use of cooked mushrooms as an ingredient in recipes often elicits a salty taste character, suggesting that either the odorants or tastants present in cooked mushrooms may help to increase the perceived saltiness in low sodium foods. This project focused on the odorants found in cooked mushrooms and explored the cross-modal effects of aroma on taste.

The first objective of this study was to identify odorants present in thermally treated hydrolyzed mushroom protein, both alone and in the presence of cysteine. This was accomplished by hydrolyzing dried mushrooms using a protease from *Aspergillus oryzae* and observing the rate of hydrolysis by gel-permeation chromatography (GPC). Once hydrolysis was complete, the enzymatically hydrolyzed mushroom protein (eHMP) was thermally treated in kitchen-like conditions alone and in the presence of cysteine. The two samples were then subjected to solvent assisted flavor evaporation (SAFE) to isolate the volatiles from the samples. The aroma extract was then serially diluted via comparative aroma extract dilution analysis (cAEDA) to identify the importance of each unique odorant in relation to the other odorants present in each sample. The flavor dilutions (FDs) were then analyzed by gas chromatography-olfactometry (GC-O) and assigned a number corresponding to the most dilute FD that the odorants were perceived.

The *second objective* was to quantitate the odorants that were responsible for the different aroma profiles between the eHMP and eHMP + cys samples. This was achieved using stable isotope dilution assay (SIDA). To calculate the concentration of an odorant, an isotope was added at a known concentration to the samples before they were subjected to analysis. The samples were then analyzed by gas chromatography-mass spectrometry (GC-MS) and the concentration of the odorants were calculated based off the ion ratio of the odorants and the internal standard isotopes.

The *third objective* was to replicate the aroma of the eHMP + cys by preparing an aroma simulation model. GC-O data was used to identify the odorants and SIDA was employed to calculate the concentration of the odorants. As a validation of the results, an aroma simulation model was prepared using commercially available odorants. The aroma simulation model was then added to eHMP and compared to eHMP + cys in a consumer sensory analysis. The odor descriptors of the samples were determined by free choice profiling and quantitated by olfactory profile analysis. The two samples were determined to be statistically similar in aroma profile by sensory analysis.

The *fourth objective* was to evaluate the perceived saltiness-enhancing effect of the aroma simulation model in a consumer sensory evaluation. The aroma simulation model was added to a low sodium chicken broth and compared to the eHMP + cys sample in the same low sodium chicken broth. Panelists were asked to judge the two samples on several qualities including saltiness, bitterness, sweetness, sourness, and umami, as well as overall taste. This study was used to identify the taste-modulating effects the added aroma simulation model might impart to the broth, as no additional tastants were added or generated to affect the taste.

The *fifth objective* of this study was to determine potential formation pathways for thermally derived odorants from mushroom precursors. Some meaty-smelling odorants are theorized to be formed through reactions of glucose and ribose, but mushrooms have low levels of glucose and ribose and higher levels of mannose and xylose. Using the precursors available in mushrooms, several new theoretical formation pathways for several meaty-smelling odorants were proposed.

## 2. LITERATURE REVIEW

### 2.1. History of Mushrooms in Food

Mushrooms have been consumed by humans for millennia. The first known documented edible mushroom was from Chile, approximately 13000 years ago.<sup>1</sup> Edible mushrooms have also been documented during the reign of the Roman Empire and for centuries in China as food and medicine. Today, over 80 countries in the world eat approximately 1000 different mushroom varieties. It is estimated that nearly 8 million tons of mushrooms are consumed globally per year, cementing mushrooms as a food staple in many cuisines around the globe.

The button mushroom, *Agaricus bisporus* (L.), was first commercialized in 1707 in France. These mushrooms were grown and harvested in caves, but cultivation expanded rapidly in the 19<sup>th</sup> century due to advances in agricultural knowledge and technology. Specific substrates for fungal growth, climate-controlled facilities, and mechanization all factored into the expansion of the consumable mushroom industry.

The white variety of button mushroom was discovered in 1926 in Pennsylvania and grew in popularity, mainly due to its color. This species of mushroom has many different common names based on its color and maturity, including names such as portabella, baby bella, and cremini mushrooms. In this study, immature white *A. bisporus* (cultivar; Delta) were used. The fruitbodies of the white button mushroom are small ellipsoids, roughly 4–6 cm across, with a stipe ~2 cm wide. The gills are underdeveloped and light brown, while the rest of the flesh is off-white.

## 2.2. Previous Mushroom Aroma Studies

The principle odorants responsible for the characteristic raw mushroom aroma, 1-octen-3-one and 1-octen-3-ol, have been studied at length.<sup>2</sup> Raw mushroom aroma is driven by 1-octen-3-one and 1-octen-3-ol, with odor activity values that are higher than other odorants present.<sup>3</sup> Drying mushrooms alters their odor profile significantly, reducing the impact of 1-octen-3-one and 1-octen-3-ol. Odorants associated with the Maillard reaction, such as pyrazines, are key contributors to the aroma of dried mushrooms.<sup>3</sup>

However, there have been comparatively few studies into the aroma of cooked mushrooms. Thermal processing of mushrooms, such as pan frying or sautéing, lower the concentration of these two odorants and generate other odorants associated with “meaty or savory-like” aroma attributes.<sup>4</sup> In addition, mushrooms are often cooked with a combination of sulfur-containing plants of the *Allium* genus, such as onions and garlic, or with other ingredients rich in sulfur-containing amino acids, that further enhance the generation of desirable odorants. Due to their pleasant flavor, mushrooms are enjoyed as ingredients included a wide variety of broths and sauces. The pleasing altered aroma profile of cooked mushrooms and their association with savory foods suggests that a better understanding of the fundamental flavor chemistry occurring during thermal processing would be useful to the food and culinary industry.

Published olfactory research on mushrooms has focused mainly on the raw mushroom-smelling odorant 1-octen-3-ol; consequently, not much is known about the odor quality of cooked mushrooms. One exception to that trend would be the work of Grosshauser and Schieberle who used gas chromatography-olfactometry (GC-O) to identify the key odorants in pan fried



mushrooms, including 3-methylbutanal, 2-(methylthio)propanal, 2-acetyl-1-pyrroline, 1-octen-3-one, 4-hydroxy-2,5-dimethylfuran-3(2H)-one, and phenylacetaldehyde.<sup>4</sup> Further research into the flavor compounds of cooked mushrooms could positively impact the knowledge base for mushroom flavor, with widespread implications.

### 2.3. Taste-Enhancing Compounds

Americans consume an average of 4 g of sodium per day, about double that of the World Health Organization's recommended 2.4 g a day.<sup>5</sup> Reduction in salt intake is suspected to be the most cost-effective method a government can take to improve health outcomes and reduce medical costs associated with cardiovascular health. Due to this, salt-enhancing flavor compounds have been a topic of both commercial and scientific interest for decades.

Monosodium glutamate (MSG) was first discovered to have a unique, savory taste attribute in 1909 by Kikunae Ikeda.<sup>6</sup> Ikeda termed this taste "umami" and was subsequently found in many savory ingredients and dishes. Taste-enhancing compounds were first reported in the 1960s when MSG was mixed with a 5'-nucleotide.<sup>7</sup> In 1967, scientists in Japan discovered that the addition of small amounts of inosine-5'-monophosphate or guanosine-5'-monophosphate significantly increased the perceived umami taste of MSG despite not possessing an umami taste individually at low concentrations.

In 1989, Tamura et al. tested the salt-enhancing effects of amino acids and their derivatives in water.<sup>8</sup> The main focus of the study, ornithyl- $\beta$ -alanine, displayed no salty taste on its own. However, modulating the pH altered the taste perception of ornithyl- $\beta$ -alanine. At pH 8.9, no

saltiness was detected. At pH 6.0 the solution was perceived as weakly salty, and at pH < 5.0 the solutions were perceived as strongly salty. At 60mM, ornithyl- $\beta$ -alanine was determined by a panel of tasters to be as salty as a 0.5% aqueous salt solution.

These results inspired Tamura et al. to further explore other amino acids and their derivatives. Lysine, asparagine, glutamine, aspartic acid, glutamic acid, glycine, serine, taurine, and the methyl esters of each of these amino acids were tested for saltiness enhancement in a similar test. Glycine methyl ester and lysine exhibited moderate saltiness enhancement, while most other amino acids were only weakly enhanced saltiness perception.

In 1998, Guerrero et al. was granted US patent 5,711,985, “*Compounds to enhance taste of salt used in reduced amounts.*”<sup>9</sup> The invention used hydrolyzed protein to enhance the saltiness perception of ammonium salts. Specifically, the amino acids lysine and arginine were specified as the precursors behind this flavor enhancement. This process of hydrolyzing protein, specifically with enzymes or heat and acid, is commonly used in processed foods as an additive to enhance flavor.

A few years later, Uchida et al. submitted a patent for enhancing the “salty or delicious” taste of food products.<sup>10</sup> Sodium chloride solutions between 1.5-12.0% in water (w/w) were considered significantly saltier when trehalose was added between 3.0-9.0% (w/w). Trehalose, a disaccharide of two glucose monomers with a 1,1-glycosidic bond, is also known as mycose or tremalose and is naturally occurring in some fungi and invertebrates. This study was unique in that several other saccharide compounds were tested by a sensory panel (n = 15). Glucose, fructose, maltose, sucrose,

erythritol, sorbitol, maltitol, lactitol, and dextrin either reduced the saltiness of the aqueous salt solution or had no effect. However, the panelists determined that trehalose enhanced the perceived saltiness of the solution.

In 1968, Bouchard et al. found that adding ppm-level concentrations of pyranones, such as maltol or ethyl maltol, to a 5% aqueous sucrose solution gave it the perceived sweetness of a 20% sucrose solution.<sup>11</sup> Further studies confirmed similar results with furanones.<sup>12</sup> Pyranones and furanones are found in cooked sugar, caramel, and fruit, indicating many people associate these odorants with sweet taste. Some studies have shown that odorants that are more commonly known for imparting aroma to foods can enhance taste even when eliminating the olfactory impact. As one of the first studies to illustrate the impact of aroma on taste perception, Bouchard et al. helped to expand the study of crossmodal effects in taste and aroma.

#### 2.4. Taste-Aroma Interaction

Flavor, by definition, is the incorporation of aroma, taste, and tactile sensation simultaneously.<sup>13</sup> Concurrent perception of taste and aroma can enhance the perception of each other. That is, the addition of a taste may suppress or enhance an aroma. The combination of these senses is limited to the retronasal perception of aroma; as tastants are sensed in the mouth, the odorants released from a food matrix during mastication enter the nasal cavity and are sensed by the olfactory epithelium. The multi-modal perception of taste, odor, and texture that simultaneously occur in the mouth is considered the benchmark that separates flavor from individual senses.

There have been several studies illustrating that odorants induce changes in taste perception.<sup>14-17</sup> Taste modulation due to odor is hypothesized to be based on two primary causes: *congruency* and *odor-taste associations*. Congruency of the taste and odor is based on how well the two sensory modalities complement each other. Odor-taste associations are thought to occur based on months or years of memory.<sup>18</sup> For example, the addition of chicken, beef, anchovy, bacon, or soy sauce aromas each has been shown to increase the saltiness perception in sodium chloride solutions. These foods are often salty and personal experience has psychologically linked these aromas with a salty taste.<sup>13</sup> Accordingly, the identification of odorants that enhance saltiness perception in low sodium foods is of substantial scientific interest in the development or augmentation of sodium reduction technologies.<sup>17, 19, 20</sup> These studies justify combined efforts for better understanding of protein hydrolysates, thermal process, and odor-induced saltiness enhancement in the pursuit of developing novel flavor technologies.

## 2.5. Hydrolysis

When mushrooms are cooked, the heat treatment, as with all foods, leads to numerous chemical reactions, including the degradation of carbohydrates into mono- and disaccharides and proteins into peptides and amino acids (Figure 1). Sugars and amino acids then serve as precursors of odorants formed in a myriad of pathways via the Maillard reaction. In the commercial preparation of protein hydrolysates, the protein breakdown is regulated through hydrolysis, which is usually performed with acid or enzymes to degrade larger molecules into smaller units. Kimatu et al. have illustrated that hydrolysis of mushroom protein increases the peptide and amino acid content of the sample.<sup>21</sup> For example, using a protease, the Kimatu team generated elevated levels of glutamine, glutamic acid, asparagine, aspartic acid, leucine, and lysine. These amino acids may

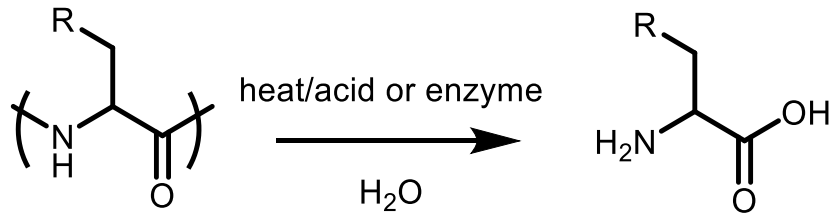


*Figure 1: Hydrolysis of protein*

themselves be taste-active, or serve as precursors for aroma active compounds, thus modifying the flavor profile and increasing the flavor intensity of the hydrolysate. As previously determined by Guerrero et al., lysing a protein yields lysine and arginine, which were purported to be the cause of enhanced saltiness perception in the 1998 patent.<sup>9</sup>

In another study, Kim et al. explored the thermal treatment of hydrolyzed protein with sugars and amino acids.<sup>22</sup> The Kim team hydrolyzed krill protein and thermally reacted it with several amino acids and sugars. Several sulfur-containing odorants were identified, including methanethiol, dimethyl sulfide, dimethyl disulfide, dimethyl trisulfide, 3-(methylsulfanyl)propanal, 6-(methylthio)-hexa-1,5-dien-3-ol, and (Z)-1-(methylthio)-1-propene. The addition of the hydrolyzed protein reaction mixture into a shrimp soup was shown to significantly increase the broth's perceived shrimp flavor as compared to the untreated control, indicating that the thermally generated odorants and/or tastants enhanced the flavor of the broth.

Insight into the flavor chemistry that takes place during the thermal treatment of mushrooms under kitchen-like cooking conditions may guide the development of reaction flavors that enhance the flavor of savory foods such as beef or chicken, other meats, and low sodium food applications.<sup>23</sup>

By isolating the odorants or tastants responsible for flavor enhancement, reactions can be optimized to generate desirable flavor.

### 3. MATERIALS AND METHODS

#### 3.1. Button Mushrooms (*A. bisporus*)

Immature white button mushrooms (*Agaricus bisporus*, cultivar Delta) were used in this study. The mushrooms were lyophilized prior to use for stability and consistency in solid content. The mushrooms were generously donated by Monterey Mushrooms (Loudon, Tennessee).

#### 3.2. Chemicals, Reference Odorants, & Labeled Odorants

##### 3.2.1. Reference Odorants

Reference odorants 1-octen-3-one (**4**), 2-furfurylthiol (**9**), acetic acid (**10**), 3-(methylsulfanyl)propanal (**11**), 2,3-diethyl-5-methylpyrazine (**13**), 2-methylpropanoic acid (**15**), butanoic acid (**16**), 2-acetylthiazole (**18**), 2-phenylacetaldehyde (**19**), 2- and 3-methylbutanoic acid (**20**), pentanoic acid (**24**), hexanoic acid (**25**), 2-methoxyphenol (**26**), HDMF (**28**), *p*-cresol (**29**), 4-allyl-2-methoxyphenol (**30**), sotolon (**31**), 5-ethyl-3-hydroxy-4-methyl-(5H)-furanone (**33**), indole (**34**), and 4-hydroxy-3-methoxybenzaldehyde (**36**) were purchased from Sigma-Aldrich (Saint Louis, MO). 3-sulfanylpentan-2-one (**6**) was purchased from VWR (Radnor, PA). 2-Methyl-3-(methylthio)furan (**17**) was purchased from Thermo Fisher Scientific (Waltham, MA). 2-Acetyl-1-pyrroline (**5**) was purchased from Aromalab (Planegg, Germany).

##### 3.2.2. Synthesis of 1-(2-furyl)ethanethiol (**8**)

1-(2-Furyl)ethanol (2 mmol, 224 mg) was dissolved in pentane (10 mL). To this solution, Lawesson's reagent (1 mmol, 404 mg) was added (Figure 2). The mixture was stirred under reflux conditions (30 min), then cooled to room temperature. The resulting solution was purified by high

vacuum distillation via SAFE isolation. The SAFE distillate was warmed to room temperature and dried over sodium sulfate before being analyzed by GC-MS (Figure 3). The final product was quantitated by GC-FID using an external calibration curve generated from 1-(2-furyl)ethanol (yield; 205 mg).

### 3.2.3. Isotopically Labeled Odorants

Labeled odorants 1-octen-3-one-d3 (**d-4**), 2-furfurylthiol-d2 (**d-9**), 3-(methylsulfanyl)propanal-d3 (**d-11**), 2-ethyl-d5-3,5-dimethylpyrazine (**d-12**), 2-acetylthiazole-<sup>13</sup>C<sub>2</sub> (**c-18**), phenylacetaldehyde-d5 (**d-19**), HDMF-<sup>13</sup>C<sub>2</sub> (**c-28**), and sotolon-<sup>13</sup>C<sub>2</sub> (**c-31**) were purchased from Aromalab (Planegg, Germany). Furfural-d3, butanoic acid-d7 (**d-16**), 3-methylbutanoic acid-d9 (**d-20**), *p*-cresol-d7 (**d-29**), and indole-d7 (**d-34**) were purchased from CDN Isotopes (Point-Claire, Canada). Phenylacetic acid-d5 (**d-35**) was purchased from Cambridge Isotopes (Tewksbury, MA). Furfural-d3 and pentadecane-d32 were purchased from Sigma Aldrich (Saint Louis, MO).

### 3.2.4. Synthesis of 1-(2-furyl)ethanethiol-d3 (d-8)

Furfural-d3 (1 mmol, 99 mg) was dissolved in dry THF (10 mL) with a magnetic stir bar. The solution was cooled to 0 °C in an ice bath and purged with N<sub>2</sub>. Then, methylmagnesium bromide (1 mmol, 0.7 mL, 1.4 M in 1:3 THF:toluene) was added drop-wise over 5 minutes (Figure 4). The reaction was allowed to react for 2 hours at 15 °C. Once complete, the reaction was quenched with 10% 2N sulfuric acid (1 mL, 10% w/w), and freshly distilled ether (5 mL) was added. The organic phase was washed with brine (2 x 5 mL) and purified by high vacuum distillation via SAFE isolation to yield 1-(2-furyl)ethanol-d3. The product was confirmed by GC-MS and used as-is in the subsequent step.



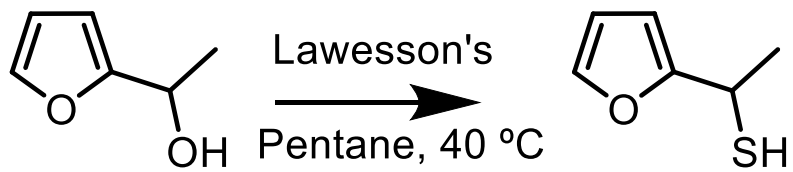


Figure 2: Synthetic pathway of 1-(2-furyl)ethanethiol

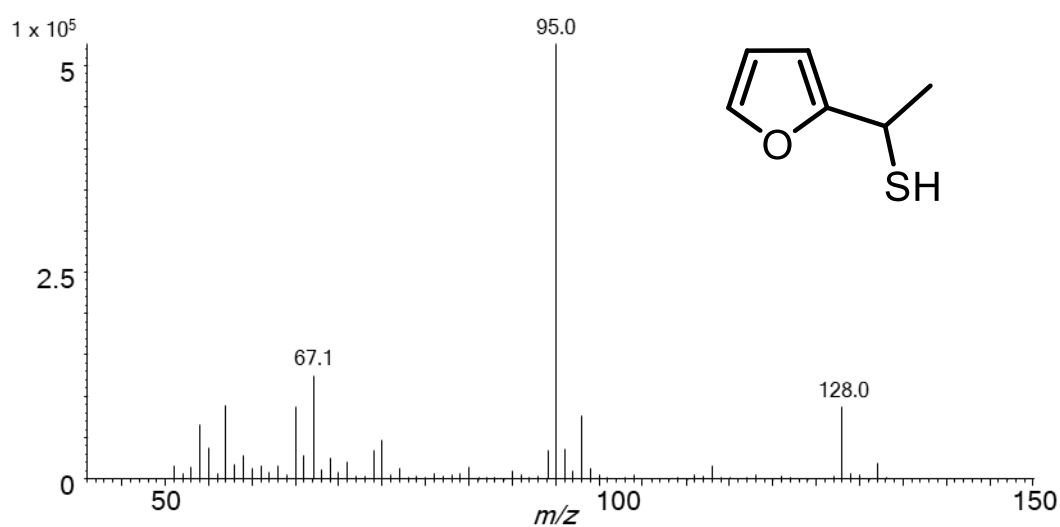


Figure 3: Mass Spectrum of 1-(2-furyl)ethanethiol (8)

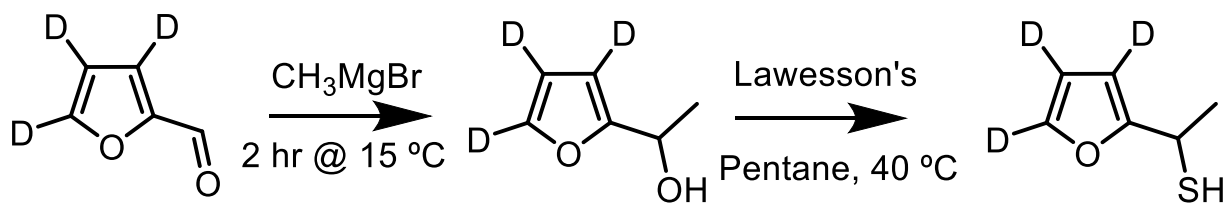


Figure 4: Synthetic pathway of 1-(2-furyl)ethanethiol-d3

1-(2-furyl)ethanol-d3 (1 mmol, 115 mg) was dissolved in pentane (5 mL) and converted to 1-(2-furyl)ethanethiol-d3 under the same conditions as described above for **8** (Figure 4). The final product was confirmed through analysis by GC-MS, and the concentration was determined by employing the same procedure as described above for the unlabeled analyte (Figure 5) (yield; 67 mg).

### 3.2.5. Miscellaneous Chemicals and Reagents

Cysteine, mannose, glucose, sucrose, fructose, ribose, xylose, maltose, protease from *Aspergillus oryzae*, triacetin, 1-(2-furyl)ethanol, sodium sulfate, Lawesson's reagent, tetrahydrofuran, 10% 2N sulfuric acid (w/w), and methylmagnesium bromide were purchased from Sigma-Aldrich (Saint Louis, MO). Sulfuric acid (1N, 10% w/w) was purchased from LabChem (Zelienople, PA). Swanson unsalted chicken broth and iodized salt were purchased at a local grocery store. Diethyl ether was purchased from Honeywell (Charlotte, NC) and freshly distilled before use. Distilled water was collected from an in-house purification system.

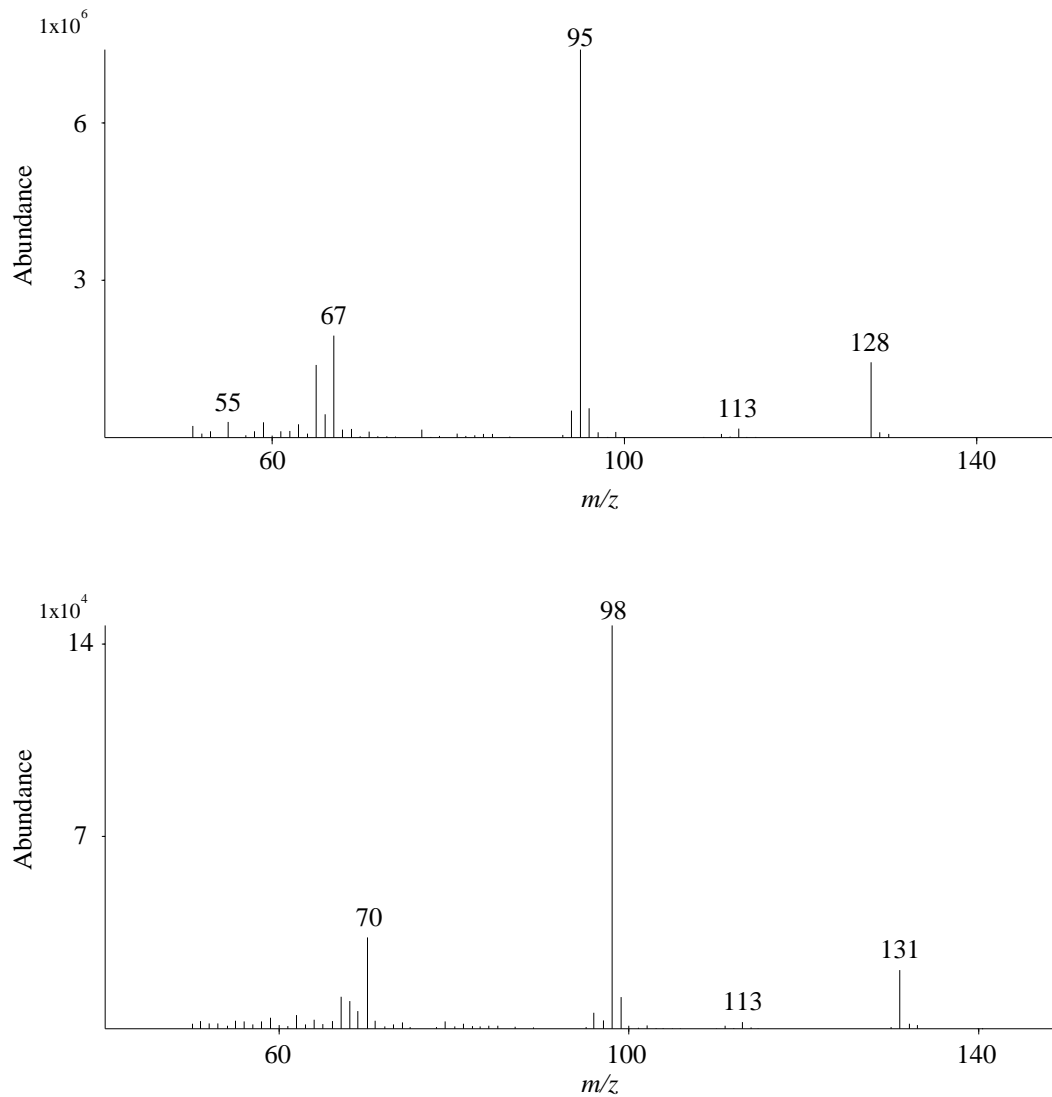


Figure 5: Mass spectra of synthesized 1-(2-furyl)ethanethiol (8, top) and 1-(2-furyl)ethanethiol-d3 (d-8, bottom)

### 3.3. Preparation of Samples

#### 3.3.1. Enzymatic Hydrolysis of Mushroom Protein (eHMP)

Fresh mushrooms were lyophilized over the course of five days. The resulting dried mushrooms were ground into a fine powder with a laboratory mill (Krupps, Solingen, Germany), and a portion of the powder (30 g) was weighed into a thermally stable 1L polyethylene bottle. Protease from *Aspergillus oryzae* (1.5 mL) was added, along with deionized water (540 mL), and shaken vigorously by hand (2 min). The bottle was placed in a water bath shaker at 50 °C for 4 hours and shaken by hand every hour (30 s). Next, the bottle was removed from the water bath shaker and cooled to room temperature and, then, vacuum filtered through a Buchner funnel to remove the solids. The filtered solution was stored at 4 °C overnight (yield; 500 mL).

#### 3.3.2. Thermal Treatment of Sample 1: eHMP (control)

eHMP (200mL) was transferred to a 500mL round bottom flask. The solution was refluxed for 4 hours while being stirred, then transferred to a large glass dish (46 cm x 31 cm) and baked in a conventional kitchen convection oven at 130 °C for 45 minutes. The resulting brown, viscous liquid (approx. 50 mL) was stored overnight at 0 °C (Figure 6).

#### 3.3.3. Thermal Treatment of Sample 2: eHMP + cystine (eHMP + cys)

eHMP (200mL) was transferred to a 500mL round bottom flask with cysteine (1.00 g). The solution was refluxed for 4 hours while stirring, then transferred to a large glass dish (46 cm x 31 cm) and baked in a conventional kitchen convection oven at 130 °C for 45 minutes. The resulting tan, viscous liquid (approx. 50 mL) was stored overnight at 0 °C.

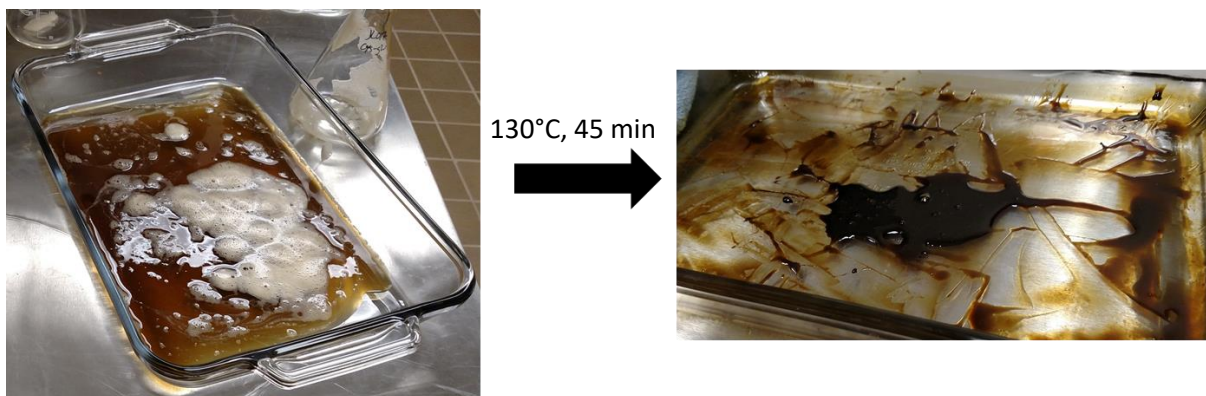


*Figure 6: eHMP Before and after thermal treatment*

#### 3.3.4. Thermal Treatment of Sample 3: Thermal treatment of cysteine (alone)

Deionized water (200mL) was transferred to a 500mL round bottom flask with cysteine (1.00 g). The solution was refluxed for 4 hours while stirring, then transferred to a large glass dish (46 cm x 31 cm) and baked in a conventional kitchen convection oven at 130 °C for 45 minutes. The resulting white liquid was stored overnight at 0 °C.

### 3.4. Sensory Analysis of eHMP Samples

#### 3.4.1. Olfactory-Profile Analysis

Trained sensory panelists were recruited from the University of Tennessee Knoxville Sensory Group for a quantitative olfactory-profile analysis. Free choice profiling was used to determine the lexicon used in the study. Samples of thermally treated eHMP and eHMP + cys were presented to panelists (n = 24) in 20 mL glass scintillation vials for orthonasal evaluation. Each panelist then provided a list of odor descriptors using their own lexicon. Based on common odor descriptors provided by the panelists, odor references were selected for the olfactory-profile analysis. Eight odorants were chosen as sensory reference standards: HDMF (caramel), 1-octen-3-one

(mushroom), 2-methyl-3-(methylthio)furan (meaty), hydrogen sulfide (egg), 2-ethyl-3,5-dimethylpyrazine (earthy), (2E, 4E)-2,4-decadienal (fatty), 2-acetylthiazole (toasty), and butanoic acid (cheesy) (Figure 7). The reference compounds were dissolved in water at 100 times greater than the threshold value for olfactory detection. The trained panelists then gauged the intensities of each sensory attribute of every sample on a scale of 0 to 3. The scores were averaged across panelists (n = 24) using Microsoft® Excel Version 16.21 for Office 360 (Microsoft Corporation, Redman, WA). For the quantitative olfactory-profile analysis of the aroma simulation model, descriptive sensory data were evaluated by a one-way analysis of variance (ANOVA) and means were separated with Tukey–Kramer HSD test ( $\alpha < 0.05$ ) using JMP Pro 14.0.0 software (SAS Institute, Cary, NC).

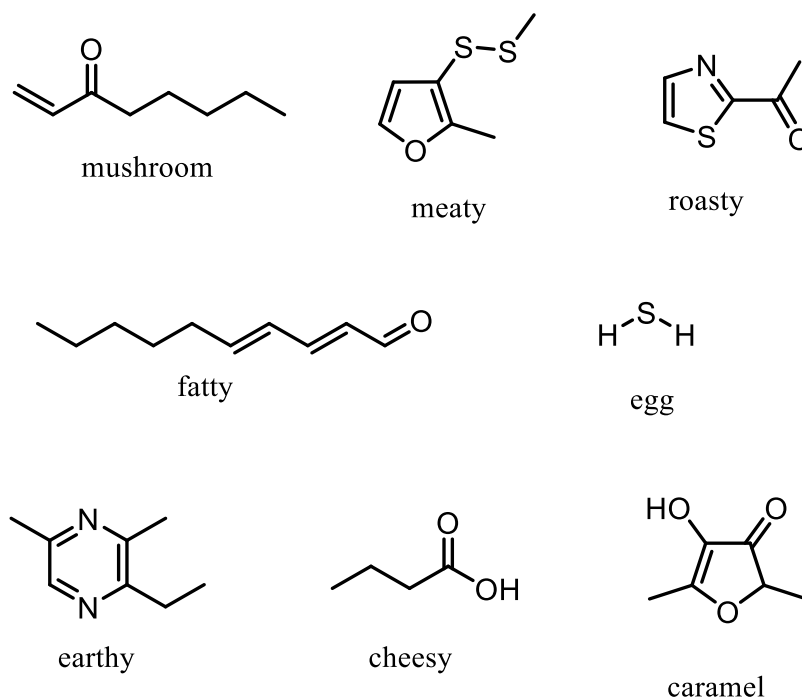


Figure 7: Reference odorants used for quantitative olfactory-profile analysis

### 3.4.2. Consumer Taste Study

The consumer sensory study was part of a high throughput screening study that used 9 participants, doing evaluations in triplicate ( $n = 27$ ). The participants were recruited using the University of Tennessee at Knoxville sensory consumer database, and each reported a healthy sense of smell and taste. All participants signed an informed consent form and were compensated for their time. This experiment was conducted according to the Declaration of Helsinki for studies on human subjects and approved by the University of Tennessee IRB review for research involving human subjects (IRB # 19-04998-XM).

Two samples were prepared for the initial sensory test. Unsalted Swanson chicken broth (Cambell's Soup Company, Camden, NJ) was chosen as a base in this study for its neutral-congruent taste and low sodium content, which allowed more control over the experiments. All eHMP samples were reduced to a thick, concentrated liquid prior to use in the sample matrices. For the eHMP sample, unsalted Swanson chicken broth (1.5 L), NaCl (3.6 g), and eHMP (1.5 g) were combined and stirred until dissolved (2.5 mg eHMP/mL broth). For the eHMP + cys sample, broth (1.5 L), NaCl (3.6 g), and eHMP + cys (1.5 g) were combined and stirred until dissolved. These broth mixtures (2.4 mg NaCl/mL) represented a 33% reduction in sodium content from the standard Swanson chicken broth (3.6 mg NaCl/mL). The samples were warmed up in a crock pot prior to evaluation.

The eHMP and eHMP + cys samples were subjected to sensory testing to evaluate the effect of each sample on saltiness perception. The participants were asked to score overall flavor intensity, umami, and saltiness attributes on a visual analog scale (500 pixel wide) ranging from “None at

all” to “Extremely high.” To test the one-tailed hypothesis of saltiness increases, the mean saltiness ratings were compared using paired t-tests with a Bonferroni correction. The attribute rating data was analyzed using JMP 14.0 (SAS Institute, Cary, NC).

### 3.5. Identification & Quantitation of Odorants

#### 3.5.1. Solvent Assisted Flavor Evaporation (SAFE)

The thermally treated eHMP was diluted with deionized water (50 mL), and pentadecane d-32 (50  $\mu$ L, 300ppm) was added as an internal standard for the concentration step. The sample was extracted with freshly distilled diethyl ether ( $2 \times 100$  mL) using a separatory funnel. The organic phases were combined, and the aqueous phase discarded. The ether extract (total volume: 200 mL) was then subjected to high-vacuum distillation ( $10^{-3}$  Pa) at 40 °C using the solvent-assisted flavor evaporation (SAFE) method (Figure 8).<sup>24</sup> The sample was then gradually dropped into the evaporation flask of the device over a 30 min period. After an additional 10 min, the vacuum was broken, and the distillate sample thawed at room temperature and, then, dried over anhydrous sodium sulfate. Next, the sample was concentrated to approximately 2 mL using a Vigreux column ( $50 \times 1$  cm) and, finally, to 200  $\mu$ L under a gentle stream of nitrogen. This process was repeated with the eHMP + cys and cysteine samples. The aroma profiles of the isolates were then evaluated sensorially to ensure that they closely matched the profiles of the concentrated reaction flavors.

#### 3.5.2. Gas Chromatography-Olfactometry (GC-O)

A 7820 series GC system (Agilent Technologies, Santa Clara, CA) was set up with an HP-FFAP capillary column ( $30 \text{ m} \times 0.32 \text{ mm}$ , 0.25  $\mu\text{m}$  film thickness) (Agilent). The samples (1  $\mu$ L) were injected using a cold-on-column inlet at 35 °C with helium as the carrier gas. The flow rate was





*Figure 8: Solvent Assisted Flavor Evaporation (SAFE) apparatus in use*

set to 1.0 mL/min. After resting at 35 °C for 1 min, the temperature of the oven was raised to 60 °C at 60 °C /min, and raised again to 240 °C at 6° C/min, where it was maintained for 10 min. The effluent was split 1:1 by volume after separation in the capillary column using a Y-type splitter into two 50 cm units of deactivated fused silica capillaries. One capillary diverted the sample to a flame ionization detector (FID) held at 250 °C, while the other capillary diverted the sample to a heated sniffing port held at 250 °C. The sniffing port was mounted on the front flame ionization detector (FID) base and consisted of a custom machined aluminum cylindrical cone (80 mm × 25 mm i.d.) housing the capillary. Throughout the GC-O analysis, a trained panelist monitored the aroma of the effluent from the sniffing port, recording odor quality and retention time as each aroma was detected.

To identify the odorants detected in the eHMP and eHMP + cys samples, retention indices (RIs) were calculated for each compound. An *n*-alkane hydrocarbon standard mixture (C-9 to C-26) was run on the GC-O and GC-MS to calculate RIs of the compounds. In order to calculate the RI for each odorant, the following equation was used:

$$RI = 100 \times \left[ n + (N - n) \frac{t_{r,a} - t_{r,n}}{t_{r,N} - t_{r,n}} \right]$$

In this equation, N is the closest alkane that elutes after the analyte of interest, *n* is the closest alkane that elutes prior to the analyte of interest,  $t_{r,a}$  is the retention time of the analyte of interest,  $t_{r,n}$  is the retention time of alkane *n*, and  $t_{r,N}$  is the retention time of alkane N. Using this formula, an RI for each odorant was calculated and compared to literature values for confirmation.

### 3.5.3. Comparative Aroma Extract Dilution Analysis (cAEDA)

The aroma isolates were sequentially diluted 1:1 with solvent to generate a series of dilutions and were analyzed by GC-O on an FFAP column following the same conditions outlined above (Figure 9). The samples were diluted 1:1 until no odorants were detected orthonasally via GC-O. The dilutions for eHMP and eHMP + cys were analyzed consecutively to ensure the most accurate comparisons possible. For both samples, each detected odorant was assigned an odor quality and an FD (flavor dilution) factor based on the highest dilution factor in which the compound was detected.

## 3.6. Quantitation of Odorants

### 3.6.1. Quantitation by Stable Isotope Dilution Assay (SIDA)

The labeled internal standards were diluted in freshly distilled diethyl ether or pentane and quantitated by calibration curves on a GC with a flame ionization detector (FID) using the GC method described below. Once quantitated, the labeled standards (50  $\mu\text{g}$  each) were added to the eHMP and eHMP + cys solutions at levels similar to the equivalent target odorants previously

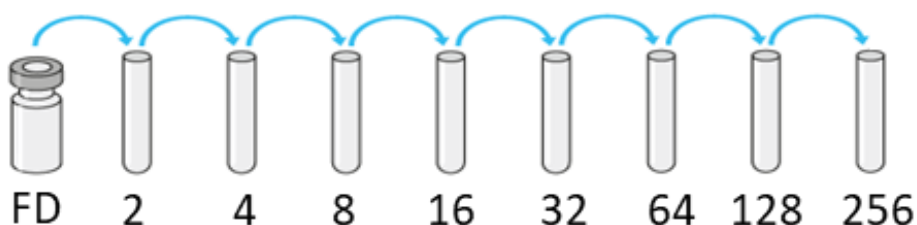


Figure 9: Stepwise dilution of sample for cAEDA

detected and shaken well by hand. After the addition, the sample was extracted with freshly distilled diethyl ether (2 x 100 mL) using a separatory funnel. The organic phases were combined, and the aqueous phase discarded. Next, the ether extract (total volume: 200 mL) was subjected to high-vacuum distillation using SAFE at 40 °C. The sample was then concentrated to 200 µL using a Vigreux column and a gentle stream of nitrogen as described earlier. The analytes were quantitated using characteristic peaks in the mass spectrum of the compound and corresponding isotope. 3-Sulfanylpentan-2-one and 2-methyl-3-(methyldithio)furan were quantitated using 2-furfurylthiol-d<sub>2</sub>.

The concentration of each odorant of interest was calculated according to the area of the integrated peak of the odorant in the GC-MS spectrum, the area of the integrated peak of the labeled standard, the amount of dried mushrooms present in the sample, the amount of labeled standard added to the sample, and a response factor (RF) created from a mixture of the unlabeled standard and the labeled standard in fixed amounts. The m/z used for each odorant and the labeled standard, as well as their RFs, are provided in Table 1.

### 3.6.2. Gas Chromatography-Mass Spectrometry (GC-MS)

Samples were analyzed on an Agilent 7800 series GC system furnished with a DB-FFAP and a DB-5 column (both 30 m × 0.25 mm, 0.25 µm film thickness) (Agilent). The column was attached to an Agilent 5973 mass spectrometer detector using a heated transfer line (250 °C). The carrier gas, Helium, was set at 1 mL/min constant flow. The sample (1 µL) was injected on-column at 35 °C, and the temperature was held for 1 min. Afterwards, the oven temperature was raised to 60 °C

Table 1: Odorants and RFs used in quantitation

no.	odorant	Ion (m/z)	labelled standard	Ion (m/z)	RF
4	1-octen-3-one	97	1-octen-3-one-d3	100	0.48
6	3-sulfanylpentan-2-one	75	2-furfurylthiol-d2	116	2.42
8	1-(2-furyl)ethanethiol	95	1-(2-furyl)ethanethiol-d3	98	1.37
9	2-furfurylthiol	114	2-furfurylthiol-d2	116	1.40
11	3-(methylsulfanyl)propanal	104	3-(methylsulfanyl)propanal-d3	107	0.82
12	2-ethyl-3,5-dimethylpyrazine	136	2-ethyl-d5-3,5-dimethylpyrazine	141	0.93
16	butanoic acid	60	butanoic acid-d7	63	0.89
17	2-methyl-3-(methyldithio)furan	160	2-furfurylthiol-d2	116	0.28
18	2-acetylthiazole	99	2-acetylthiazole- <sup>13</sup> C <sub>2</sub>	100	1.00
19	phenylacetaldehyde	91	phenylacetaldehyde-d5	96	1.07
20	3-methylbutanoic acid	60	3-methylbutanoic acid-d9	63	1.02
28	HDMF	128	HDMF- <sup>13</sup> C <sub>2</sub>	130	0.96
29	<i>p</i> -cresol	108	<i>p</i> -cresol-d7	115	1.04
31	sotolon	128	sotolon- <sup>13</sup> C <sub>2</sub>	130	1.23
34	indole	117	indole-d7	123	0.34
35	phenylacetic acid	91	phenylacetic acid-d5	96	0.90

at 60 °C/min and then to 250 °C at 6 °C/min, then held at the final temperature of 250 °C for 5 min.

The single quadrupole mass spectrometer was fixed at 70 eV and run in electron impact (EI) ionization mode with a scan range of m/z 50-450.

### 3.6.3. Calculation of Odor Activity Values

Odor activity values (OAVs) were calculated for each quantitated odorant. This provided a measure of impact or contribution to the overall aroma of the sample from each odorant. The OAV is calculated using the following formula:

$$OAV = \frac{C}{t}$$

In this formula, the OAV is calculated by dividing C, the concentration of the odorant in the sample, by t, the odor threshold in the appropriate matrix (water). Any odorant with an OAV > 1 is considered to have impact in the odor profile of the sample, with higher numbers usually

providing more impact. An odorant with an OAV < 1 is below the detectable odor threshold and is usually not impactful.

Odor thresholds determined in water were taken from literature.<sup>25-28</sup> The odor threshold for 1-(2-furyl)ethanethiol was determined through a triangle test with decreasing concentrations of 1-(2-furyl)ethanethiol in water. Odorless glass scintillation vials were filled with deionized water (10 mL) to function as blanks or with the diluted odorant (10 mL). A panel of trained assessors (n = 21) were given the test samples in increasing concentrations of the odorant and instructed to mark the samples based on detection. Calculation of the odor threshold was performed as described in the literature.<sup>25</sup>

### 3.7. Quantitation of Sugar Content

Sugar analysis of the eHMP samples were performed by ion chromatography using pulsed amperometric detection (IC-PAD). The samples were fully hydrolyzed and filtered through a 0.45 µm PTFE filter and analyzed (injection volume; 400 µL) at 35 °C on a 945 Professional Detector Vario (Metrohm, Herisau, Switzerland). The samples were separated on a Metrosep Carb 2 column (150 x 4 mm; 5µm). The mobile phase consisted of isocratic 100 mmol/L sodium hydroxide : 10 mmol/L sodium acetate (1:1; v/v). The flow rate was set to 0.5 mL/min and the column temperature was set to 35 °C. The detector temperature was set to 40 °C and the potential profile was as follows: 300 ms, 0.05 V; 50 ms, 0.55 V; 200 ms, -0.1 V. Cycle duration was 550 ms; duration, 100 ms; range, 200 µA. Each pure sugar standard was run individually and compared to eHMP to determine the sugar content of each sample.

### 3.8. Model Reaction of Mannose and Cysteine

To gain insight into the formation pathway of key sulfur-containing odorants 1-(2-furyl)ethanethiol and 2-furfurylthiol, a model reaction was created using analytical standards. Mannose (1.80 g, 10 mmol) and cysteine (0.40g, 3.3 mmol) were dissolved in a phosphate buffer (pH 5, 100 mL). The solution was placed in a glass reaction vessel and sealed inside a high-pressure reactor (Parr Instrument company, Moline, IL). The solution was stirred slowly and heated to 140 °C for 1 hour, cooled to room temperature, and extracted with freshly distilled diethyl ether (2 x 50 mL). The ether extract (total volume: 100 mL) was dried over sodium sulfate, concentrated as described above, and analyzed using GC-O and GC-MS.

### 3.9. Sensory Analysis of Aroma Simulation Model

#### 3.9.1. Aroma Simulation Model

An aroma simulation model was created based on the quantitative differences calculated in odorant concentrations between eHMP + cys and eHMP. Commercially available odorants were chosen due to their OAVs in eHMP + cys. These odorants were combined in triacetin based on the difference in concentration between the eHMP + cys and eHMP samples. This aroma simulation model was then added to thermally treated eHMP at the concentration detected in eHMP + cys and mixed until fully dissolved. The eHMP with aroma simulation model was subjected to an olfactory-profile analysis and compared to a sample of eHMP + cys. The eHMP with aroma simulation model was further tested in a consumer sensory taste panel in low sodium chicken broth and compared to eHMP.

### 3.9.2. Olfactory-Profile Analysis

As previously tested with the eHMP samples, trained sensory panelists were recruited from the University of Tennessee Knoxville Sensory Group for a quantitative olfactory-profile analysis. The aroma simulation model was compared to eHMP + cys using the same odorants, descriptors, and methodology as before: HDMF (caramel), 1-octen-3-one (mushroom), 2-methyl-3-(methylthio)furan (meaty), hydrogen sulfide (egg), 2-ethyl-3,5-dimethylpyrazine (earthy), (2*E*, 4*E*)-2,4-decadienal (fatty), 2-acetylthiazole (toasty), and butanoic acid (cheesy).

### 3.9.3. Consumer Taste Evaluation

The sensory portion of this study was performed in two separate sessions. Large consumer panels ( $n = 96$  and  $87$ , respectively) were used for evaluation. The participants were recruited using the University of Tennessee at Knoxville sensory consumer database, and each reported a healthy sense of smell and taste. All participants signed an informed consent form and were compensated for their time. This experiment was conducted according to the Declaration of Helsinki for studies on human subjects and approved by the University of Tennessee IRB review for research involving human subjects (IRB # 19-04998-XM).

Three samples were prepared for the consumer sensory evaluations: broth (warm-up), broth with thermally treated eHMP (eHMP), and broth with thermally treated eHMP and the aroma simulation model. The warm-up sample, unsalted chicken broth (2.5 L) combined with NaCl (6.0 g), was used as a baseline for the other two samples to be based off. For the eHMP sample, broth (4.75 L), NaCl (11.4 g), and eHMP (4.75 g) were combined and stirred until dissolved. For the



aroma simulation model, broth (4.75 L), NaCl (11.4 g), eHMP (4.75 g), and the aroma model (added at levels previously calculated) were combined and stirred until dissolved.

In the first sensory test, participants were asked to rate the taste attributes of chicken broths in a sequential monadic format (with and without the compounds of interest), using a visual analog scale (500 pixel wide) ranging from “None at all” to “Extremely high”. The taste attributes, salty, sweet, sour, bitter, and umami, were evaluated along with an overall flavor rating. Each sample was labeled with a random three-digit code and served in 60mL plastic cup at 50° C. For palate cleansing, participants were given water and carrots between samples. 25mL of each sample was provided per judgment.

In the second sensory test, the samples were evaluated using a 2 alternative forced choice (2-AFC) task, in which the panelists were asked to select the sample that was saltier. Each sample was labeled with a random three-digit code and served in 60mL plastic cup at 50° C. For palate cleansing, participants were given water and carrots between samples. 25mL of each sample was provided per judgment.

In a sequential monadic paradigm, the participants were asked to score overall flavor intensity and all five basic tastes (sweet, salty, bitter, umami, and sour) on a visual analog scale (500 pixel wide) ranging from “None at all” to “Extremely high”. In the discrimination task the participants were presented with broth containing eHMP and broth containing eHMP with the aroma model. Each participant was instructed to “taste the samples from left to right and select the sample that is saltier.” The presentation of the sample was randomized. The mean saltiness ratings were

compared using paired t-tests with a Bonferroni correction. The attribute rating data was analyzed using JMP 14.0 (SAS Institute, Cary, NC) and the 2-AFC data was analyzed using exact binomial test, comparing  $d'$  to zero in the sensR R package.

## 4. RESULTS AND DISCUSSION

### 4.1. First Consumer Sensory Panel

An initial screening of taste activity was performed for a baseline understanding of salt-enhancing properties of eHMP and eHMP + cys. Previous studies have shown that protein hydrolysates can enhance the perceived saltiness and overall flavor of foods.<sup>22</sup> Accordingly, thermally treated mushroom hydrolysates (with and without the addition of cysteine) were generated and screened for enhancement of perceived saltiness in a consumer sensory study. First, the mushrooms were lyophilized, ground into a fine powder, and enzymatically hydrolyzed. The resulting hydrolysate was filtered and split into two equal samples. One sample was thermally treated under kitchen-like cooking conditions for 4 hours (eHMP), and the second sample was mixed with cysteine (eHMP + cys) and thermally treated in the same manner as the eHMP. The concentrated samples were separately dissolved in low-sodium chicken broth and evaluated in a consumer sensory study to determine their effect on perceived saltiness enhancement. The results of the experiment showed that the eHMP sample had a higher saltiness rating than the control sample (broth alone). Interestingly, the broth containing eHMP + cys had a significantly higher mean saltiness rating as compared to the sample with only eHMP ( $t_8 = 2.300$ ,  $p = 0.0252$ , Figure 10). This suggests that the thermal treatment of the eHMP in the presence of cysteine (eHMP + cys) generated either tastants or odorants that further enhance the perceived saltiness of the broth. To test the hypothesis that odorants generated from the thermal treatment of eHMP in the presence of cysteine (eHMP + cys) were responsible for the increased perceived saltiness of the sample, the following series of experiments were conducted.

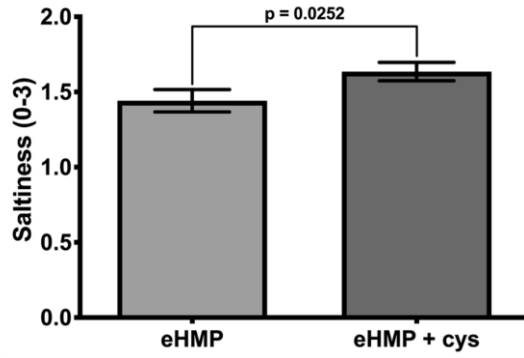


Figure 10: Consumer sensory data comparing eHMP and eHMP + cys saltiness ratings in chicken broth

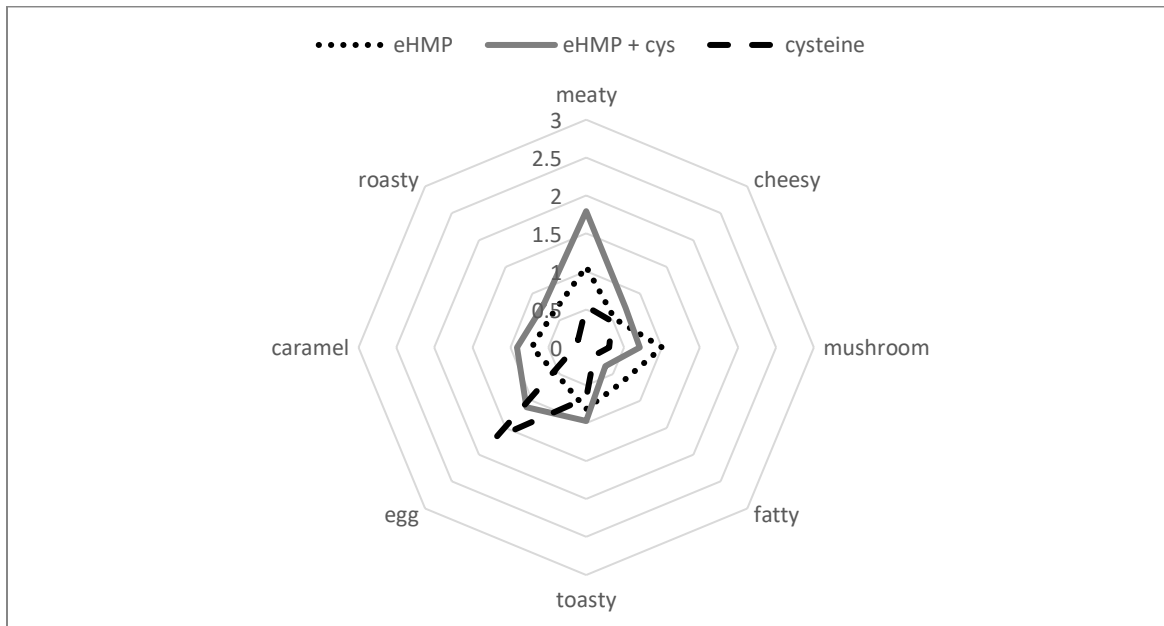


Figure 11: Olfactory-profile analysis of eHMP, cys, and eHMP + cys

#### 4.2. Olfactory-Profile Analysis of eHMP & eHMP + cys

The initial consumer sensory panel identified eHMP and eHMP + cys enhanced the perceived saltiness of a chicken broth at different levels. To determine if this difference was caused by the aroma, we performed olfactory-profile analyses of eHMP and eHMP + cys, along with a thermally treated sample of cysteine (no mushroom). Orthonasal olfactory-profile analysis of the samples was performed in water to determine overall odor quality. The first sample, eHMP, was described as having a caramel, mushroom, and toasty aroma, with a weak meaty character (Figure 11). The second sample, cysteine refluxed in water (alone) with no eHMP added, was described as having an egg-like smell. The third sample, eHMP + cys, was described as toasty and mushroom-like with a strong meaty character, higher than that of the eHMP. While neither eHMP nor the cysteine samples were perceived as meaty individually, the combined reaction flavor (eHMP + cys) was predominantly meaty. The results of the quantitative olfactory profile analysis suggest that the reaction between eHMP and cysteine is important to the formation of the meaty odorants detected in the sample.

#### 4.3. Identification of Odorants by GC-O & GC-MS

To identify the odorants contributing to the aroma character of eHMP and eHMP + cys, and which odorants drive a difference in odor quality, a comparative aroma extract dilution analysis (cAEDA) was performed. The samples were separately extracted with ether, nonvolatile compounds were removed by SAFE, and the distillates were collected. The distillates were then concentrated on a Vigreux column, followed by a gentle stream of nitrogen, prior to GC-O analysis. The aroma isolates were serially diluted (1:2 by vol.) with freshly distilled diethyl ether. The samples were then submitted to a cAEDA,<sup>29, 30</sup> which led to the identification of 36 odorants (Table 2). To assign

Table 2: Odorants identified in eHMP and eHMP + cys

no. <sup>a</sup>	odorant <sup>b</sup>	odor quality <sup>c</sup>	RI <sup>d</sup>		FD <sup>e</sup> factor	
			FFAP	DB-5	eHMP	eHMP + cys
1	2- and 3-methylbutanal	malty	930	668	1	
2	butane-2,3-dione	buttery	985	<600	1	
3	hexanal	green	1085	802	1	1
4	1-octen-3-one	mushroom	1295	975	4	4
5	2-acetyl-1-pyrroline	roasty	1322	920	16	
6	3-sulfanylpentan-2-one	catty	1347	907		16
7	dimethyl trisulfide	sulfurous	1365	968	4	
8	1-(2-furyl)ethanethiol	meaty	1396	951		16
9	2-furfurylthiol	coffee	1431	909		64
10	acetic acid	vinegar	1439	600	4	4
11	3-(methylsulfanyl)propanal	cooked potato	1443	902	256	256
12	2-ethyl-3,5-dimethylpyrazine	earthy	1450	1095	4	1
13	2,3- diethyl-5-methylpyrazine	earthy	1480	1158	4	1
14	(2E)-non-2-enal	green	1530	1161	4	1
15	2-methylpropanoic acid	sweaty, rancid	1565	1215	1	1
16	butanoic acid	sweaty, rancid	1610	820	16	16
17	2-methyl-3-(methyldithio)furan	meaty	1615	1184		16
18	2-acetylthiazole	roasty	1624	1018	64	16
19	2-phenylacetaldehyde	floral, honey	1640	1045	64	
20	2- and 3-methylbutanoic acid	sweaty, rancid	1660	885	256	256
21	(2E,4E)-2,4-nonadienal	fatty	1697	1212	4	4
22	3-methylnonane-2,4-dione	hay-like	1715	1246	1	4
23	2-acetyl-2-thiazoline	roasty	1743	1106	16	16
24	pentanoic acid	sweaty, rancid	1731	904	1	1
25	hexanoic acid	sweaty, rancid	1840	1085	4	4
26	2-methoxyphenol	smoky	1860	1187	4	1
27	trans-4,5-epoxy-(2E)-2-decenal	metallic	1989	1380	4	1
28	HDMF	caramel	2006	1080	64	4
29	<i>p</i> -cresol	barnyard	2063	1072	4	64
30	4-allyl-2-methoxyphenol	clove	2142	1359	1	1
31	sotolon	maple	2171	1135	64	256
32	2-amino acetophenone	foxy	2222	1260	64	64
33	5-ethyl-3-hydroxy-4-methyl-(5H)-furan-2-one	maple	2238	1184	16	16
34	indole	animal	2446	1288	16	64
35	phenylacetic acid	honey	2570	1262	16	64
36	4-hydroxy-3-methoxybenzaldehyde	vanilla	2600	1411	64	64

<sup>a</sup>Odorants were numbered according to their retention time on the FFAP column. <sup>b</sup>Identified by comparing the retention indices on the FFAP and DB-5 column, the mass spectra, as well as aroma quality and intensity with data obtained from authentic reference standards analyzed in parallel. <sup>c</sup>Odor quality as perceived during GC-O. <sup>d</sup>RI = linear retention index. <sup>e</sup>FD factor = flavor dilution factor.

the structures of the odorants, their RIs, odor characteristics, and mass spectra were compared to data obtained from reference standards.

#### 4.3.1. FD Chromatograms of eHMP

AEDA was performed for every other FD from FD 1 to FD 256. The odorants, along with the highest FD they were detected at, were plotted in an FD chromatogram (Figure 13). Only 2 odorants were detected at the highest FD, 256: 3-(methylsulfanyl)propanal (**11**, cooked potato) and 2- and 3-methylbutanoic acid (**20**, sweaty, rancid). The structures of these compounds are provided in Figure 12.

The next highest FD tested, FD 64, contained 6 other odorants: 2-acetylthiazole (**18**, roasty), 2-phenylacetaldehyde (**19**, floral, honey), HDMF (**28**, caramel), sotolon (**31**, maple), 2-aminoacetophenone (**32**, foxy), and 4-hydroxy-3-methoxybenzaldehyde (**36**, vanilla) (Figure 14). The olfactory-profile analysis of the eHMP sample was characterized as roasted, caramelized mushroom (Figure 11). The roasty character is likely due in part to the presence of **18**. Additionally, **28** and **31** are common odorants found in food, and they often impart a cooked, caramel and maple flavor to foods.

Six more odorants were detected at FD 16: 2-acetyl-1-pyrroline (**5**, roasty), butanoic acid (**16**, sweaty, rancid), 2-acetyl-2-thiazoline (**23**, roasty), 5-ethyl-3-hydroxy-4-methyl-(5H)-furan-2-one (**33**, maple), indole (**34**, animal), and phenylacetic acid (**35**, honey) (Figure 15). Along with **18**, **5** and **23** are likely sources of the roast character that was prevalent in the olfactory-profile analysis of the eHMP. Despite high FDs for **16** and **20**, eHMP did not rate highly in cheese character,

suggesting these odorants do not significantly contribute to the overall aroma. These are likely products of the maillard reaction, as **5**, **16**, **23**, **35**, **4**, **10**, and **13** were previously detected in cooked mushrooms.<sup>4</sup>

1-octen-3-one (**4**, mushroom), dimethyl trisulfide (**7**, sulfurous), acetic acid (**10**, vinegar), 2-ethyl-3,5-dimethylpyrazine (**12**, earthy), 2,3-diethyl-5-methylpyrazine (**13**, earthy), (2*E*)-non-2-enal (**14**, green), (2*E*, 4*E*)-2,4-nona-2,4-dienal (**21**, green), hexanoic acid (**25**, sweaty, rancid), 2-methoxyphenol (**26**, smoky), trans-4,5-epoxy-(2*E*)-decenal (**27**, metallic), and *p*-cresol (**29**, barnyard) were all detected at FD 4 (Figure 16).

2- and 3-Methylbutanal (**1**, malty), butane-2,3-dione (**2**, buttery), hexanal (**3**, green), 2-methylpropanoic acid (**15**, sweaty, rancid), 3-methylnonan-2,4-dione (**22**, hay-like), pentanoic acid (**24**, sweaty, rancid), and 4-allyl-2-methoxyphenol (**30**, clove) were all weakly detected at FD 1 (Figure 17).

#### 4.3.2. FD Chromatograms of eHMP + cys

Like the AEDA for eHMP, every other FD of the eHMP + cys sample was analyzed, from FD 1 to FD 256. The odorants, along with the highest FD they were detected at, were plotted on an FD chromatogram (Figure 18). 3 odorants were detected at FD 256: 3-(methylsulfanyl)propanal (**11**, cooked potato), 2- and 3-methylbutanoic acid (**20**, sweaty, rancid), and sotolon (**31**, maple) (Figure 19).



Six more odorants were detected at FD 64: 2-furfurylthiol (**9**, coffee), *p*-cresol (**29**, barnyard), 2-aminoacetophenone (**32**, foxy), indole (**34**, animal), phenylacetic acid (**35**, honey), and 4-hydroxy-3-methoxybenzaldehyde (**36**, vanilla) (Figure 20). The olfactory-profile analysis of the eHMP + cys sample is consistent with high levels of **9**, which is a common odorant found in roasted meat. Furthermore, **9** was not detected in the eHMP sample at any FD. **29**, **32**, and **34** are also associated with meaty aromas, and are likely contributors to the meat-like aroma of eHMP + cys.

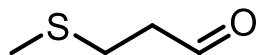
Seven additional odorants were detected at FD 16: 3-sulfanylpentan-2-one (**6**, catty), 1-(2-furyl)ethanethiol (**8**, meaty), butanoic acid (**16**, sweaty, rancid), 2-methyl-3-(methylthio)furan (**17**, meaty), 2-acetylthiazole (**18**, roasty), 2-acetyl-2-thiazoline (**23**, roasty), and 5-ethyl-3-hydroxy-4-methyl-(5H)-furan-2-one (**33**, maple) (Figure 21).

1-Octen-3-one (**4**, mushroom), acetic acid (**10**, vinegar), (2*E*, 4*E*)-2,4-nona-2,4-dienal (**21**, green), 3-methylnonan-2,4-dione (**22**, hay-like), hexanoic acid (**25**, sweaty, rancid), and HDMF (**28**, caramel) were all detected at FD 4 (Figure 22).

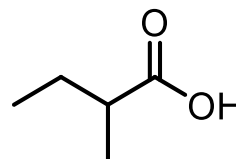
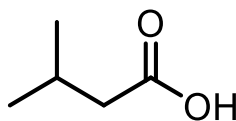
Figure 23 lists the odorants detected at FD 1 in eHMP + cys: Hexanal (**3**, green), 2-ethyl-3,5-dimethylpyrazine (**12**, earthy), 2,3-diethyl-5-methylpyrazine (**13**, earthy), (2*E*)-non-2-enal (**14**, green), 2-methylpropanoic acid (**15**, sweaty, rancid), pentanoic acid (**24**, sweaty, rancid), 2-methoxyphenol (**26**, smoky), trans-4,5-epoxy-(2*E*)-decenal (**27**, metallic), and 4-allyl-2-methoxyphenol (**30**, clove).

Table 3: List of odorants detected at FD 256 in eHMP

no.	odorant	odor quality	RI		
			FFAP	DB-5	FD Factor
11	3-(methylsulfanyl)propanal	cooked potato	1443	902	256
20	2- and 3-methylbutanoic acid	sweaty, rancid	1660	885	256



cooked potato, **11**



sweaty, rancid, **20**

Figure 12: Structures of odorants detected at FD 256 in eHMP

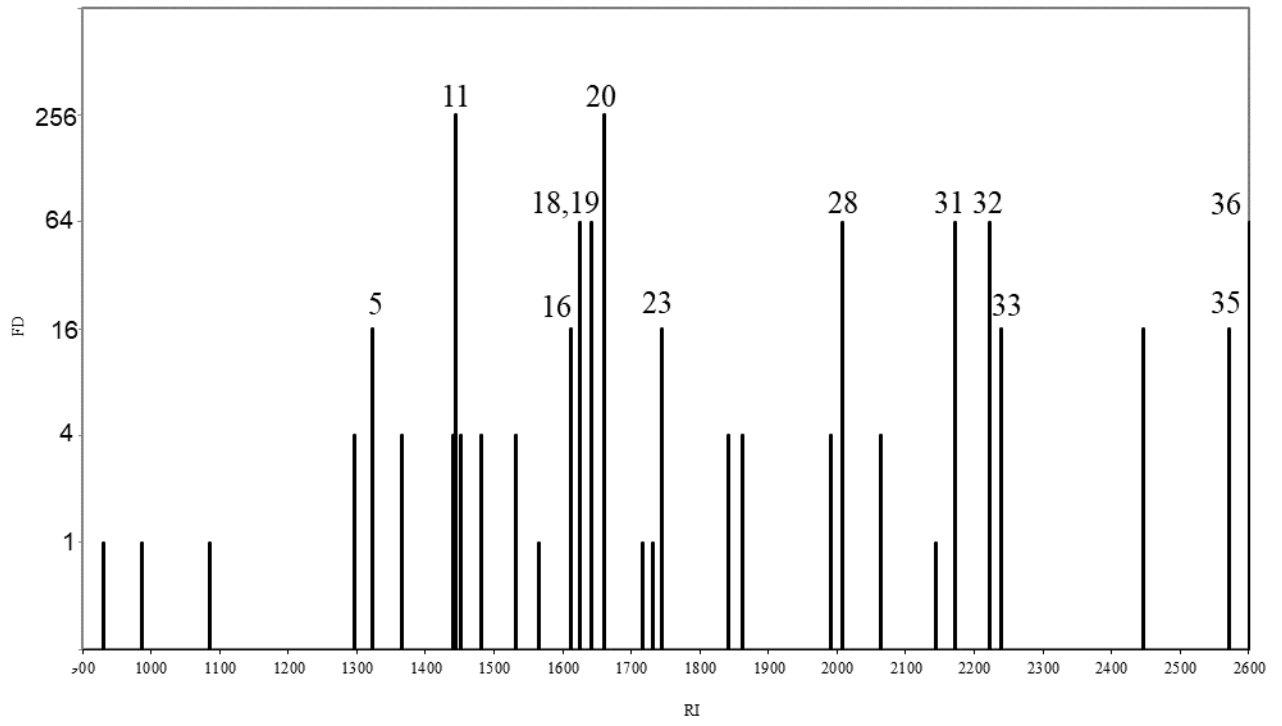
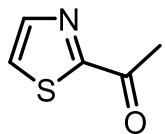


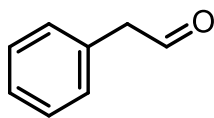
Figure 13: FD chromatogram of eHMP

Table 4: List of odorants detected at FD 64 in eHMP

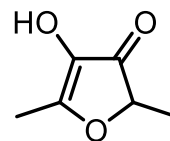
no.	odorant	odor quality	RI		FD Factor
			FFAP	DB-5	
18	2-acetylthiazole	roasty	1624	1018	64
19	2-phenylacetaldehyde	floral, honey	1640	1045	64
28	HDMF	caramel	2006	1080	64
31	sotolon	maple	2171	1135	64
32	2-amino acetophenone	foxy	2222	1260	64
36	4-hydroxy-3-methoxybenzaldehyde	vanilla	2600	1411	64



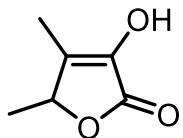
roasty, **18**



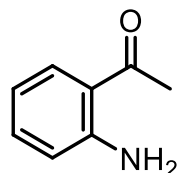
floral, honey, **19**



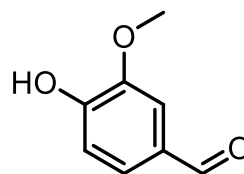
caramel, **28**



maple, **31**



foxy, **32**

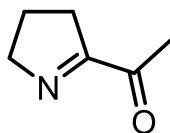


vanilla, **36**

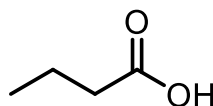
Figure 14: Structures of odorants detected at FD 64 in eHMP

Table 5: List of odorants detected at FD 16 in eHMP

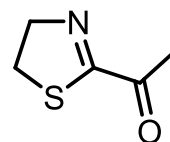
no.	odorant	odor quality	RI		FD Factor
			FFAP	DB-5	
5	2-acetyl-1-pyrroline	roasty	1322	920	16
16	butanoic acid	sweaty, rancid	1610	820	16
23	2-acetyl-2-thiazoline	roasty	1743	1106	16
33	5-ethyl-3-hydroxy-4-methyl-(5H)-furan-2-one	maple	2238	1184	16
34	indole	animal	2446	1288	16
35	phenylacetic acid	honey	2570	1262	16



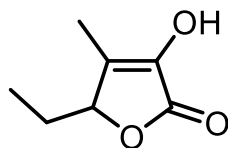
roasty, **5**



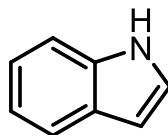
sweaty, rancid, **16**



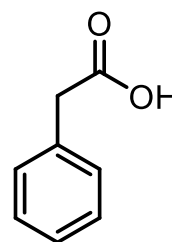
roasty, **23**



maple, **33**



animal, **34**



honey, **35**

Figure 15: Structures of odorants detected at FD 16 in eHMP

Table 6: List of odorants detected at FD 4 in eHMP

no.	odorant	odor quality	RI		
			FFAP	DB-5	FD Factor
4	1-octen-3-one	mushroom	1295	975	4
7	dimethyl trisulfide	sulfurous	1365	968	4
10	acetic acid	vinegar	1439	600	4
12	2-ethyl-3,5-dimethylpyrazine	earthy	1450	1095	4
13	2,3- diethyl-5-methylpyrazine	earthy	1480	1158	4
14	(2E)-non-2-enal	green	1530	1161	4
21	(2E, 4E)-2,4-nonadienal	fatty	1697	1212	4
25	hexanoic acid	sweaty, rancid	1840	1085	4
26	2-methoxyphenol	smoky	1860	1187	4
27	trans-4,5-epoxy-(2E)-2-decenal	metallic	1989	1380	4
29	p-cresol	barnyard	2063	1072	4

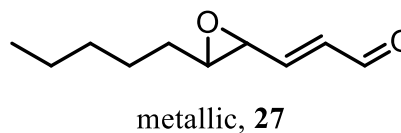
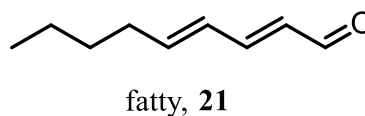
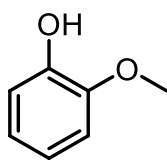
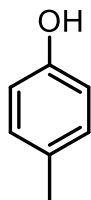
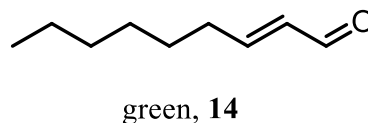
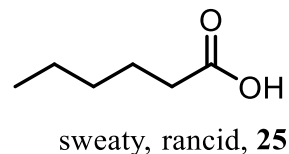
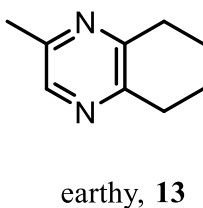
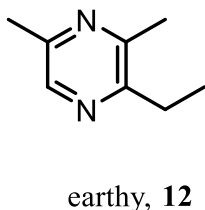
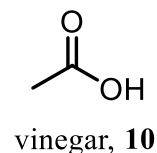
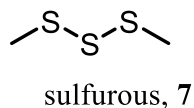
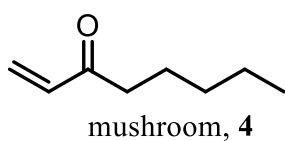


Figure 16: Structures of odorants detected at FD 4 in eHMP

Table 7: List of odorants detected at FD 1 in eHMP

no.	odorant	odor quality	RI		FD Factor
			FFAP	DB-5	
1	2- and 3-methylbutanal	malty	930	668	1
2	butane-2,3-dione	buttery	985	<600	1
3	hexanal	green	1085	802	1
15	2-methylpropanoic acid	sweaty, rancid	1565	1215	1
22	3-methylnonane-2,4-dione	hay-like	1715	1246	1
24	pentanoic acid	sweaty, rancid	1731	904	1
30	4-allyl-2-methoxyphenol	clove	2142	1359	1

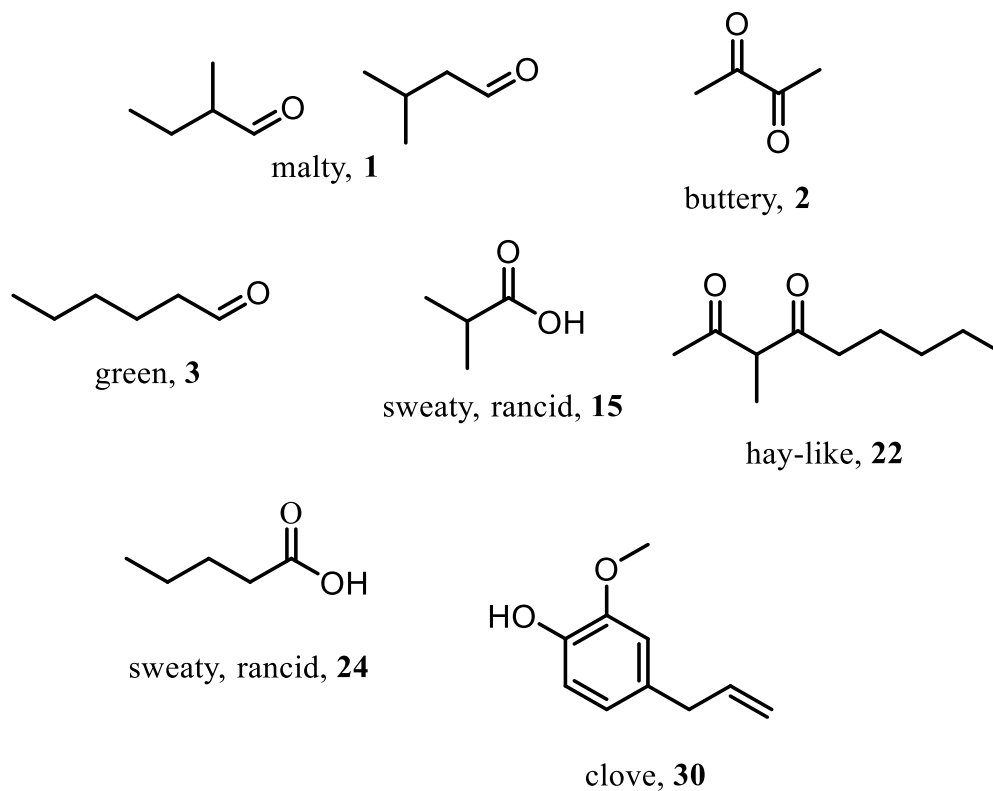


Figure 17: Structures of odorants detected at FD 1 in eHMP

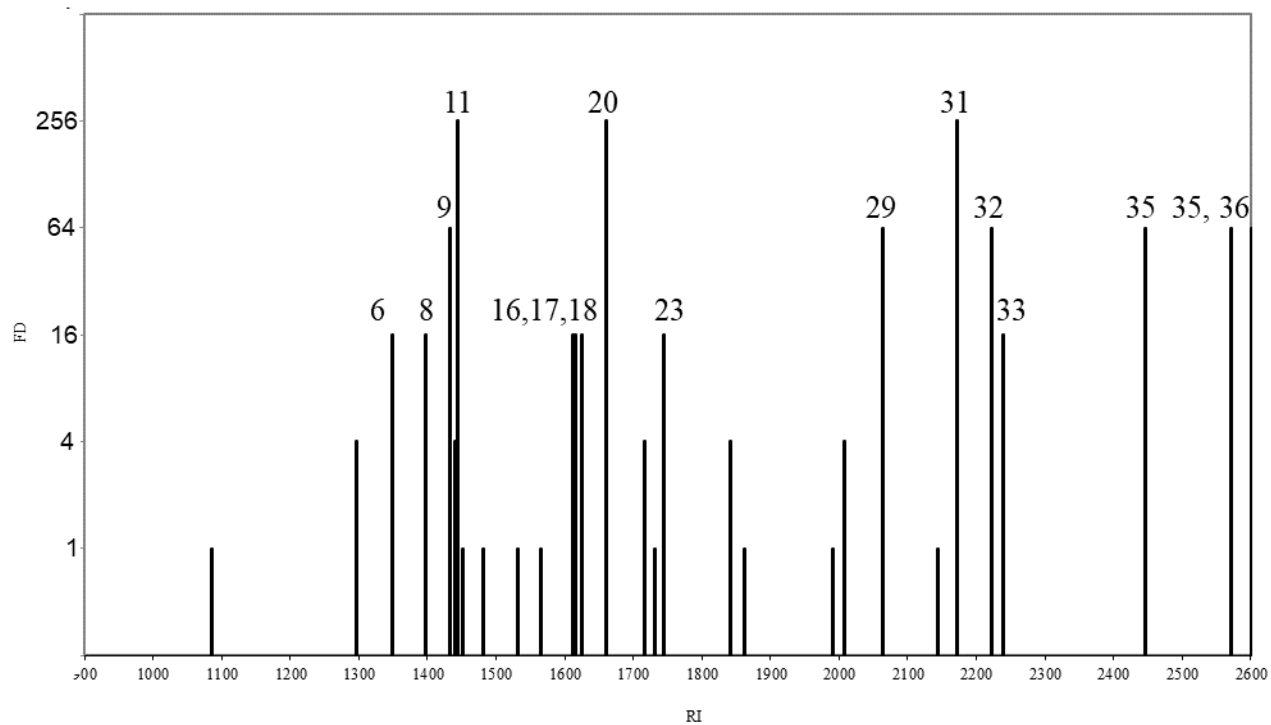
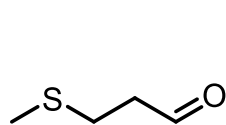


Figure 18: FD chromatogram of eHMP + cys

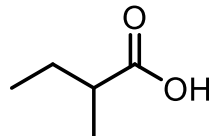
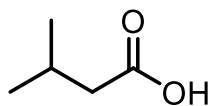


Table 8: List of odorants detected at FD 256 in eHMP + cys

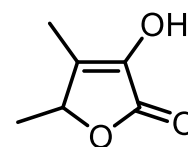
no.	odorant	odor quality	RI		FD Factor
			FFAP	DB-5	
11	3-(methylsulfanyl)propanal	cooked potato	1443	902	256
20	2- and 3-methylbutanoic acid	sweaty, rancid	1660	885	256
31	sotolon	maple	2171	1135	256



cooked potato, **11**



sweaty, rancid, **20**



maple, **31**

Figure 19: Structures of odorants detected at FD 256 in eHMP + cys

Table 9: List of odorants detected at FD 64 in eHMP + cys

no.	odorant	odor quality	RI		FD Factor
			FFAP	DB-5	
9	2-furfurylthiol	coffee	1431	909	64
29	<i>p</i> -cresol	barnyard	2063	1072	64
32	2-amino acetophenone	foxy	2222	1260	64
34	indole	animal	2446	1288	64
35	phenylacetic acid	honey	2570	1262	64
36	4-hydroxy-3-methoxybenzaldehyde	vanilla	2600	1411	64

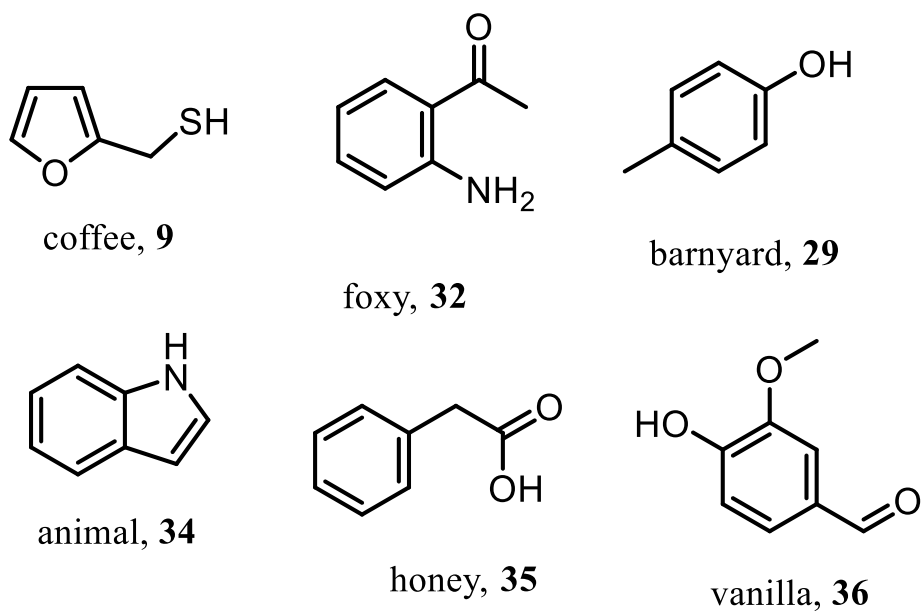
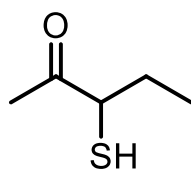


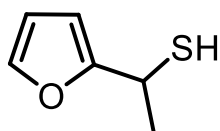
Figure 20: Structures of odorants detected at FD 64 in eHMP + cys

Table 10: List of odorants detected at FD 16 in eHMP + cys

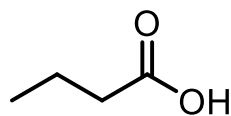
no.	odorant	odor quality	RI		FD Factor
			FFAP	DB-5	
6	3-sulfanylpentan-2-one	catty	1347	907	16
8	1-(2-furyl)ethanethiol	meaty	1396	951	16
16	butanoic acid	sweaty, rancid	1610	820	16
17	2-methyl-3-(methylthio)furan	meaty	1615	1184	16
18	2-acetylthiazole	roasty	1624	1018	16
23	2-acetyl-2-thiazoline	roasty	1743	1106	16
33	5-ethyl-3-hydroxy-4-methyl-(5H)-furan-2-one	maple	2238	1184	16



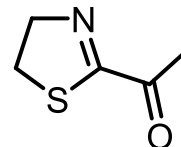
catty, **6**



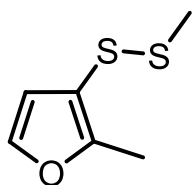
meaty, **8**



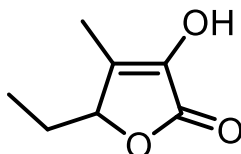
sweaty, rancid, **16**



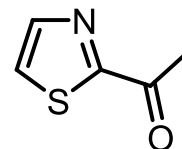
roasty, **23**



meaty, **17**



maple, **33**



roasty, **18**

Figure 21: Structures of odorants detected at FD 16 in eHMP + cys

Table 11: List of odorants detected at FD 4 in eHMP + cys

no.	odorant	odor quality	RI		
			FFAP	DB-5	FD Factor
4	1-octen-3-one	mushroom	1295	975	4
10	acetic acid	vinegar	1439	600	4
21	(2E, 4E)-2,4-nonadienal	fatty	1697	1212	4
22	3-methylnonane-2,4-dione	hay-like	1715	1246	4
25	hexanoic acid	sweaty, rancid	1840	1085	4
28	HDMF	caramel	2006	1080	4

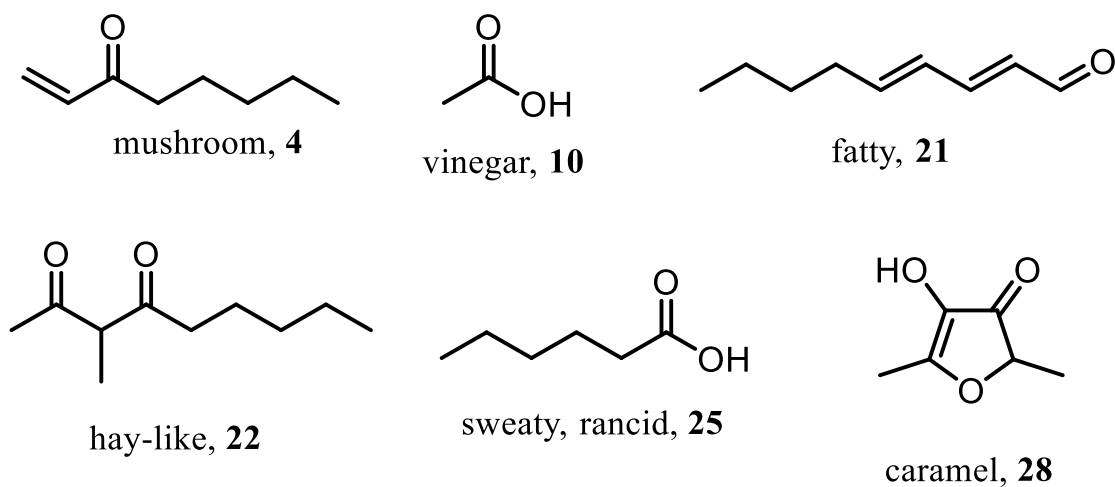
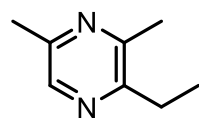


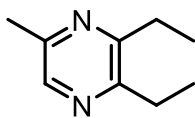
Figure 22: Structures of odorants detected at FD 4 in eHMP + cys

Table 12: List of odorants detected at FD 1 in eHMP + cys

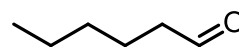
no.	odorant	odor quality	RI		FD Factor
			FFAP	DB-5	
3	hexanal	green	1085	802	1
12	2-ethyl-3,5-dimethylpyrazine	earthy	1450	1095	1
13	2,3- diethyl-5-methylpyrazine	earthy	1480	1158	1
14	(2E)-non-2-enal	green	1530	1161	1
15	2-methylpropanoic acid	sweaty, rancid	1565	1215	1
24	pentanoic acid	sweaty, rancid	1731	904	1
26	2-methoxyphenol	smoky	1860	1187	1
27	trans-4,5-epoxy-(2E)-2-decenal	metallic	1989	1380	1
30	4-allyl-2-methoxyphenol	clove	2142	1359	1



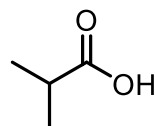
earthy, 12



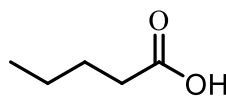
earthy, 13



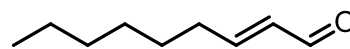
green, 3



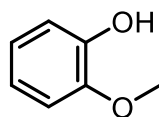
sweaty, rancid, 15



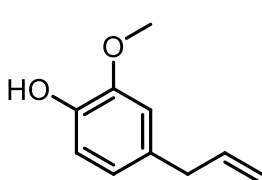
sweaty, rancid, 24



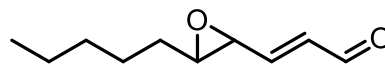
green, 14



smoky, 26



clove, 30



metallic, 27

Figure 23: Structures of odorants detected at FD 1 in eHMP + cys

#### 4.3.3. Comparison of Odorants in eHMP & eHMP + cys by cAEDA

Comparing the FDs of odorants differentially present in eHMP, as compared to eHMP + cys, suggests which compounds are most likely responsible for the high meat-like aroma of the eHMP + cys. The sulfur-containing odorants **6**, **8**, **9**, and **17** were detected at  $FD \geq 16$  in eHMP + cys, but none were detected in the eHMP sample. Odorants **22**, **29**, **31**, **34**, and **35** were present in the eHMP sample; however, they were detected at higher FDs in the eHMP + cys sample, suggesting that they may also play a role in the sample's meat-like aroma (Figure 24).

The odorants **1**, **2**, **5**, **7**, and **19** were detected in eHMP, but not detected in eHMP + cys. Additionally, **12**, **13**, **14**, **18**, **19**, and **28** were all detected at higher FDs in eHMP, suggesting that they were driven off, degraded, or are possible precursors to other compounds. Several odorants,

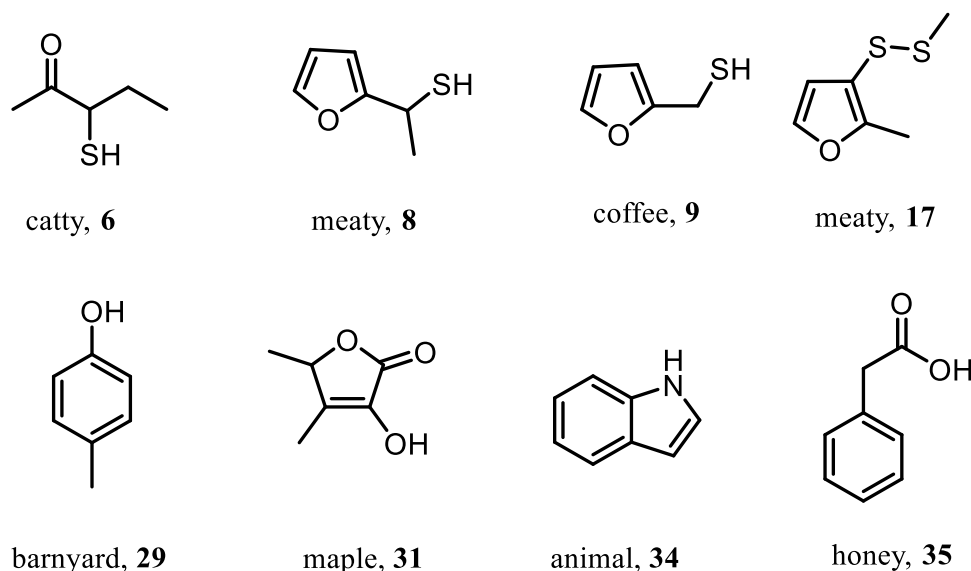


Figure 24: Odorants detected at a higher FD in eHMP + cys compared to eHMP

including 1-octen-3-one (**4**, mushroom), **11**, **16**, **20**, **23**, **32**, and **36**, were detected at similar FDs between both samples, suggesting that their impact on the unique meat-like aroma of eHMP + cys, as compared to eHMP, is minimal.

#### 4.4. Quantitation of Odorants

Due to the complex food matrix of sugars and proteins, an exhaustive extraction of the odorants was difficult. To determine the effect of each odorant on the overall aroma of the two samples, stable isotope dilution assay (SIDA) was conducted and odor activity values (OAVs) were calculated. Sixteen odorants were selected, based on the results of the cAEDA, and quantitated by SIDA (Table 2). Concentrations were determined and OAVs were then calculated for each odorant.

The eHMP sample was prepared as before, and the labeled odorants were added to the sample at known concentrations and amounts prior to solvent extraction. The high vacuum SAFE distillation was performed, and the samples were concentrated and, then, analyzed by GC-MS. The concentration and OAV of each odorant were then calculated. Total ion chromatograms for eHMP and eHMP + cys are provided in Figures 25 & 26. The mass spectra for each odorant, which were used for identification of the odorants of interest, and the corresponding mass spectra of the isotopes used for quantitation, are provided in Figures 27-42.

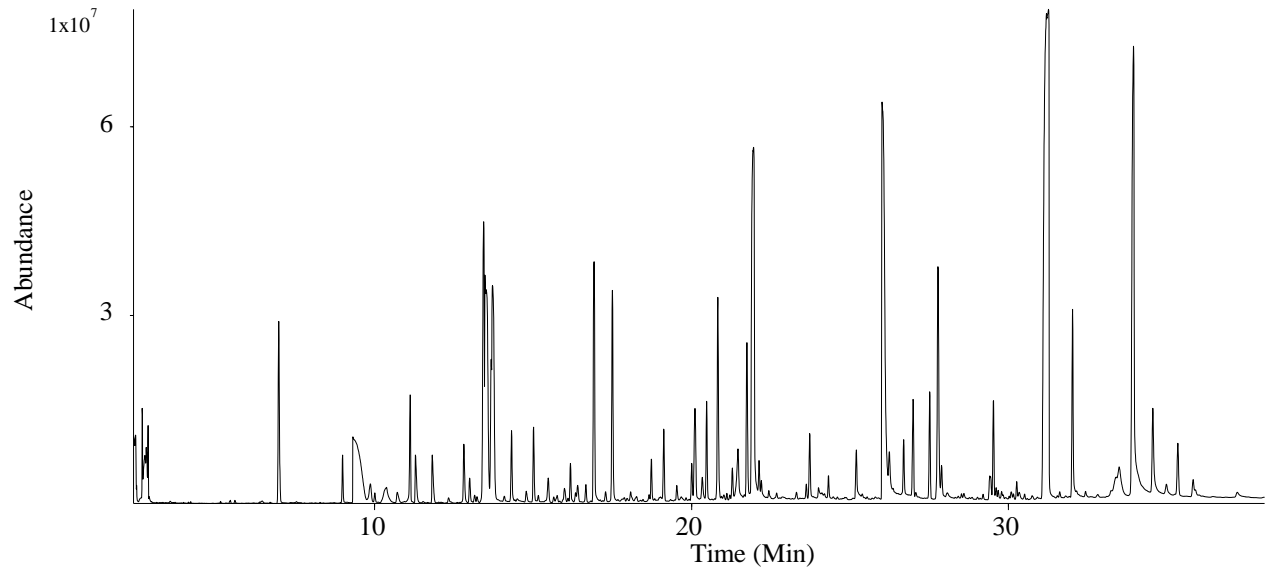


*Figure 25: Total ion chromatogram of eHMP*



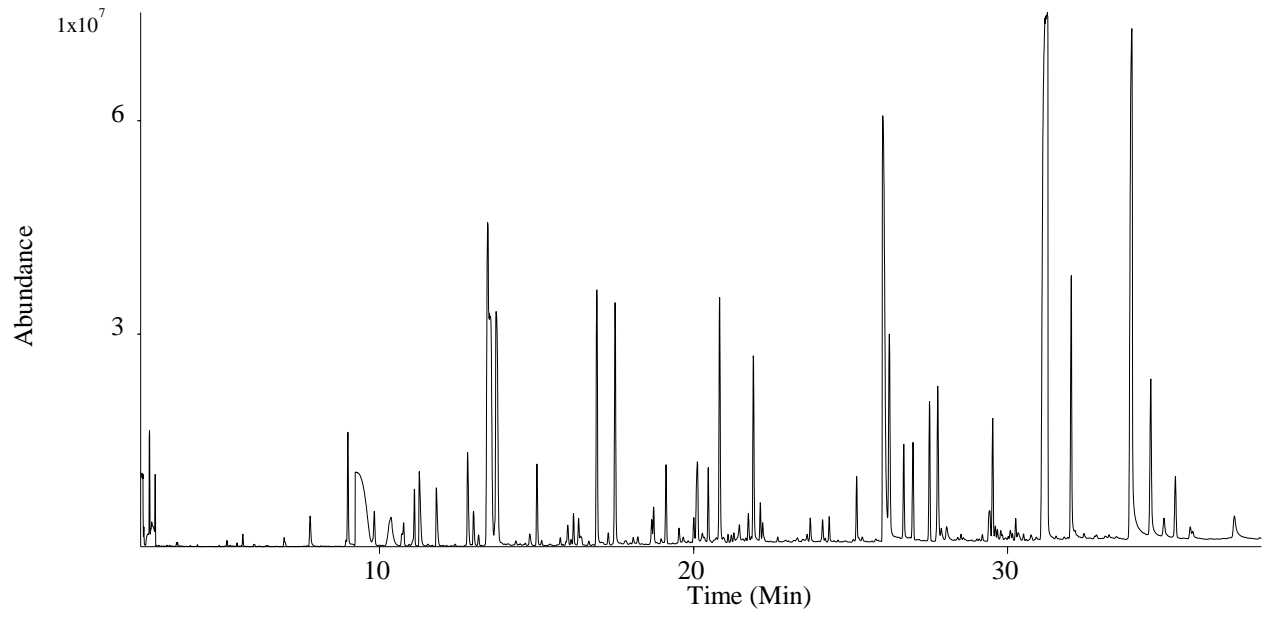


Figure 26: Total ion chromatogram of eHMP + cys

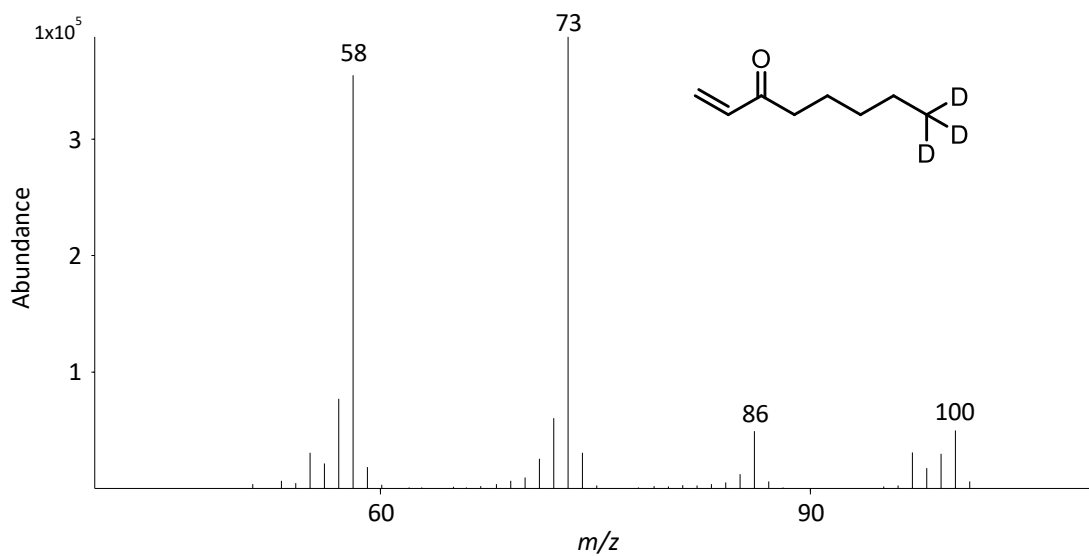
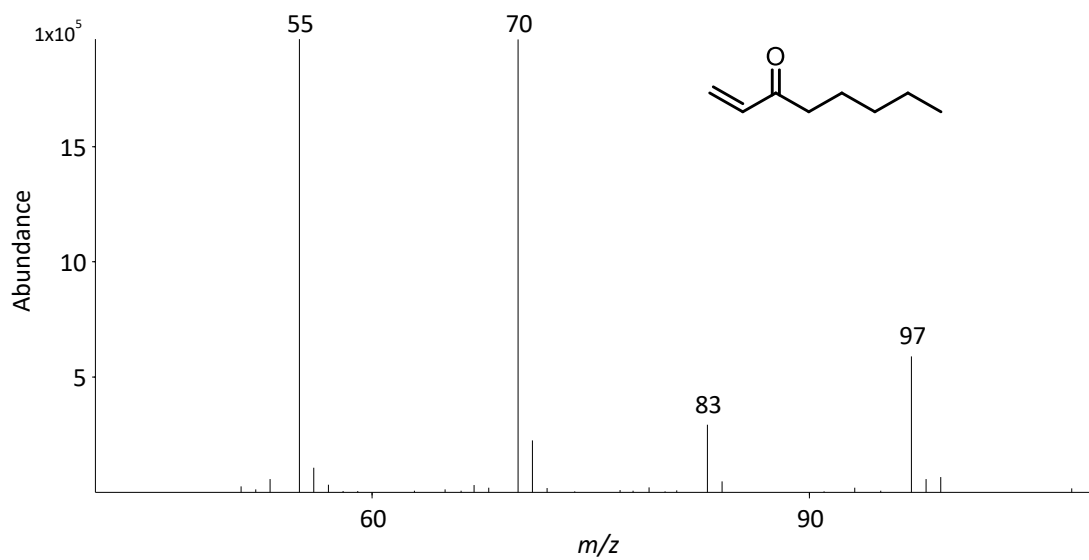


Figure 27: Mass spectra for 1-octen-3-one and 1-octen-3-one- $d_3$

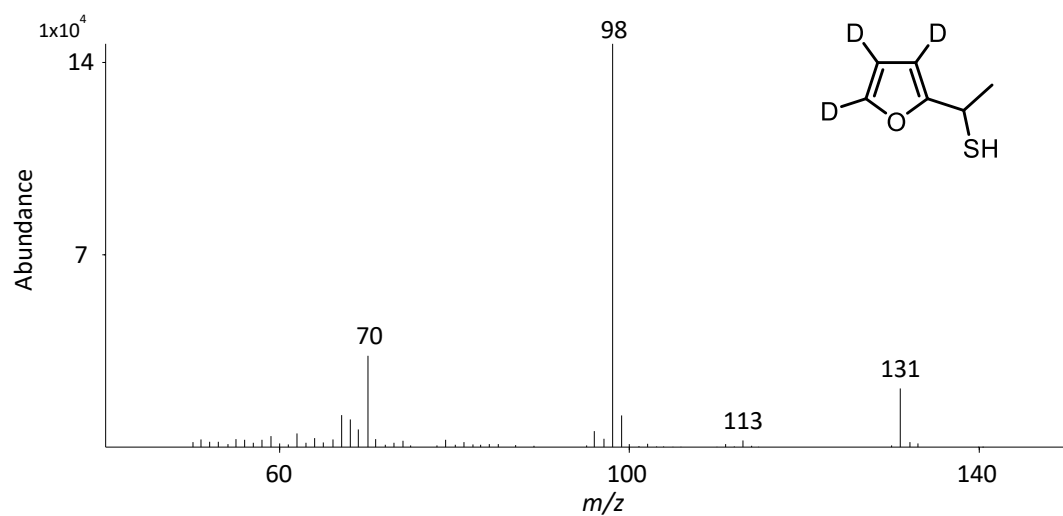
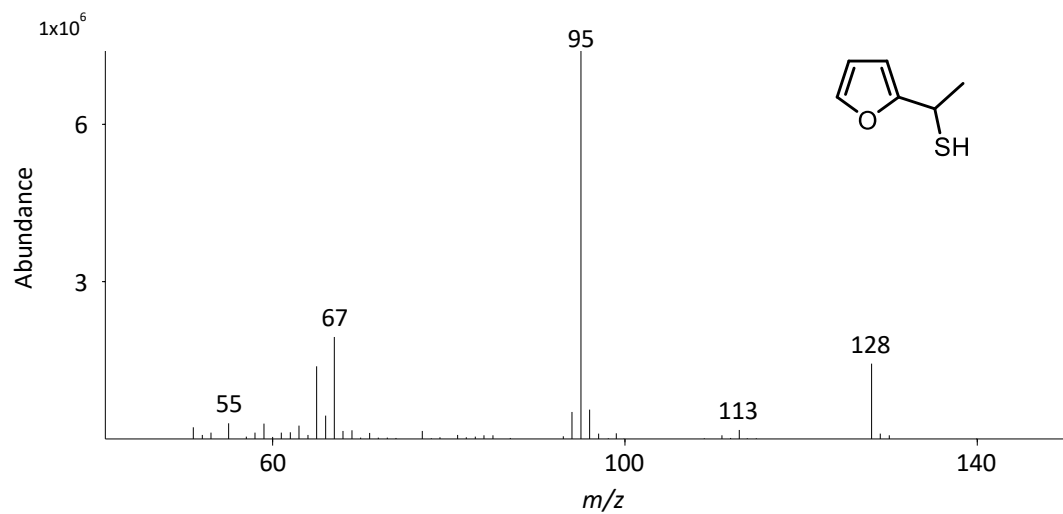


Figure 28: Mass spectra for 1-(2-furyl)ethanethiol and 1-(2-furyl)ethanethiol- $d_3$

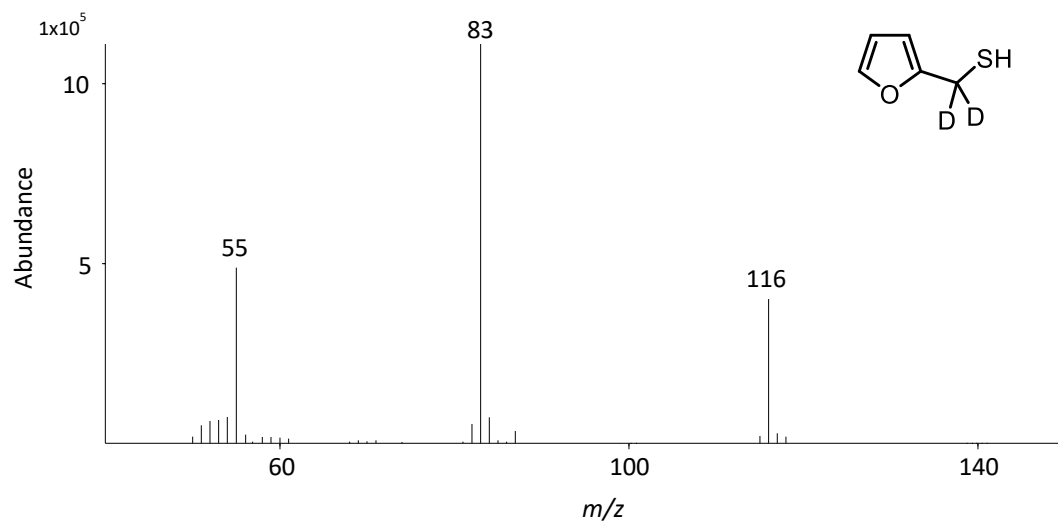
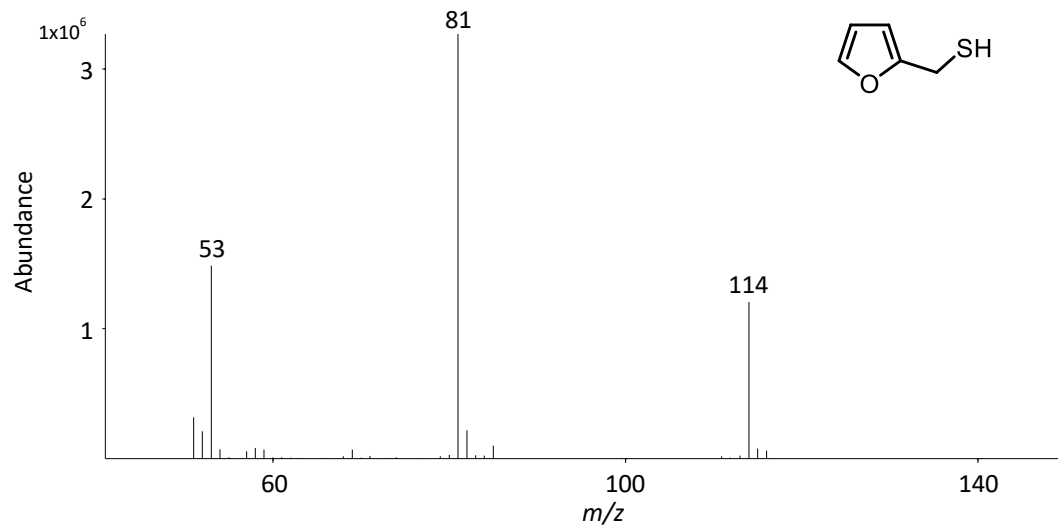


Figure 29: Mass spectra for 2-furfurylthiol and 2-furfurylthiol- $d_2$

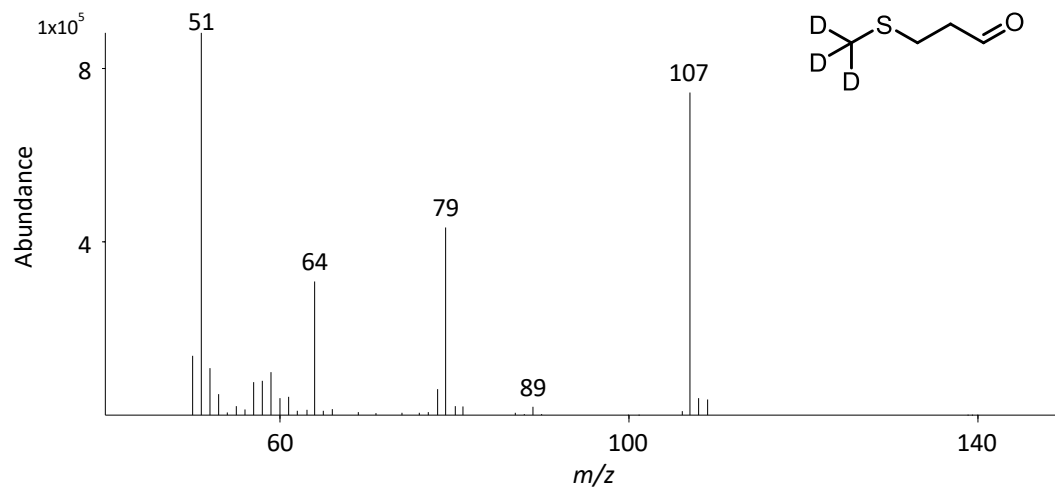
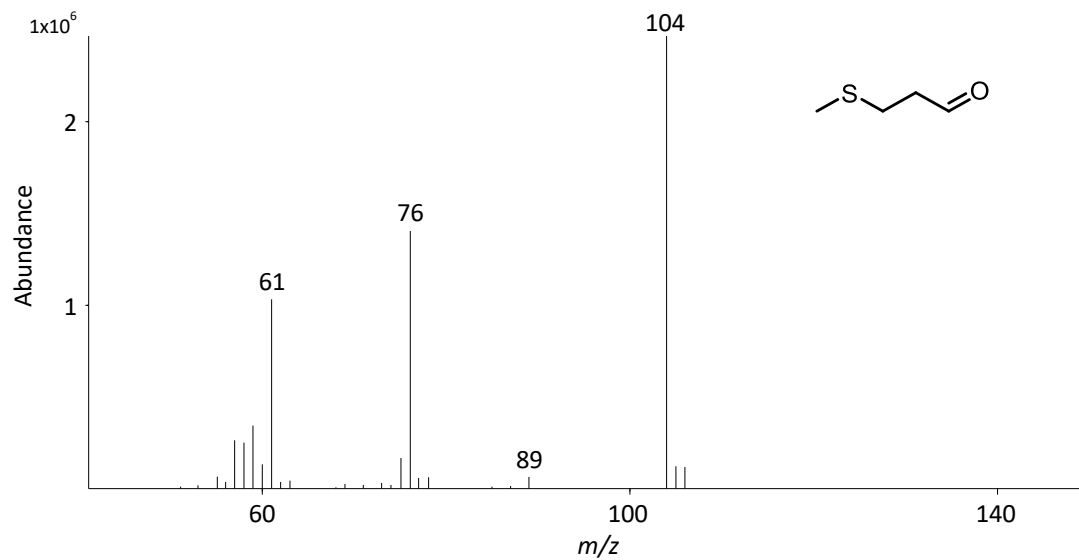


Figure 30: Mass spectra for 3-(methylsulfanyl)propanal and 3-(methylsulfanyl)propanal- $d_3$

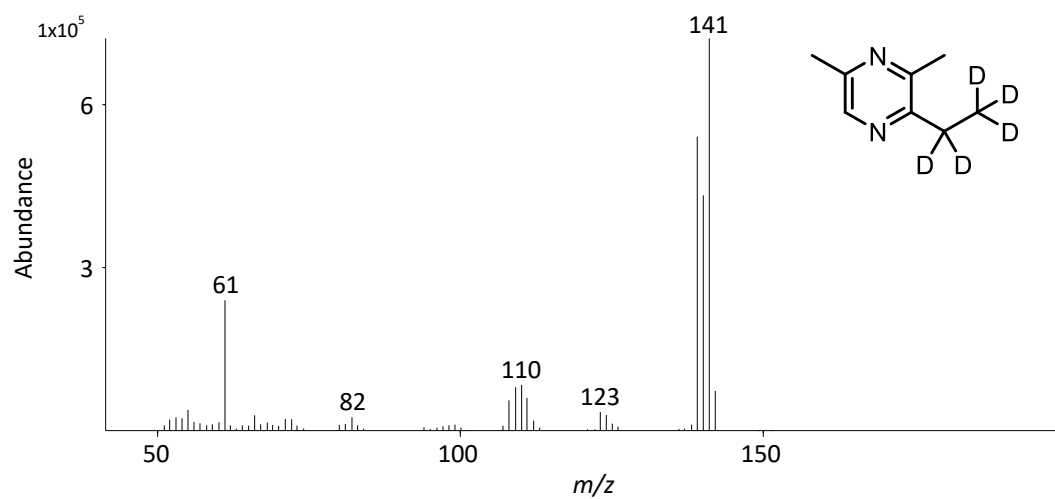
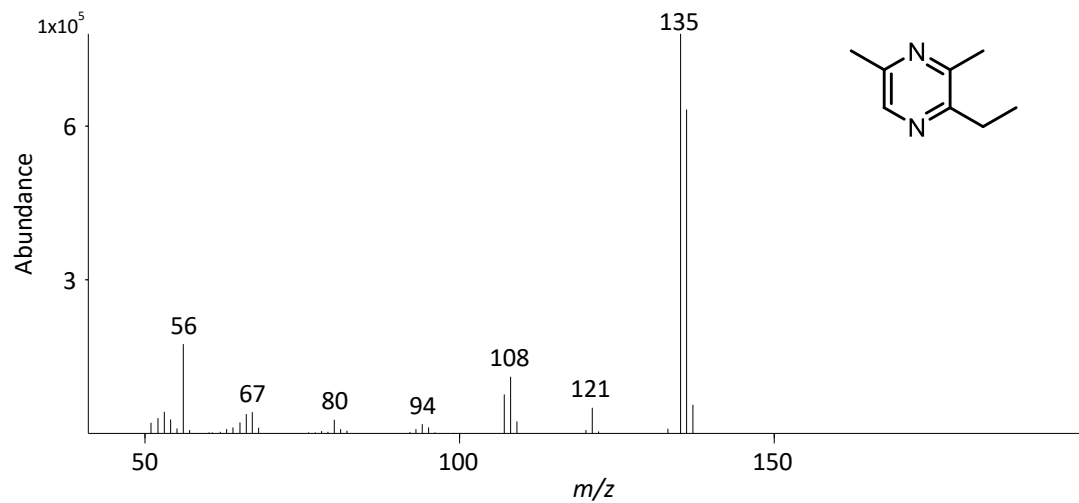


Figure 31: Mass spectra of 2-ethyl-3,5-dimethylpyrazine and 2-ethyl- $d_5$ -3,5-dimethylpyrazine

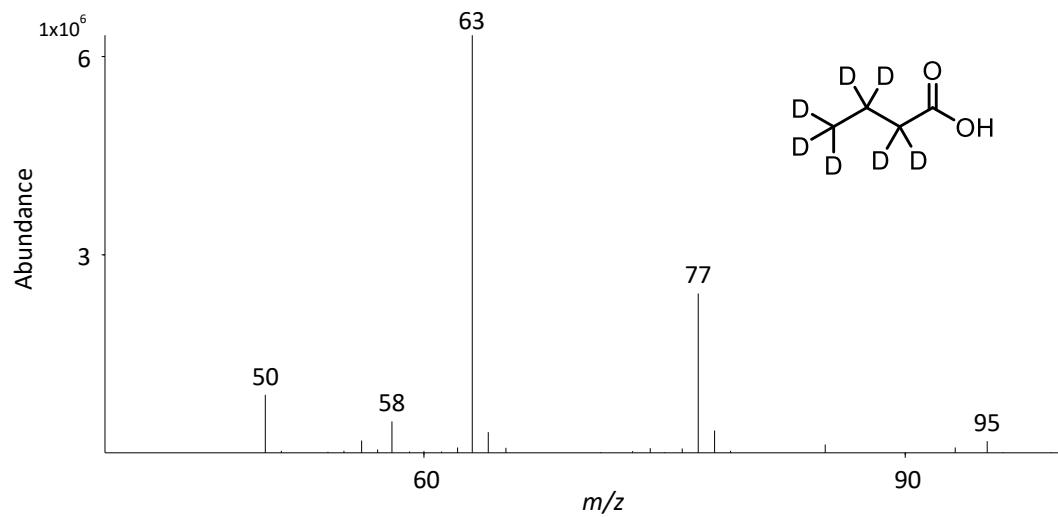
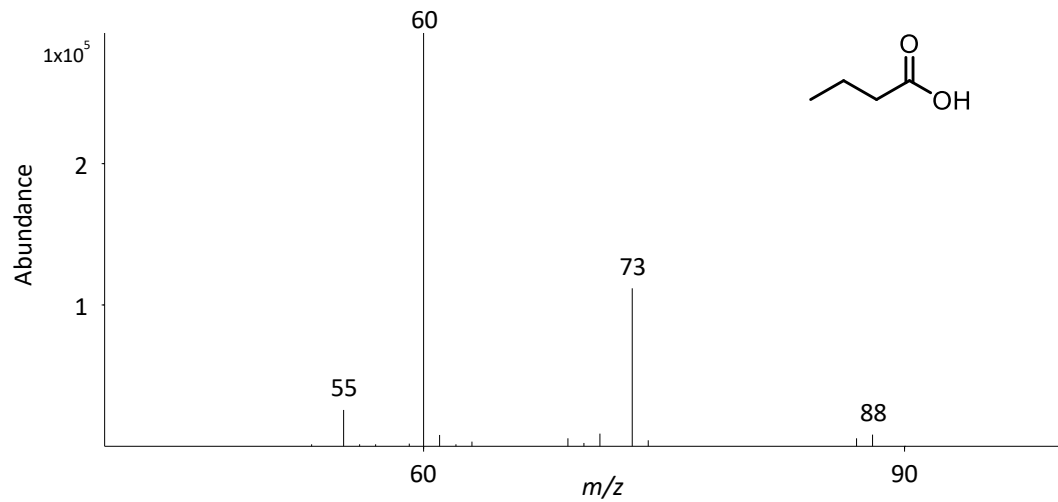


Figure 32: Mass spectra of butanoic acid and butanoic acid- $d_7$

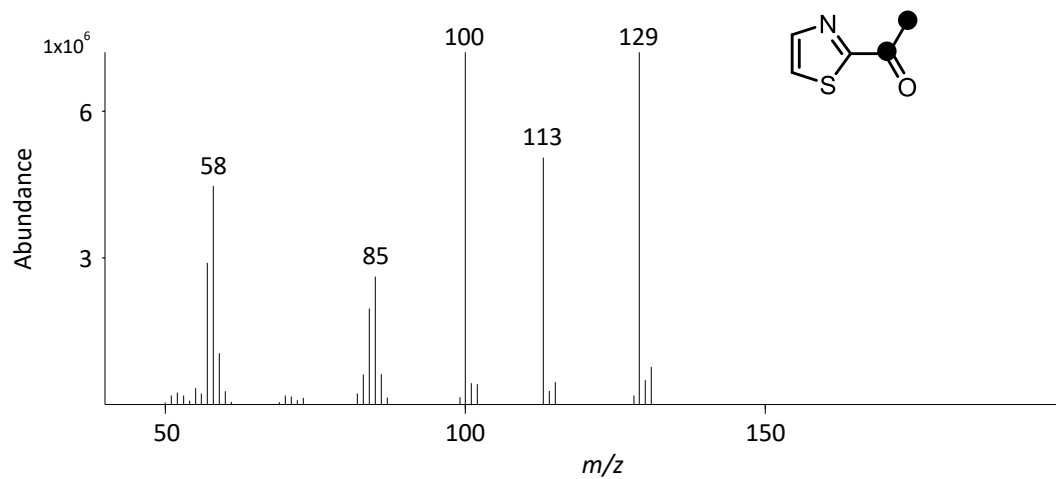
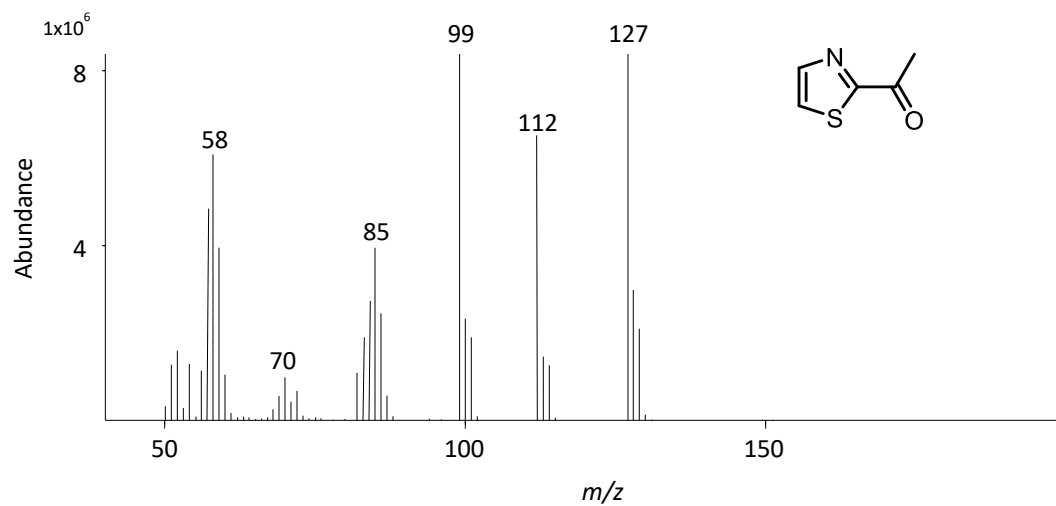


Figure 33: Mass spectra of 2-acetylthiazole and 2-acetylthiazole- $^{13}\text{C}_2$



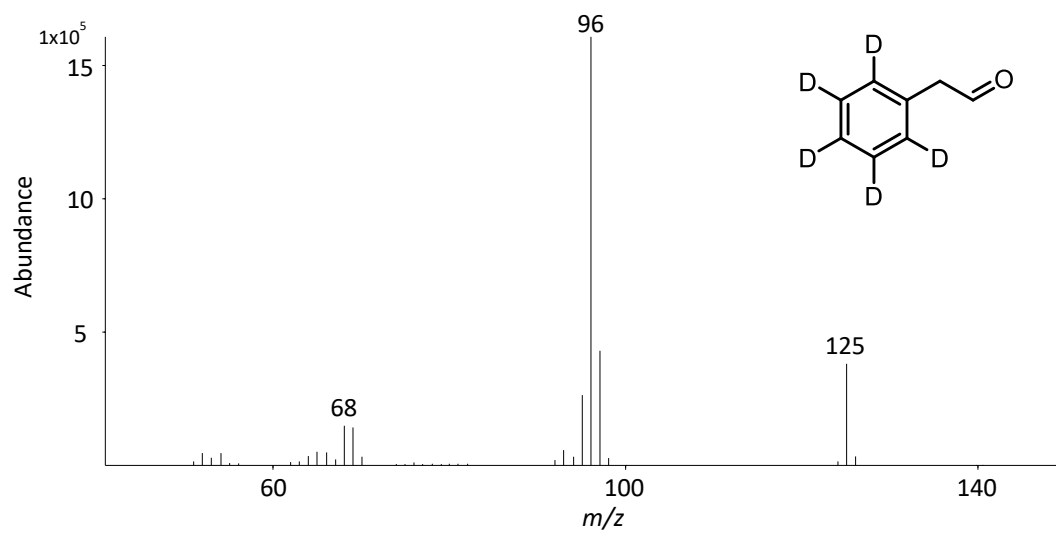
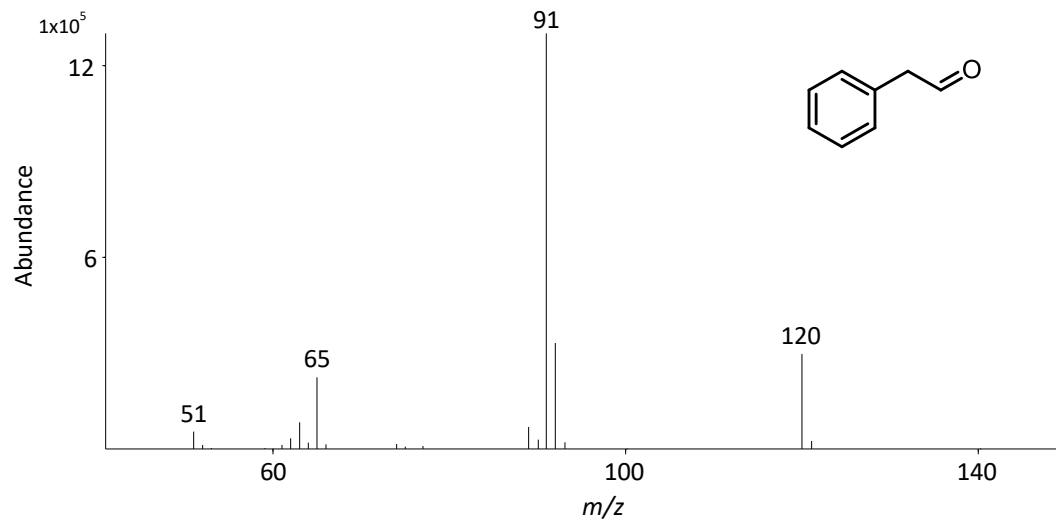


Figure 34: Mass spectra of phenylacetaldehyde and phenylacetaldehyde- $d_5$

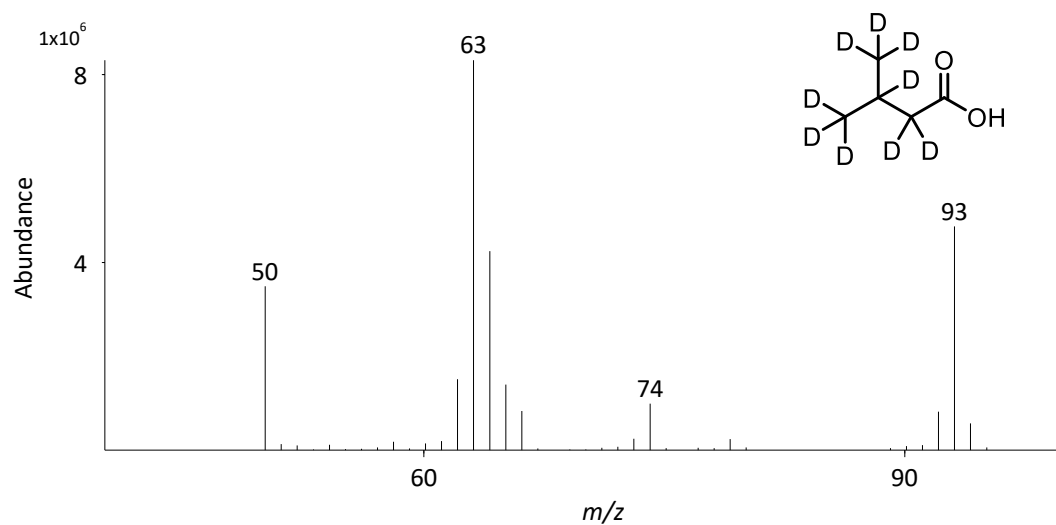
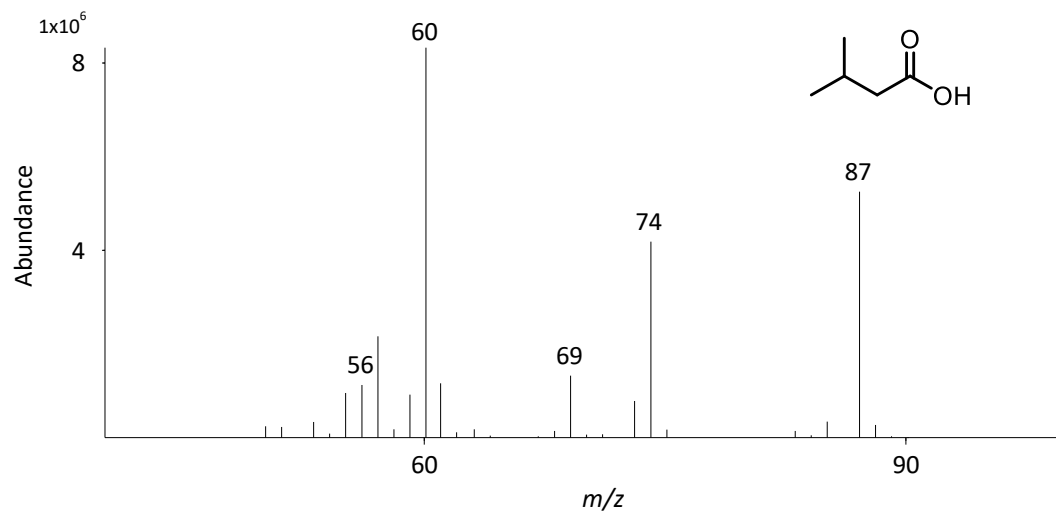


Figure 35: Mass spectra of 3-methylbutanoic acid and 3-methylbutanoic acid- $d_9$

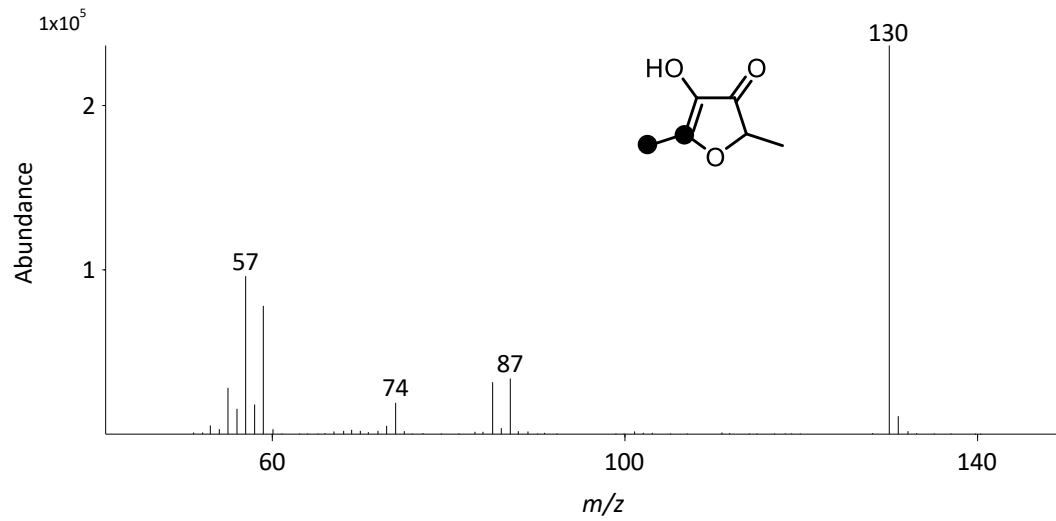
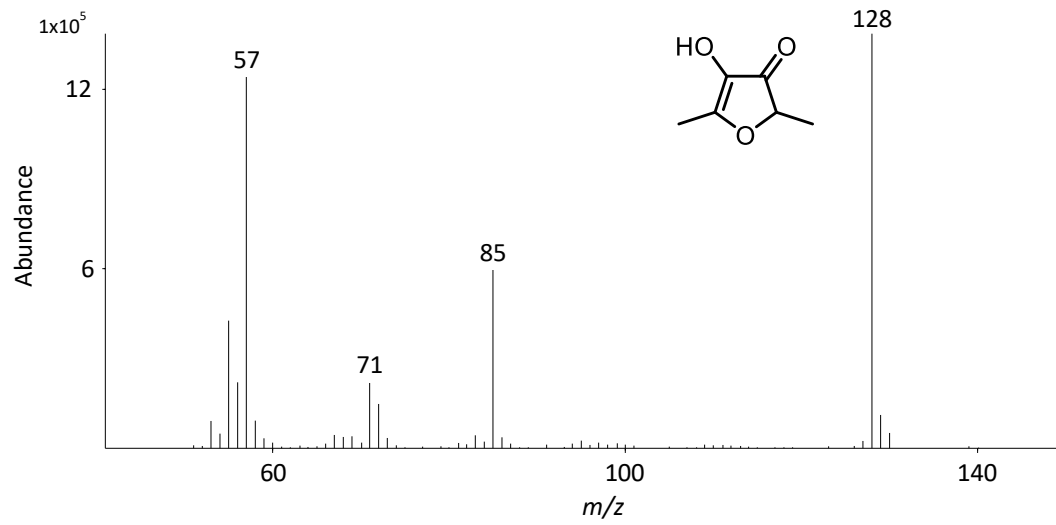


Figure 36: Mass spectra of HDMF and HDMF- $^{13}\text{C}_2$

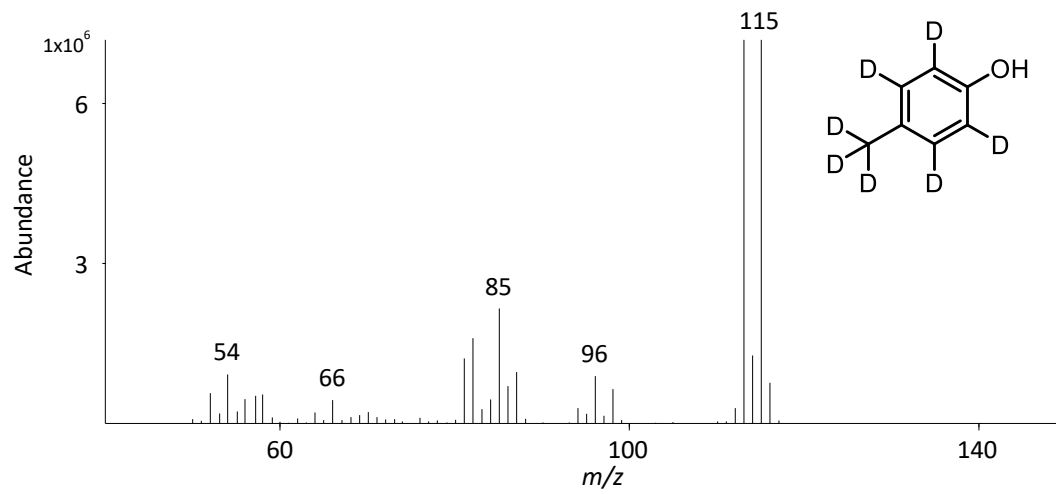
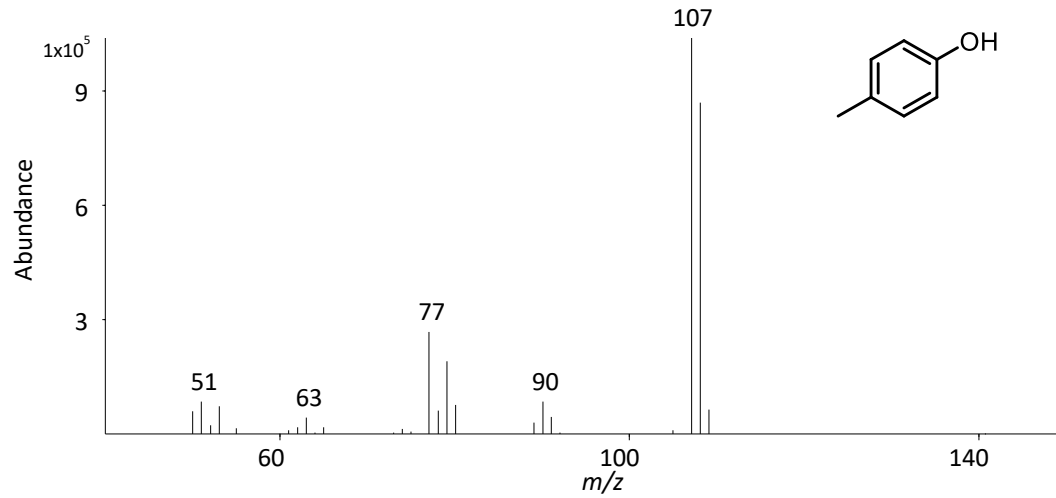


Figure 37: Mass spectra of p-cresol and p-cresol- $d_7$

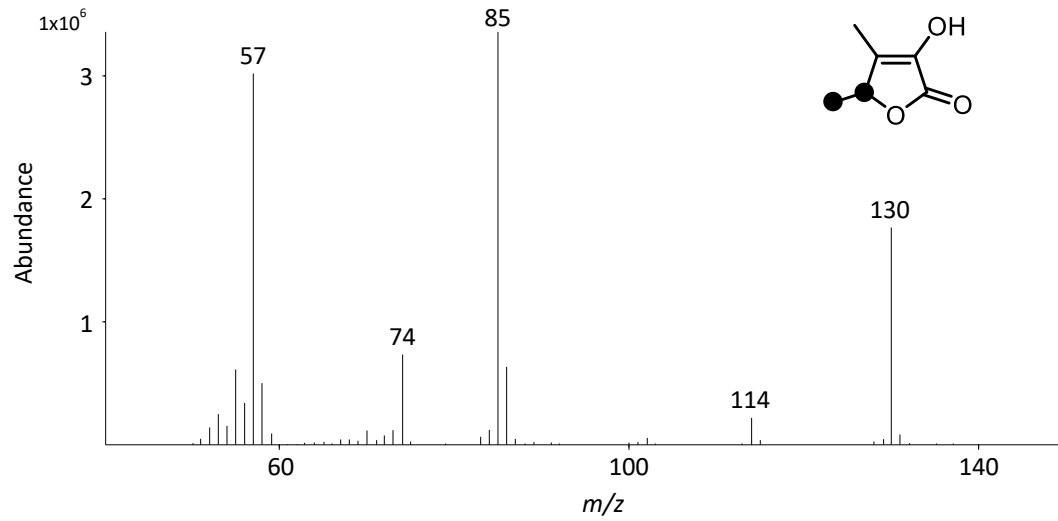
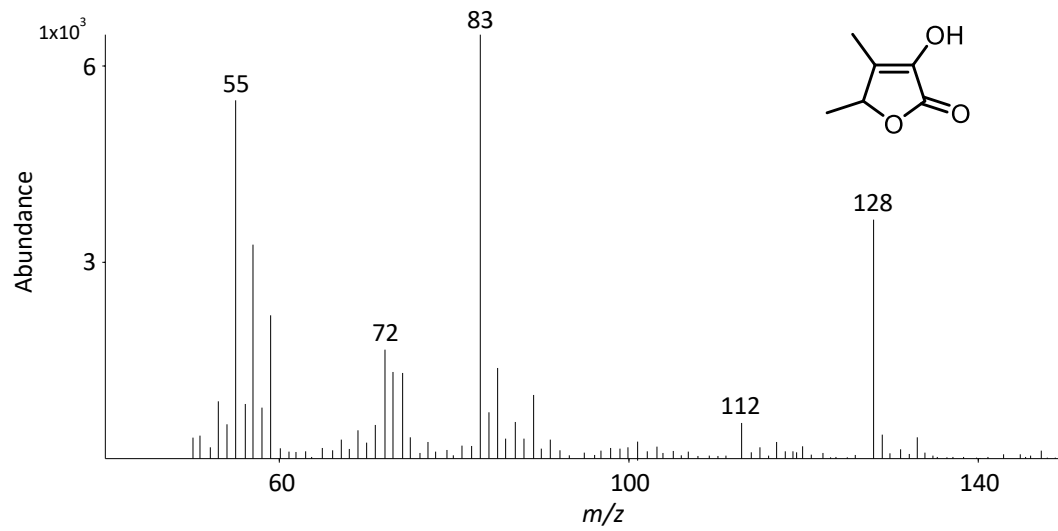


Figure 38: Mass spectra of sotolon and sotolon- $^{13}\text{C}_2$

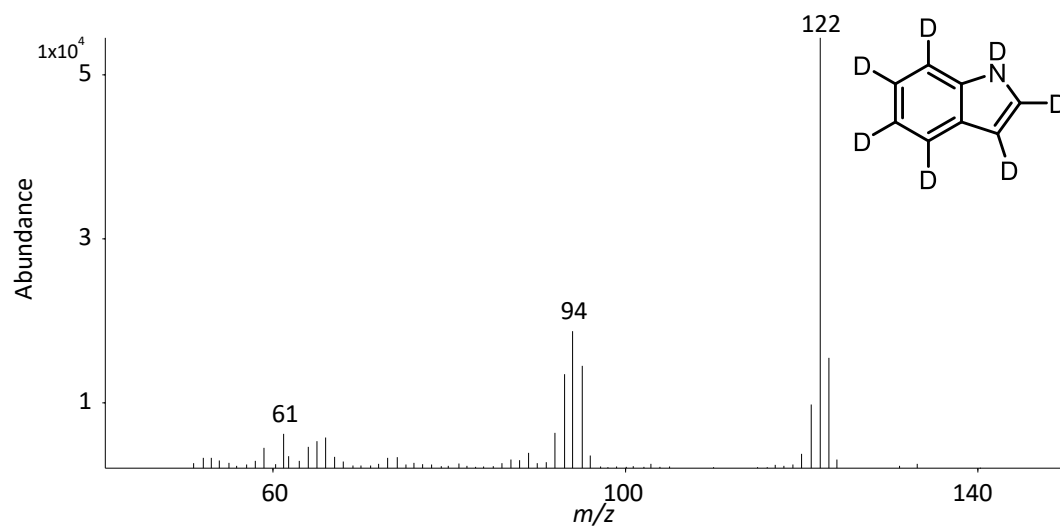
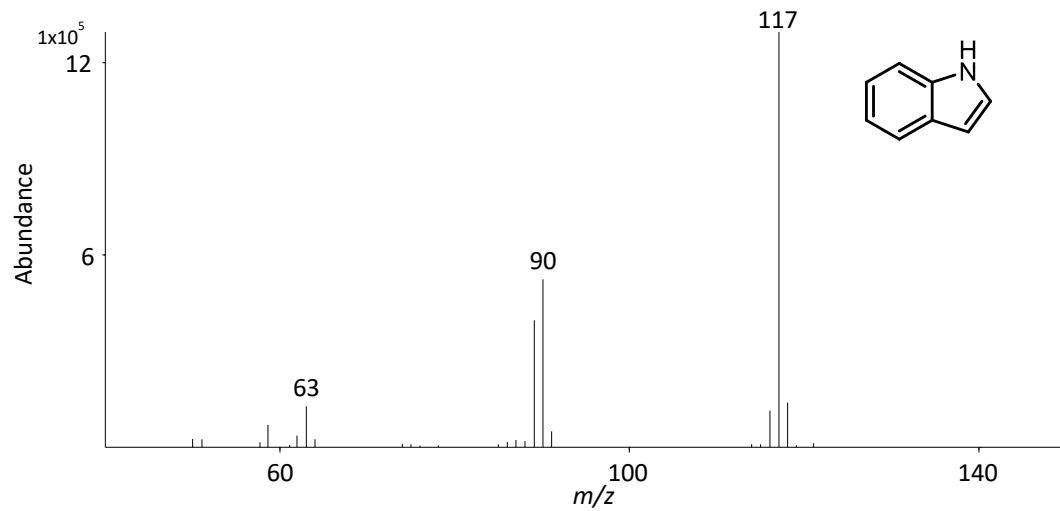


Figure 39: Mass spectra of indole and indole- $d_7$

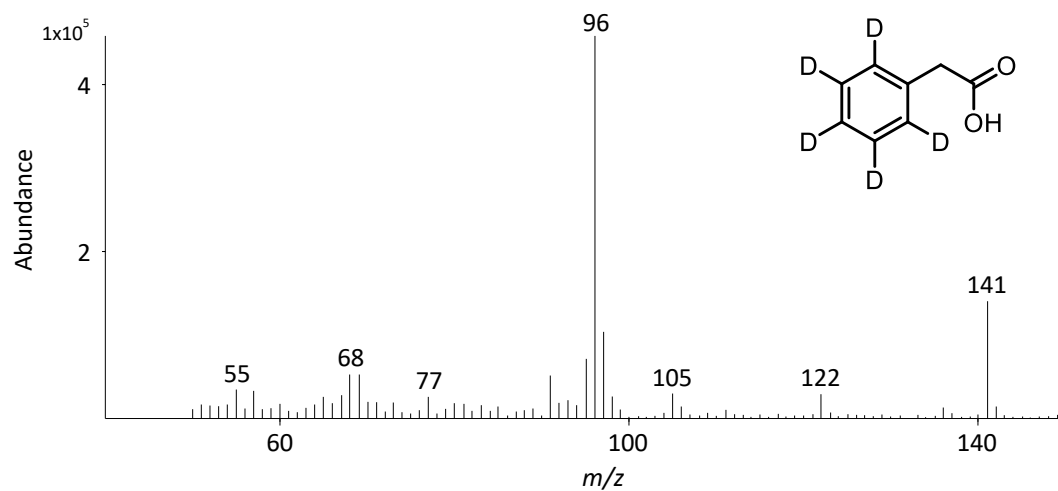
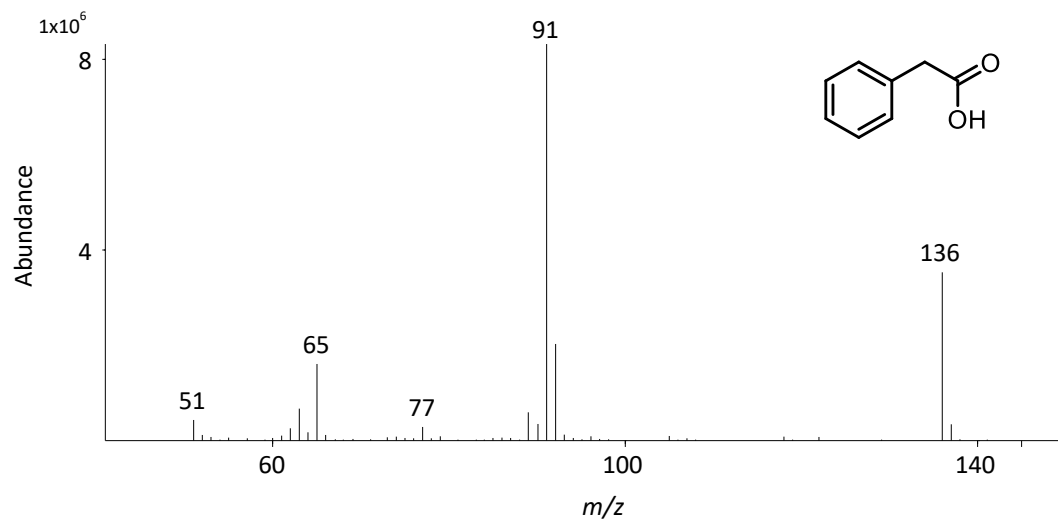


Figure 40: Mass spectra of phenylacetic acid and phenylacetic acid- $d_5$

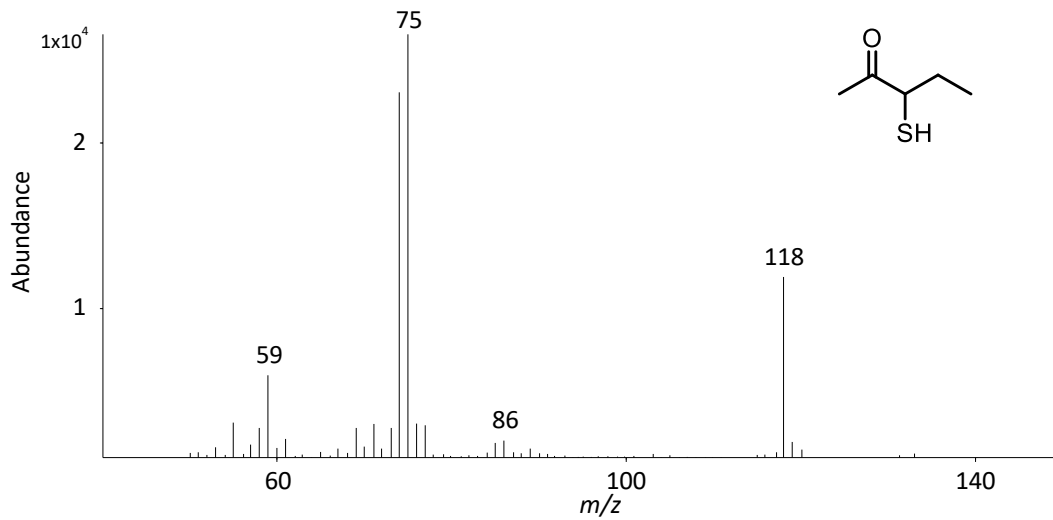


Figure 41: Mass spectrum for 3-sulfanylpentan-2-one

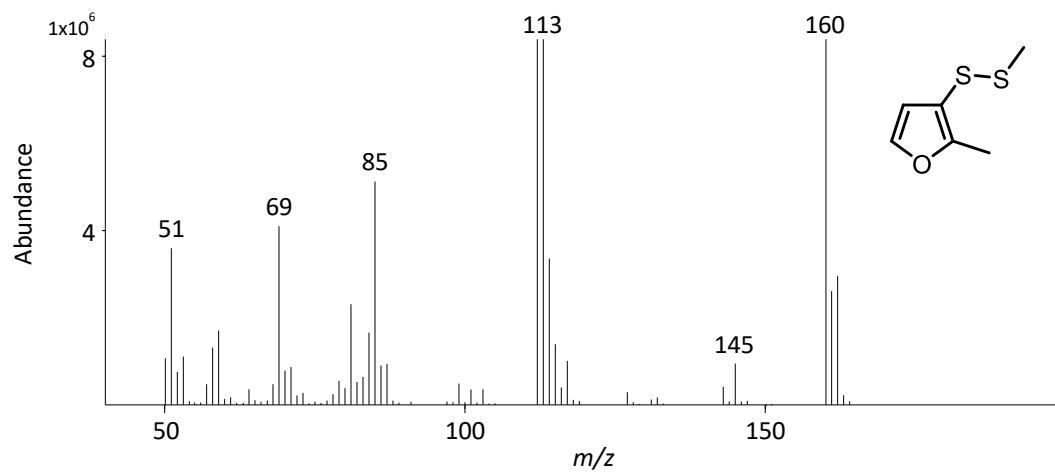


Figure 42: Mass spectrum for 2-methyl-3-(methyldithio)furan



#### 4.4.1. Aroma Profile of eHMP

The concentration and OAV of each odorant in the eHMP sample was calculated using SIDA (Table 13). The odorant with the highest OAV in eHMP, 1-octen-3-one (**4**, OAV 1356), was likely a major contributor to the perceived mushroom-like aroma of the sample. HDMF (**28**, OAV 16), sotolon (**31**, OAV 16), 2-phenylacetaldehyde (**19**, OAV 6), 3-(methylsulfanyl)propanal (**11**, OAV 4), 2-acetylthiazole (**18**, OAV 3), indole (**34**, OAV 3), and 2-ethyl-3,5-dimethylpyrazine (**12**, OAV 1) were also calculated to have an OAV  $\geq 1$ , and thus are all at least somewhat impactful in the overall aroma of eHMP. Despite calculating high concentrations of 3-methylbutanoic acid (**20**) and phenylacetic acid (**35**), neither compound was concentrated enough to eclipse its odor threshold, and thus both odorants had OAVs  $< 1$ .

#### 4.4.2. Aroma Profile of eHMP + cys

The concentration and OAV of each odorant in the eHMP sample was calculated using SIDA (Table 14). In the eHMP + cys sample, 1-octen-3-one (**4**, OAV 1342) showed the highest OAV, followed by 2-furfurylthiol (**9**, OAV 610). 2-Furfurylthiol (**9**) is a potent odorant and key aroma compound in coffee and cooked beef.<sup>31</sup> It has been generated in model systems through the reaction of cysteine with a variety of sugars, including ribose.<sup>32</sup> 1-(2-furyl)ethanethiol (**8**, OAV 78) has previously been identified in glucose/cysteine reaction mixtures.<sup>33</sup> 3-sulfanylpentan-2-one (**6**, OAV 42), like **9**, has been detected in cooked beef and coffee and has been synthesized from cysteine and ribose in a previous study.<sup>31</sup> 2-Methyl-3-(methylthio)furan (**17**, OAV 3) has also been reported in cooked meat, yeast extracts, and hydrolyzed vegetable proteins.<sup>34,35</sup> In hydrolyzed vegetable protein, thiamin, cysteine, and methionine were added to generate the odorant. Baek et al. theorized that **17** and similar compounds were formed from methanethiol reacting with 2-

methyl-3-furanthiol through the Maillard reaction.<sup>35</sup> Other odorants with OAVs  $\geq 1$  were: sotolon (**34**, OAV 20), HDMF (**28**, OAV 9), indole (**34**, OAV 8), 3-(methylsulfanyl)propanal (**11**, OAV 3), *p*-cresol (**29**, OAV 1), and 2-ethyl-3,5-dimethylpyrazine (**12**, OAV 1).

A direct comparison between the odorant concentrations in eHMP and eHMP + cys showed differences between the two samples (Table 15). The sulfur compounds not detected in eHMP, 3-sulfanylpentan-2-one (**6**), 1-(2-furyl)ethanethiol (**8**), 2-furfurylthiol (**9**), and 2-methyl-3-(methylthio)furan (**17**), were all important to the aroma profile of eHMP + cys, suggesting that their absence from eHMP was because of a lack of cysteine. Also, compared to eHMP, eHMP + cys showed higher concentrations of *p*-cresol (**29**), sotolon (**31**), indole (**34**), and phenylacetic acid (**35**). All 8 odorants that were detected at a higher concentration in eHMP + cys compared to eHMP were detected at a FD  $\geq 16$ . While **35** was detected at elevated levels in eHMP + cys, the calculated OAV was still below 1 and, thus, left out of the aroma simulation model.

Table 13: Concentrations, odor thresholds, and odor activity values (OAV) of key odorants in eHMP

no.	odorant	RT	concentration (µg/kg)	odor threshold (µg/kg)	OAV
4	1-octen-3-one	6.983	21.7	0.0	1355.6
31	sotolon	22.676	7.7	0.5	15.7
28	HDMF	20.089	629.6	40.0	15.7
19	phenylacetaldehyde	13.414	30.4	5.4	5.6
11	3-(methylsulfanyl)propanal	9.489	1.5	0.4	3.5
18	2-acetylthiazole	13.449	12.4	4.0	3.1
34	indole	26.256	30.6	11.0	2.8
12	2-ethyl-3,5-dimethylpyrazine	9.837	0.1	0.1	1.4
6	3-sulfanylpentan-2-one	7.933	0.0	0.2	<1
17	2-methyl-3-(methylthio)furan	14.115	0.0	0.4	<1
16	butanoic acid	12.993	12.5	2400.0	<1
20	3-methylbutanoic acid	13.700	348.4	490.0	<1
29	<i>p</i> -cresol	20.895	0.7	3.9	<1
8	1-(2-furyl)ethanethiol	8.992	0.0	0.1	<1
9	2-furfurylthiol	9.389	0.0	0.0	<1
35	phenylacetic acid	27.498	334.9	6100.0	<1

Table 14: Concentrations, odor thresholds, and odor activity values (OAV) of key odorants in eHMP + cys

no.	odorant	RT	concentration ( $\mu\text{g}/\text{kg}$ )	odor threshold ( $\mu\text{g}/\text{kg}$ )	OAV
4	1-octen-3-one	6.983	21.5	0.0	1342.4
9	2-furfurylthiol	9.389	22.0	0.0	610.4
8	1-(2-furyl)ethanethiol	8.992	4.1	0.1	78.2
6	3-sulfanylpentan-2-one	7.933	8.0	0.2	41.9
31	sotolon	22.676	9.9	0.5	20.2
28	HDMF	20.089	338.0	40.0	8.5
34	indole	26.256	83.5	11.0	7.6
17	2-methyl-3-(methyldithio)furan	14.115	1.4	0.4	3.4
11	3-(methylsulfanyl)propanal	9.489	1.4	0.4	3.2
29	<i>p</i> -cresol	20.895	4.9	3.9	1.3
12	2-ethyl-3,5-dimethylpyrazine	9.837	0.1	0.1	<1
16	butanoic acid	12.993	10.5	2400.0	<1
18	2-acetylthiazole	13.449	0.5	4.0	<1
19	phenylacetaldehyde	13.414	4.1	5.4	<1
20	3-methylbutanoic acid	13.700	324.2	490.0	<1
35	phenylacetic acid	27.498	458.2	6100.0	<1

Table 15: Concentrations of 16 odorants in eHMP and eHMP + cys

no.	odorant	concentration ( $\mu\text{g}/\text{kg}$ )		
		eHMP cys	eHMP	difference
1	1-octen-3-one	21.5	21.7	-0.2
6	3-sulfanylpentan-2-one	8.0	0.0	8.0
8	1-(2-furyl)ethanethiol	4.1	0.0	4.1
9	2-furfurylthiol	22.0	0.0	22.0
11	3-(methylsulfanyl)propanal	1.4	1.5	-0.1
12	2-ethyl-3,5-dimethylpyrazine	0.1	0.1	0.0
16	butanoic acid	10.5	12.5	-2.0
17	2-methyl-3-(methyldithio)furan	1.4	0.0	1.4
18	2-acetylthiazole	0.5	12.4	-11.9
19	phenylacetaldehyde	4.1	30.4	-26.3
20	3-methylbutanoic acid	324.2	348.4	-24.1
28	HDMF	338.0	629.6	-291.5
29	<i>p</i> -cresol	4.9	0.7	4.2
31	sotolon	9.9	7.7	2.2
34	indole	83.5	30.6	52.9
35	phenylacetic acid	458.2	334.9	123.3

#### 4.4.3. Aroma Simulation Model of eHMP + cys

In order to confirm which odorants were responsible for the odor quality difference between the eHMP and eHMP + cys samples, an aroma simulation model was created. The data obtained from cAEDA identified four sulfur containing odorants that were found in eHMP + cys, but not in eHMP. The odorants were 3-sulfanylpentan-2-one (**6**), 1-(2-furyl)ethanethiol (**8**), 2-furfurylthiol (**9**), and 2-methyl-3-(methylthio)furan (**17**). Initially, an aroma simulation model was created using these odorants at the quantitated levels detected by SIDA in eHMP as the carrier matrix. The aroma simulation model was tested by olfactory-profile analysis (n = 21) but proved unsatisfactory. This was due to inadequate aroma of the aroma simulation model with only the sulfur compounds added (data not shown). The odorants *p*-cresol (**29**), sotolon (**31**), and indole (**34**) were then added to the aroma simulation model at the calculated values (Table 16). The addition of these odorants resulted in a close match to eHMP + cys (Figure 43). This experiment determined that **6, 8, 9, 17, 29, 31, and 34** were contributors to the meat-like aroma character of the eHMP + cys sample; however, omission studies are needed to determine the minimum number of odorants required to match the olfactory profile. A one-way ANOVA statistical analysis suggested no significant differences existed between the eHMP + cys and the aroma simulation model ( $p > 0.05$ ).

#### 4.5. Second & Third Consumer Taste Panels

Two consumer sensory evaluations were conducted to determine if the thermally generated odorants were responsible for the increased saltiness perception of the eHMP + cys, as compared to eHMP alone. To test this, eHMP was compared to eHMP with addition of the aroma model (7 odorants: **6, 8, 9, 17, 29, 31, 34**) in low sodium chicken broth.

Table 16: Odorants and concentrations used in simulation flavor formula

no.	Odorant	ppb in flavor
6	3-sulfanylpentan-2-one	147
8	1-(2-furyl)ethanethiol	81
9	2-furfurylthiol	439
17	2-methyl-3-(methyldithio)furan	28
29	<i>p</i> -cresol	90
31	sotolon	40
34	indole	993

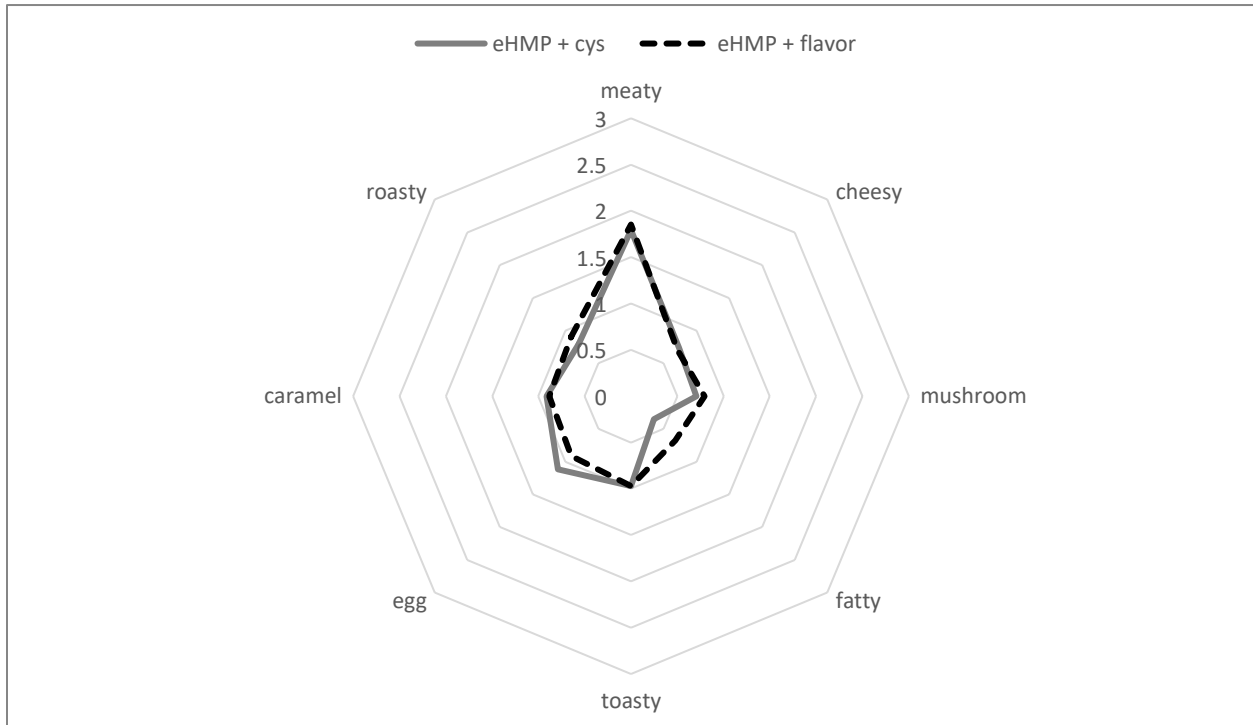


Figure 43: Olfactory-profile analysis of eHMP + aroma model versus eHMP + cys

In the first consumer sensory test, consumers rated the overall flavor, saltiness, sourness, bitterness, sweetness, and umami (n = 96). The results of the first consumer sensory test showed that the sample with eHMP and the aroma model had a higher perceived saltiness when compared to the model broth containing eHMP alone ( $t_{95} = 3.626$ ,  $p = 0.0005$ ; Figure 44). Additionally, overall flavor was rated to be higher in the eHMP with aroma model sample ( $t_{95} = 3.0437$ ,  $p = 0.0030$ ). The perceived intensity of the other basic tastes (sweet, sour, umami, and bitter) were not found to be significantly different across the samples ( $p > 0.05$ ).

In the second consumer sensory test, the samples were subjected to a 2-alternative forced choice test. The eHMP with the aroma model was significantly selected as the saltier of the two samples ( $d' = 0.5647$ ,  $p = 0.0025$ ).

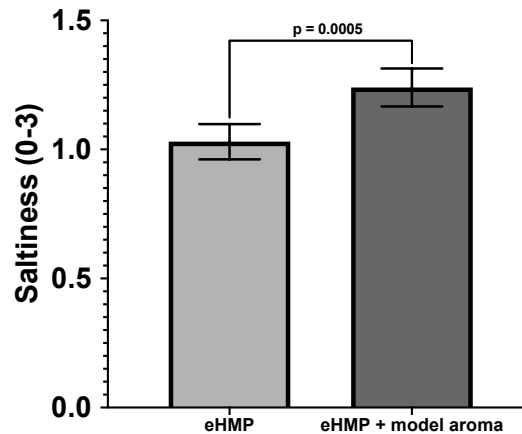


Figure 44: Consumer sensory data comparing eHMP vs. eHMP + aroma model saltiness ratings in low sodium chicken broth



The results from these studies provide strong evidence that the addition of the aroma model (7 odorants differentially higher in eHMP + cys) into the eHMP enhances the saltiness perception of the broth greater than that of eHMP alone. In general, these findings coincide with previous work on using mushrooms to increase the palatability of a reduced sodium food.<sup>36</sup> Going further, the additional saltiness enhancement from the model aroma confirmed the notion that specific odors could enhance saltiness perception through crossmodal effects.<sup>19, 20, 37, 38</sup>

#### 4.6. Proposed Mechanisms of Formation

##### 4.6.1. Sugar Analysis

Analysis of the mushroom carbohydrates was performed to determine which monosaccharides could be precursors to the potent odorants determined by cAEDA and SIDA (**6**, **8**, **9**, and **17**). To identify which sugars were present in each sample, eHMP and eHMP + cys were run by IC-PAD and compared to sugar standards (Table 17). The overall sugar profile was similar for both samples and matched well with the previous mushroom sugar content performed by Kim et al.<sup>39</sup> Mannose was the major sugar identified, with xylose and glucose also detected. Trace amounts of other sugars, including fructose, sucrose, and maltose, were found in the mushrooms.

Table 17: Sugar content of eHMP as determined by IC-PAD ( $n = 3$ )

Sugar	mg/g dry weight	std dev
glucose	17.10	0.91
fructose	5.95	0.34
sucrose	2.25	0.08
maltose	10.19	1.10
mannose	117.95	4.93
xylose	47.01	2.61

#### 4.6.2. Reaction of Mannose and Cysteine

After determining the importance of the sulfur-containing odorants 1-(2-furyl)ethanethiol (**8**) and 2-furfurylthiol (**9**) in the meat-like aroma and saltiness-perception enhancing effect of eHMP + cys, a model system was used to gain insight into potential formation pathways. In this model reaction, mannose was combined with cysteine and dissolved in a phosphate buffer. The mixture was then heated to 140 °C in a pressurized reactor for 1 hour. The resulting solution was extracted with ether and analyzed by GC-MS and GC-O for the formation of odorants. Both **8** and **9** were detected in the model reaction, confirming that mannose was an acceptable monosaccharide for the formation of **8** and **9**. The generation of **8**, which has only been reported previously in model reaction mixtures using glucose, was a new discovery. Mannose was earlier identified as the major sugar in mushrooms (Table 17) and, thus, a potential starting material for **8**, though no previous studies have reported a link between mannose and **8** before.

#### 4.6.3. Proposed Mechanisms of Formation

Further research was done to gain insight into the formation pathway of 1-(2-furyl)ethanethiol (**8**), which had never been reported from mannose in a food system before. Previously, Wang and Ho proposed a mechanism for the formation of 2-acetylfuran from ribose and the 1-deoxysone of glucose.<sup>40,41</sup> In the study, they used a model system and measured the formation of 2-acetylfuran. In the current study, thermally treated eHMP + cys generated **8**, with mannose being a possible precursor from *A. bisporus*, considering the relatively high concentration of mannose as compared to glucose in mushrooms.<sup>39</sup> Rearrangement of monosaccharides in water suggested that the mechanisms proposed by Wang and Ho could also be applied to mannose. Furthermore, the model reaction performed in this study, using only mannose and cysteine, yielded **8** in detectable levels

by GC-O and GC-MS. A possible formation pathway of **8** from mannose and cysteine is proposed here, based on the pathways described by Münch et al, as well as Wang and Ho (Figure 45).<sup>40,41,42</sup> First, mannose rearranges in water to form the 2,3-enediol, and the 1-deoxysone of mannose is then formed via the 2,3-enediol. The 1-deoxysone of mannose rearranges and loses water, generating the 1,4-dideoxysone. Next, the 1,4-dideoxysone cyclizes into a furan ring and generates 2-acetylfuran through dehydration. Alternatively, 2-acetylfuran could also be generated from mannose fragments via the condensation of hydroxyacetone and methylglyoxal.<sup>43</sup> Finally, a substitution of the carbonyl on the 2-acetylfuran with a sulfur, provided by cysteine, yields **8**. According to Ho and Wang, the reaction of glucose with amino acids generated 2-acetylfuran. However, in their study, it was observed that when glucose was reacted with cysteine, no 2-acetylfuran was detected. This might be due to the consumption of 2-acetylfuran to generate 1-(2-furyl)ethanethiol (**8**), not measured in the study. This result suggested that 2-acetylfuran might be an intermediate product during the formation of **8**. Furthermore, a similar formation pathway for thiofuran compounds was proposed by Hofmann and Schieberle, with positive confirmation through testing of a model experiment.<sup>33</sup>

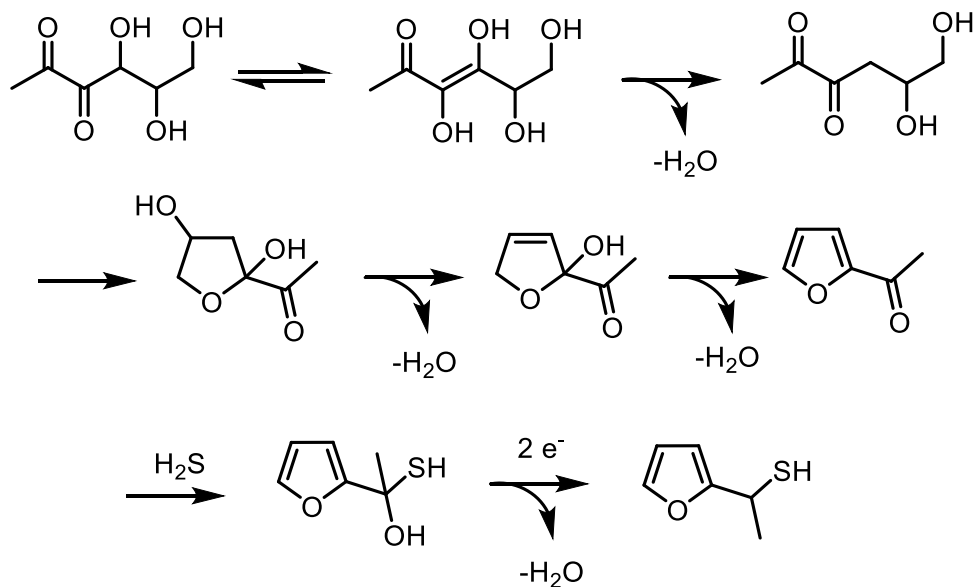


Figure 45: Theoretical pathway of formation of 1-(2-furyl)ethanethiol via the reaction of mannose with cysteine.

Analysis of odor activity values suggests 2-furfurylthiol (**9**) as a major contributor to the aroma differences between the samples. Due to a low odor threshold, **9** is a potent odorant that is a key odorant in coffee and cooked beef.<sup>31</sup> It was previously generated through the reaction of cysteine with several different sugars, including ribose.<sup>32</sup> Preceding studies were performed after identification of the compound in yeast extracts,<sup>42</sup> and model studies were created to demonstrate formation of **9** from 2-furaldehyde was possible. The proposed mechanism of formation involves the reaction of 2-furaldehyde and hydrogen sulfide with the loss of water. *Agaricus bisporus* is replete with xylose, a pentose similar to ribose, and a theoretical mechanism is proposed here based off of the reaction pathway devised by Munch, Hofmann, and Schieberle

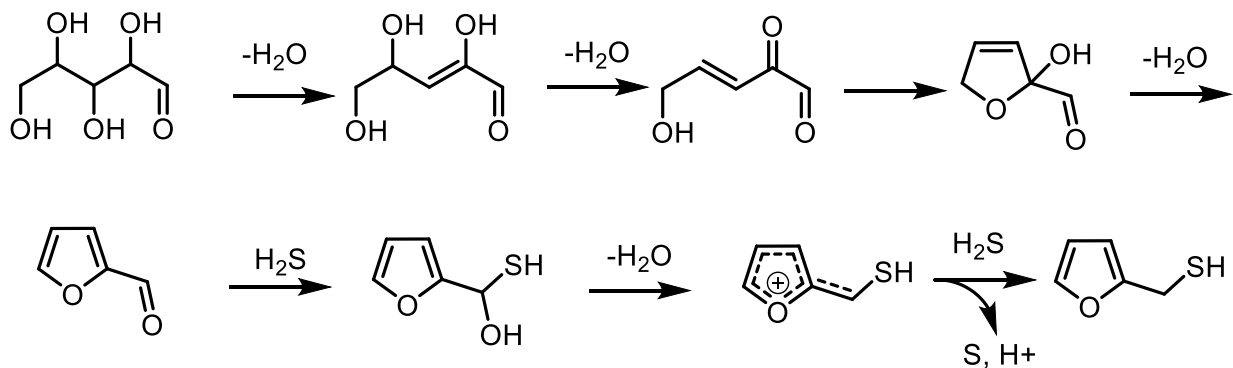


Figure 46: Theoretical pathway of formation for 2-furfurylthiol via the reaction of xylose and cysteine.

(Figure 46).<sup>42</sup> Similar to the proposed mechanism of formation of **8**, xylose rearranges in water to form the 2,3-enediol, and the 3-deoxyxylose of xylose is then formed via the 2,3-enediol. Then, the 3-deoxyxylose of xylose rearranges and loses water, cyclizing into a furan ring and generating 2-furfural through dehydration. Hydrogen sulfide then attacks the carbonyl group, leading to the loss of water and a positively charged furan ring. Another hydrogen sulfide molecule donates electrons, stabilizing the ring and generating **9**.

The catty, animal-like 3-sulfanylpentan-2-one (**6**) was also present in the eHMP + cys sample at a high OAV. Like 2-furfurylthiol (**9**), **6** has been detected in cooked beef and coffee and has previously been synthesized from cysteine and ribose.<sup>31</sup> Chu proposes a complicated formation pathway of 2,3-pentanedione from glucose fragments generated during the Maillard process.<sup>44</sup> Compound **6** is easily formed after introduction of hydrogen sulfide to 2,3-pentanedione. Due to the relative dearth of glucose in *Agaricus bisporus* compared to mannose, we considered a pathway of formation starting with mannose. Mannose is a hexose like glucose and can rearrange into glucose in an aqueous environment. Using Chu's pathway as a model, a formation mechanism for **6** is proposed based on fragments of mannose reacting with cysteine (Figure 47). Mannose first

forms the 3-deoxyglucosone in water, which is broken down into 2,3-dihydroxypropanal and 2-oxopropanal under maillard-like conditions. Alanine, a common amino acid in mushrooms, may then react with the 2-oxopropanal fragment to generate an intermediate. The loss of the azanide yields 2,3-pentanedione. The addition of hydrogen sulfide leads to an intermediate, which then forms **6** via loss of water.

2-methyl-3-(methylthio)furan (**17**) has previously been identified in cooked meat.<sup>34</sup> Interestingly, it has also been reported in yeast extracts, as well as hydrolyzed vegetable proteins.<sup>35</sup> In hydrolyzed vegetable protein, thiamin, cysteine, and methionine were added to generate the odorant. Baek et al<sup>35</sup> theorized that **17** and similar compounds were formed through the Maillard reaction of ribose and cysteine or methanethiol reacting with 2-methyl-3-furanthiol. We propose a theoretical pathway for the formation of **17** based on a previous pathway suggested by Mottram and Whitfield (Figure 48).<sup>45</sup> First, xylose and an amino group from a peptide or amino acid form an amadori product. The amadori product of xylose and an amino acid rearrange and form a 1-deoxypentosone. The 1-deoxypentosone then cyclizes and loses a water, generating the 2-methylfuran-3(2*H*)-one. Hydrogen sulfide attacks the carbonyl, generating 2-methylfuran-3-thiol. Finally, an addition reaction of the sulfur and methanethiol from the degradation of cysteine generates **17**. Once again, xylose is structurally similar enough to ribose that it might play the same role as ribose during the maillard reaction, and could be a key reagent in formation of compound **17**. Earlier studies on this compound showed that increased cysteine did not alter the concentration of **17** in cooked ham, suggesting the reaction is limited by other precursors.<sup>46</sup> Data collected from the eHMP and eHMP + cys samples suggests in the case of hydrolyzed mushroom, cysteine is the limiting factor, as no **17** was generated in the control.

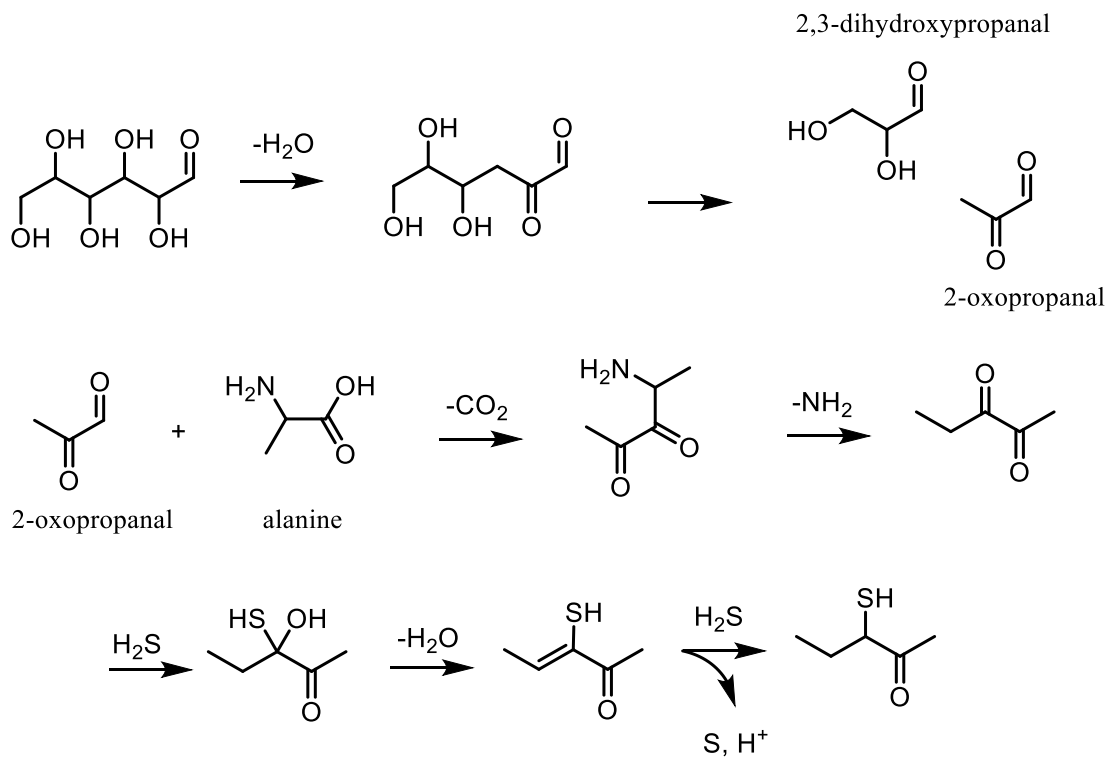


Figure 47: Theoretical pathway of formation for 3-sulfanylpentan-2-one via the reaction of mannose, cysteine, and alanine.

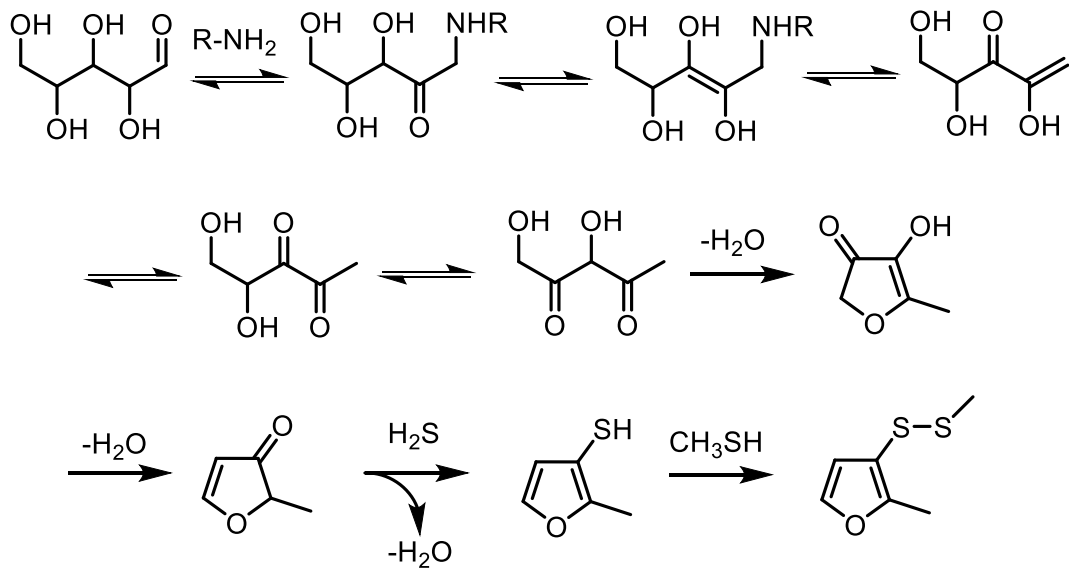


Figure 48: Theoretical pathway of formation of 2-methyl-3-(methylthio)furan via the reaction of xylose and cysteine.



## 5. CONCLUSION

In conclusion, this study demonstrated the saltiness perception-enhancing effects of eHMP and eHMP + cys in low sodium chicken broth through several sensory evaluations. Thirty-six odorants were identified between both eHMP and eHMP + cys, and sixteen odorants were quantitated by SIDA to determine OAVs for odorants in both eHMP and eHMP + cys. The key odorants that drove the olfactory differences between the samples were 3-sulfanylpentan-2-one (**6**), 1-(2-furyl)ethanethiol (**8**), 2-furfurylthiol (**9**), 2-methyl-3-(methylthio)furan (**17**), *p*-cresol (**29**), sotolon (**31**), and indole (**34**). An aroma simulation model was created using these odorants at the calculated differences between eHMP and eHMP + cys and was tested in additional consumer sensory evaluations, eliciting similar salt-enhancing properties as the eHMP + cys sample. This sensory testing illustrated the crossmodal functionality of these odorants. Using a model system, this study proposed a mechanism of formation for 1-(2-furyl)ethanethiol from mannose, the predominant sugar in button mushrooms. Additionally, we theorized a mechanism of formation for 3-sulfanylpentan-2-one via the reaction of mannose and cysteine. Furthermore, this study offered potential mechanisms of formation for 2-furfurylthiol and 2-methyl-3-(methylthio)furan from the reaction of xylose and cysteine.

This study illustrated the complex, interconnected relationship between aroma and taste that occurs during eating. Affecting the perception of one sense can alter another sense, or provide a new, unique sensation. Through better knowledge of this phenomenon, advances in flavor technology can be made to enhance the flavor of healthful foods. Discovering new sources of meaty, salt-enhancing odorants suggests potential future innovation for meat substitutes derived from mushrooms. This technology can most crucially be used to increase the desirability of low-sodium

diets, one of the most important areas of dietary improvement according to the USDA. Overall, this research identified potential sources of saltiness-enhancing odorants from mushrooms and provided a foundation for future crossmodal studies between odor and taste.

## REFERENCES

1. Ferreira, I. C.; Morales, P.; Barros, L., *Wild plants, mushrooms and nuts: functional food properties and applications*. John Wiley & Sons: 2016.
2. Nijssen, L.; Visscher, C.; Maarse, H.; Willemsens, L.; Boelens, M., Volatile compounds in food: qualitative and quantitative data. *Central Institute for Nutrition and Food Research, TNO: Zeist, The Netherlands 1996*.
3. Zhang, H.; Pu, D.; Sun, B.; Ren, F.; Zhang, Y.; Chen, H., Characterization and comparison of key aroma compounds in raw and dry porcini mushroom (*Boletus edulis*) by aroma extract dilution analysis, quantitation and aroma recombination experiments. *Food chemistry* **2018**, *258*, 260-268.
4. Grosshauser, S.; Schieberle, P., Characterization of the key odorants in pan-fried white mushrooms (*Agaricus bisporus* L.) by means of molecular sensory science: comparison with the raw mushroom tissue. *Journal of agricultural and food chemistry* **2013**, *61*, 3804-3813.
5. Organization, W. H. Salt Reduction. (September 26),
6. Lindemann, B.; Ogiwara, Y.; Ninomiya, Y., The discovery of umami. *Chemical senses* **2002**, *27*, 843-844.
7. Yamaguchi, S., The synergistic taste effect of monosodium glutamate and disodium 5'-inosinate. *Journal of Food Science* **1967**, *32*, 473-478.
8. Tamura, M.; Seki, T.; Kawasaki, Y.; Tada, M.; Kikuchi, E.; Okai, H., An enhancing effect on the saltiness of sodium chloride of added amino acids and their esters. *Agricultural and Biological Chemistry* **1989**, *53*, 1625-1633.
9. Guerrero, A.; Kwon, S. S.-Y.; Vadehra, D. V., Compositions to enhance taste of salt used in reduced amounts. In Google Patents: 1998.

10. Uchida, Y.; Iritani, S.; Miyake, T., Method for enhancing the salty-taste and/or delicious-taste of food products. In Google Patents: 2000.
11. Bouchard, E. F.; Hetzel, C. P.; Olsen, R. D., Process of sweetening foods with maltol and sugar. In Google Patents: 1968.
12. Namiki, T.; Nakamura, T., Enhancement of sugar sweetness by furanones and/or cyclotene. *Japanese Patent, JP* **1992**, 4008264.
13. Noble, A. C., Taste-aroma interactions. *Trends in Food Science & Technology* **1996**, 7, 439-444.
14. Schifferstein, H. N.; Verlegh, P. W., The role of congruency and pleasantness in odor-induced taste enhancement. *Acta psychologica* **1996**, 94, 87-105.
15. Clark, C. C.; Lawless, H. T., Limiting response alternatives in time-intensity scaling: an examination of the halo-dumping effect. *Chemical senses* **1994**, 19, 583-594.
16. Frank, R. A.; Byram, J., Taste–smell interactions are tastant and odorant dependent. *Chemical Senses* **1988**, 13, 445-455.
17. Batenburg, M.; van der Velden, R., Saltiness enhancement by savory aroma compounds. *Journal of food science* **2011**, 76, S280-S288.
18. Dalton, P.; Doolittle, N.; Nagata, H.; Breslin, P., The merging of the senses: integration of subthreshold taste and smell. *Nature neuroscience* **2000**, 3, 431.
19. Lawrence, G.; Salles, C.; Septier, C.; Busch, J.; Thomas-Danguin, T., Odour–taste interactions: A way to enhance saltiness in low-salt content solutions. *Food Quality and Preference* **2009**, 20, 241-248.
20. Djordjevic, J.; Zatorre, R.; Jones-Gotman, M., Odor-induced changes in taste perception. *Experimental Brain Research* **2004**, 159, 405-408.

21. Kimatu, B. M.; Zhao, L.; Biao, Y.; Ma, G.; Yang, W.; Pei, F.; Hu, Q., Antioxidant potential of edible mushroom (*Agaricus bisporus*) protein hydrolysates and their ultrafiltration fractions. *Food chemistry* **2017**, *230*, 58-67.
22. Kim, Y.-J.; Park, J.-Y.; Park, H.-J.; Kim, S.-B.; Chun, B.-S.; Lee, Y.-B., Development of Reaction Flavors with Enzymatic Hydrolysate of Krill *Euphausia superba* in Ramen Sauce. *Fisheries and aquatic sciences* **2014**, *17*, 403-408.
23. Myrdal Miller, A.; Mills, K.; Wong, T.; Drescher, G.; Lee, S.; Sirimuangmoon, C.; Schaefer, S.; Langstaff, S.; Minor, B.; Guinard, J. X., Flavor-enhancing properties of mushrooms in meat-based dishes in which sodium has been reduced and meat has been partially substituted with mushrooms. *Journal of food science* **2014**, *79*, S1795-S1804.
24. Engel, W.; Bahr, W.; Schieberle, P., Solvent assisted flavour evaporation—a new and versatile technique for the careful and direct isolation of aroma compounds from complex food matrices. *European Food Research and Technology* **1999**, *209*, 237-241.
25. Czerny, M.; Christlbauer, M.; Christlbauer, M.; Fischer, A.; Granvogl, M.; Hammer, M.; Hartl, C.; Hernandez, N. M.; Schieberle, P., Re-investigation on odour thresholds of key food aroma compounds and development of an aroma language based on odour qualities of defined aqueous odorant solutions. *European Food Research and Technology* **2008**, *228*, 265-273.
26. Tamura, H.; Fujita, A.; Steinhaus, M.; Takahisa, E.; Watanabe, H.; Schieberle, P., Assessment of the aroma impact of major odor-active thiols in pan-roasted white sesame seeds by calculation of odor activity values. *Journal of agricultural and food chemistry* **2011**, *59*, 10211-10218.

27. Steinhaus, P.; Schieberle, P., Characterization of the key aroma compounds in soy sauce using approaches of molecular sensory science. *Journal of agricultural and food chemistry* **2007**, *55*, 6262-6269.
28. Culleré, L.; Escudero, A.; Pérez-Trujillo, J. P.; Cacho, J.; Ferreira, V., 2-Methyl-3-(methylthio) furan: A new odorant identified in different monovarietal red wines from the Canary Islands and aromatic profile of these wines. *Journal of food composition and analysis* **2008**, *21*, 708-715.
29. Schieberle, P., Recent developments in methods for analysis of flavor compounds and their precursors. . In *Characterization of Food: Emerging Methods* Goankar, A., Ed. Elsevier: Amsterdam, The Netherlands, 1995; pp 403–431.
30. Schieberle, P.; Grosch, W., Evaluation of the Flavor of Wheat and Rye Bread Crusts by Aroma Extract Dilution Analysis. *Zeitschrift Fur Lebensmittel-Untersuchung Und-Forschung* **1987**, *185*, 111-113.
31. Kerscher, R.; Grosch, W., Quantification of 2-methyl-3-furanthiol, 2-furfurylthiol, 3-mercapto-2-pentanone, and 2-mercapto-3-pentanone in heated meat. *Journal of agricultural and food chemistry* **1998**, *46*, 1954-1958.
32. Hofmann, T.; Schieberle, P., Identification of key aroma compounds generated from cysteine and carbohydrates under roasting conditions. *Zeitschrift für Lebensmitteluntersuchung und-Forschung A* **1998**, *207*, 229-236.
33. Hofmann, T.; Schieberle, P., Identification of potent aroma compounds in thermally treated mixtures of glucose/cysteine and rhamnose/cysteine using aroma extract dilution techniques. *Journal of Agricultural and Food Chemistry* **1997**, *45*, 898-906.

34. Mottram, D. S., Flavour formation in meat and meat products: a review. *Food chemistry* **1998**, *62*, 415-424.
35. Baek, H. H.; Kim, C. J.; Ahn, B. H.; Nam, H. S.; Cadwallader, K. R., Aroma extract dilution analysis of a beeflike process flavor from extruded enzyme-hydrolyzed soybean protein. *Journal of agricultural and food chemistry* **2001**, *49*, 790-793.
36. Wong, K. M.; Decker, E. A.; Autio, W. R.; Toong, K.; DiStefano, G.; Kinchla, A. J., Utilizing mushrooms to reduce overall sodium in taco filling using physical and sensory evaluation. *Journal of food science* **2017**, *82*, 2379-2386.
37. Djordjevic, J.; Zatorre, R. J.; Jones-Gotman, M., Effects of perceived and imagined odors on taste detection. *Chemical Senses* **2004**, *29*, 199-208.
38. Seo, H. S.; Iannilli, E.; Hummel, C.; Okazaki, Y.; Buschhüter, D.; Gerber, J.; Krammer, G. E.; van Lengerich, B.; Hummel, T., A salty-congruent odor enhances saltiness: Functional magnetic resonance imaging study. *Human brain mapping* **2013**, *34*, 62-76.
39. Kim, M.-Y.; Lee, S.-J.; Ahn, J.-K.; Kim, E.-H.; Kim, M.-J.; Kim, S.-L.; Moon, H.-I.; Ro, H.-M.; Kang, E.-Y.; Seo, S.-H., Comparison of free amino acid, carbohydrates concentrations in Korean edible and medicinal mushrooms. *Food Chemistry* **2009**, *113*, 386-393.
40. Wang, Y.; Ho, C.-T., Comparison of 2-acetylfuran formation between ribose and glucose in the Maillard reaction. *Journal of agricultural and food chemistry* **2008**, *56*, 11997-12001.
41. Wang, Y.; Juliani, H. R.; Simon, J. E.; Ho, C.-T., Amino acid-dependent formation pathways of 2-acetylfuran and 2, 5-dimethyl-4-hydroxy-3 [2H]-furanone in the Maillard reaction. *Food chemistry* **2009**, *115*, 233-237.
42. Münch, P.; Hofmann, T.; Schieberle, P., Comparison of key odorants generated by thermal treatment of commercial and self-prepared yeast extracts: influence of the amino acid



composition on odorant formation. *Journal of Agricultural and Food Chemistry* **1997**, *45*, 1338-1344.

43. Zhao, J.; Wang, T.; Xie, J.; Xiao, Q.; Du, W.; Wang, Y.; Cheng, J.; Wang, S., Meat flavor generation from different composition patterns of initial Maillard stage intermediates formed in heated cysteine-xylose-glycine reaction systems. *Food chemistry* **2019**, *274*, 79-88.

44. Chu, F. L. Elucidation of Selected Maillard Reaction Pathways in Alanine and Phenylalanine Model Systems through Isotope Labelling and Pyrolysis-GC/MS Based Techniques. McGill University, 2009.

45. Mottram, D. S.; Whitfield, F. B., Maillard-lipid interactions in nonaqueous systems: volatiles from the reaction of cysteine and ribose with phosphatidylcholine. *Journal of agricultural and food chemistry* **1995**, *43*, 1302-1306.

46. Thomas, C.; Mercier, F.; Tournayre, P.; Martin, J.-L.; Berdagué, J.-L., Identification and origin of odorous sulfur compounds in cooked ham. *Food chemistry* **2014**, *155*, 207-213.

## APPENDIX

## Abbreviations

cAEDA, comparative aroma extract dilution analysis; eHMP, enzymatically hydrolyzed mushroom protein; eHMP + cys, enzymatically hydrolyzed mushroom protein reacted with cysteine; FD factor, flavor dilution factor; FFAP, free fatty acid phase; FID, flame ionization detector; GC-O, gas chromatography-olfactometry; GC-MS, gas chromatography/mass spectrometry; OAV, odor activity value; QDA, quantitative descriptive analysis; RI, retention index; SAFE, solvent-assisted flavor evaporation; SIDA, stable isotope dilution assay.

## IUPAC Nomenclature

2-acetyl-1-pyrroline, 1-(3,4-dihydro-2H-pyrrol-5-yl)ethanone; dimethyl trisulfide, (methyltrisulfanyl)methane; 1-(2-furyl)-ethanethiol, 1-(furan-2-yl)ethanethiol; 2-furfurylthiol, (furan-2-yl)methanethiol; 2-methyl-3-(methylthio)furan, 2-methyl-3-(methylsulfanyl)furan; 2-acetylthiazole, 1-(1,3-thiazol-2-yl)-ethenone); 2-acetyl-2-thiazoline, 1-(4,5-dihydro-1,3-thiazol-2-yl)ethenone; trans-4,5-epoxy-(2E)-2-decenal, (E)-3-(3-pentylloxiran-2-yl)prop-2-enal; HDMF, 4-hydroxy-2,5-dimethyl-3(2H)-furanone; *p*-cresol, 4-methylphenol; 4-allyl-2-methoxyphenol, 2-methoxy-4-prop-2-enylphenol; sotolon, 3-hydroxy-4,5-dimethylfuran-2(5H)-one; 2-aminoacetophenone, 2-amino-1-phenyl ethanone; indole, 1H-indole

## ACS Publications Copyright Certification



RightsLink®

Home

Create Account

Help



ACS Publications  
Most Trusted. Most Cited. Most Read.

**Title:** Odorants from the Thermal Treatment of Hydrolyzed Mushroom Protein and Cysteine Enhance Saltiness Perception  
**Author:** Jordan Lopez, Trent Kerley, Lindsay Jenkinson, et al  
**Publication:** Journal of Agricultural and Food Chemistry  
**Publisher:** American Chemical Society  
**Date:** Oct 1, 2019  
Copyright © 2019, American Chemical Society

LOGIN

If you're a **copyright.com user**, you can login to RightsLink using your copyright.com credentials. Already a **RightsLink user** or want to [learn more?](#)

### PERMISSION/LICENSE IS GRANTED FOR YOUR ORDER AT NO CHARGE

This type of permission/license, instead of the standard Terms & Conditions, is sent to you because no fee is being charged for your order. Please note the following:

- Permission is granted for your request in both print and electronic formats, and translations.
- If figures and/or tables were requested, they may be adapted or used in part.
- Please print this page for your records and send a copy of it to your publisher/graduate school.
- Appropriate credit for the requested material should be given as follows: "Reprinted (adapted) with permission from (COMPLETE REFERENCE CITATION). Copyright (YEAR) American Chemical Society." Insert appropriate information in place of the capitalized words.
- One-time permission is granted only for the use specified in your request. No additional uses are granted (such as derivative works or other editions). For any other uses, please submit a new request.

BACK

CLOSE WINDOW

Copyright © 2019 [Copyright Clearance Center, Inc.](#) All Rights Reserved. [Privacy statement.](#) [Terms and Conditions.](#) Comments? We would like to hear from you. E-mail us at [customer@copyright.com](mailto:customer@copyright.com)

## VITA

Jordan grew up in New Jersey, in the suburbs of New York City. He attended Montclair High School and graduated in 2004. He earned a Bachelor's of Science in Chemistry from Worcester Polytechnic Institute, Worcester, MA, in 2008. Jordan briefly worked as a technician at Benjamin Moore in 2008, synthesizing latex paint bases and testing for physical properties. In late 2008, he accepted a job at Mars Chocolate, NA, where he was first introduced to flavor chemistry and food science. In 2013, Jordan relocated to Chicago and worked at a flexible electronics company. He provided support on the chemistry side, synthesizing monomers and other building blocks for prototype products. In 2016, Jordan accepted a position at Prinova, a food ingredient supplier and small flavor house. He decided to pursue a Master's degree with the University of Tennessee, Knoxville, to learn more of the field of food science.